CARPAL TUNNEL PATHOMECHANICS: VASCULAR DYNAMICS, TISSUE KINEMATICS, & NERVE FUNCTION

CARPAL TUNNEL PATHOMECHANICS: VASCULAR DYNAMICS, TISSUE

KINEMATICS, & NERVE FUNCTION

By AMANDA FARIAS ZUNIGA, M.Sc., B.Sc.

A Thesis Submitted to the Department of Kinesiology and the School of Graduate Studies

in Partial Fulfilment of the Requirements for the Degree Doctor of Philosophy

McMaster University DOCTOR OF PHILOSOPHY (2020) Hamilton, Ontario (Kinesiology)

TITLE: Carpal Tunnel Pathomechanics: Vascular Dynamics, Tissue Kinematics, & Nerve Function

AUTHOR: Amanda Farias Zuniga, M.Sc, B.Sc (McGill University)

SUPERVISOR: Dr. Peter J. Keir

NUMBER OF PAGES: xxviii, 198

LAY ABSTRACT

Carpal tunnel syndrome (CTS) is due to compression of the median nerve as it passes

through the carpal tunnel which is located at the base of the palm. Nerve compression

leads to nerve dysfunction, resulting in symptoms of tingling, numbness and weakness of

the hand. The purpose of this thesis was to improve our understanding of the effects of

altered blood flow on the development of CTS. I conducted three unique studies to

investigate the relationship among nerve blood flow, nerve function, and motion of the

tendons and connective tissue within the carpal tunnel. The use of ultrasound allowed for

real-time, non-invasive investigation of function in these tissues. Results from these three

studies clearly demonstrate the interrelationship between nerve function, tendon-

connective tissue motion and adequate nerve blood flow. These findings have

implications for individuals with cardiovascular conditions and for people working under

conditions that may compromise normal blood flow.

ABSTRACT

Carpal tunnel syndrome (CTS) is a common peripheral compression neuropathy which is often idiopathic in etiology. There is evidence that the development of CTS may result from circulatory disturbances. The purpose of this thesis was to improve our understanding of the vascular component to the development and progression of CTS. Ultrasound allowed for non-invasive investigation of median nerve intraneural blood flow and morphology, tissue stiffness, and mechanics of the flexor digitorum superficialis (FDS) tendon and its adjacent subsynovial connective tissue (SSCT). Nerve conduction study (NCS) allowed for investigation of median nerve function. Three studies were completed, two with patients and one involving healthy participants, to investigate the relationship between local blood flow and carpal tunnel tissue function, morphology, and mechanics. Nerve function, intraneural blood flow, individual FDS and SSCT displacements, and measures of shear strain (relative FDS-SSCT displacement and shear strain index (SSI)) were quantified in CTS patients (Chapter 2). These patients were followed-up six months later and the measures were repeated (Chapter 3), allowing me to determine the prognostic value of ultrasound measures. Results from these two studies suggested a high interdependency among intraneural blood flow velocity, nerve function, and FDS-SSCT relative displacement and SSI. Intraneural blood flow velocity, peak FDS-SSCT relative displacement, and SSI were also significant predictors of median nerve function at 6-months follow-up. To directly investigate the effects of circulatory disturbances, temporary partial ischemia of the carpal tunnel was induced in healthy participants through a 30-minute occlusion protocol (Chapter 4). Partial ischemia

iv

immediately decreased intraneural blood flow velocity. Nerve dysfunction, and increased

SSI and relative displacement were observed soon after. This thesis clearly demonstrates

the interrelationship among median nerve vascular dynamics, tendon-SSCT kinematics,

and nerve function. Altered nerve blood flow may be a driver in the development of

CTS.

ACKNOWLEDGEMENTS

CONTRIBUTIONS TO PAPERS WITH MULTIPLE AUTHORS

<u>*Chapter 2*</u>

Farias Zuniga, A., Ghavanini, A.A., Israelian, G., Keir, P.J. 2020. Blood flow velocity but not tendon mechanics related to nerve function in carpal tunnel syndrome patients. Journal of the Neurological Sciences, 411: 116694.

Contributions

This study was conceived by Amanda Farias Zuniga and Dr. Peter J. Keir. Method development was conducted by Amanda Farias Zuniga with substantial input from Dr. Peter J. Keir. Data collection and analysis was conducted by Amanda Farias Zuniga with the exception of the neurological outcomes which were collected and analyzed by Dr. Amer Ghavanini and Dr. Gaspar Israelian. Interpretation and manuscript preparation were completed by Amanda Farias Zuniga, with input from Dr. Keir, Dr. Ghavanini and Dr. Israelian. All co-authors contributed to the final manuscript.

<u>*Chapter 3*</u>

Farias Zuniga, A., Ghavanini, A.A., Israelian, G., Keir, P.J. Ultrasound examination predicts 6-month progression in carpal tunnel syndrome patients. Submitted June 16, 2020, to the Journal of Orthopaedic Research.

Contributions

This study was conceived by Amanda Farias Zuniga with input from Dr. Peter Keir, Dr. Amer Ghavanini, and Dr. Gaspar Israelian. Methodology was developed by Amanda Farias Zuniga with substantial input from Dr. Peter J. Keir. Data collection and analysis were conducted by Amanda Farias Zuniga with the exception of the neurological outcomes which were collected and analyzed by Dr. Amer Ghavanini and Dr. Gaspar Israelian. Interpretation and manuscript preparation were completed by Amanda Farias

Zuniga, with input from Dr. Keir, Dr. Ghavanini and Dr. Israelian. All co-authors contributed to the final manuscript.

Chapter 4

Farias Zuniga, A., Keir, P.J. Thirty minutes of Sub-Diastolic Blood Flow Occlusion Alters Carpal Tunnel Tissue Function and Mechanics. Prepared for submission to Ultrasound in Medicine and Biology.

Contributions

Study conception and methodology were developed by Amanda Farias Zuniga, with substantial input from Dr. Peter Keir. Data collection and analysis were completed by Amanda Farias Zuniga. Interpretation of results and writing of the manuscript were completed by Amanda Farias Zuniga, with input from Dr. Peter J. Keir. Both co-authors contributed to this manuscript.

TABLE OF CONTENTS

LIST OF TABLES

LIST OF FIGURES

CHAPTER 1

CHAPTER 2

CHAPTER 4

LIST OF ABBREVIATIONS AND SYMBOLS

ANOVA……………………………………………………Analysis of Variance

APB…………………………………………………….Abductor Pollicis Brevis

ARFI…………………………………..Acoustic Radiation Force Impulse Imaging

CNN………………………………………………..Convolutional Neural Network

CSA…………………………………………………..Cross-Sectional Area

CTP…………………………………………………...Carpal Tunnel Pressure

CTS…………………………………………………Carpal Tunnel Syndrome

CV…………………………………………………………Conduction Velocity

DBP……………………………………………………….Diastolic Blood Pressure

DLC………………………………………………………………DeepLabCut

E……………………………………………………………..Young's modulus

EMG…………………………………………………………..Electromyography

FDP………………………………………………...Flexor Digitorum Profundus

FDS………………………………………………Flexor Digitorum Superficialis

FPL………………………………………………….Flexor Pollicis Longus

FR……………………………………………………………….Flattening Ratio

HR…………………………………………………………………Heart Rate

HSD……………………………………………….Honestly Significant Difference

ICC………………………………………………Intraclass Correlation Coefficient

MRI………………………………………………Magnetic Resonance Imaging

MVCAS……………...Microvascular Collagenous Dynamic Absorbing System

NCS…………………………………………………….Nerve Conduction Study

PD…………………………………………………...Power Doppler

PW Doppler………………………………………...Pulse Wave Doppler

RMSE……………………………………………Root Mean Squared Error

ROC………………………………………..Receiver Operating Characteristic

ROI……………………………………………………Region of Interest

RPD…………………………………………….Rating of Perceived Discomfort

SD…………………………………………………Standard Deviation

SEM……………………………………………….Standard Error of Measurement

SpO$_2$…………………………………………Peripheral Oxygen Saturation

SSCT………………………………………...Sub-synovial Connective Tissue

SSI……………………………………………………….Shear Strain Index

SWE……………………………………………..Shear Wave Elastography

TCL……………………………………………...Transverse Carpal Ligament

LIST OF APPENDICES

Chapter 1: Introduction and General Literature Review

Carpal tunnel syndrome (CTS) is a commonly diagnosed peripheral neuropathy. The lifetime prevalence of clinically diagnosed CTS is estimated to be between 6.7 – 8.0% (Dale et al., 2013; Luckhaupt et al., 2013), with an overall estimated incidence rate of 0.38– 2.3 per 100 person-years (Dale et al., 2013; Roquelaure et al., 2017). CTS has associated medical costs upwards of $2 billion annually in the United States (Stapleton, 2006). Several laboratory and epidemiological studies have identified work-related risk factors of CTS, including repetitive hand use (Bernard et al., 1997; Latko et al., 1999; Nordander et al., 2013; Rempel et al., 1994; Szabo et al., 1989; Thomsen et al., 2002; Werner et al., 1998), forceful exertions (Ferguson et al., 1993; Gabra et al., 2016; Keir et al., 1998; Marquardt et al., 2015; Nathan et al., 2005; Nordander et al., 2013; Rempel et al., 1997; Thomsen et al., 2002; Werner et al., 1983), and non-neutral wrist postures (Babski-Reeves et al., 2003; Bauman et al., 1981; Gelberman et al., 1981b; Rojviroj et al., 1990; Szabo et al., 1989; Werner et al., 1983). However, median nerve compression is the primary mechanism for CTS development. Compression of the median nerve within the carpal tunnel results in several changes in nerve function that manifest into characteristic symptoms associated with CTS, including pain, tingling and numbness of the hands (Ferry et al., 1998). Compression also impairs blood flow to the nerve, further contributing to physiological changes resulting in nerve dysfunction (Topp et al., 2006).

1.1 Carpal Tunnel Anatomy

The average area of the carpal tunnel in a neutral wrist posture is approximately 200 mm^2 in men and approximately 150 mm^2 in women (Bower et al., 2006). The

borders of the carpal tunnel are comprised of four carpal bones: the hamate, capitate,

trapezoid and trapezium. The volar surface is enclosed by the transverse carpal ligament

(TCL)/ flexor retinaculum (D'Arcy et al., 2010; Jayaraman et al., 2004). This small space

contains the median nerve and nine finger flexor tendons: the four tendons of the flexor

digitorum superficialis (FDS), four tendons of the flexor digitorum profundus (FDP) and

the flexor pollicis longus (FPL) tendon (Figure 1.1). The median nerve sits radially,

immediately below the TCL (Jayaraman et al., 2004). Two bursae, the radial and ulnar

bursa, surround the tendons (Ettema et al., 2004).
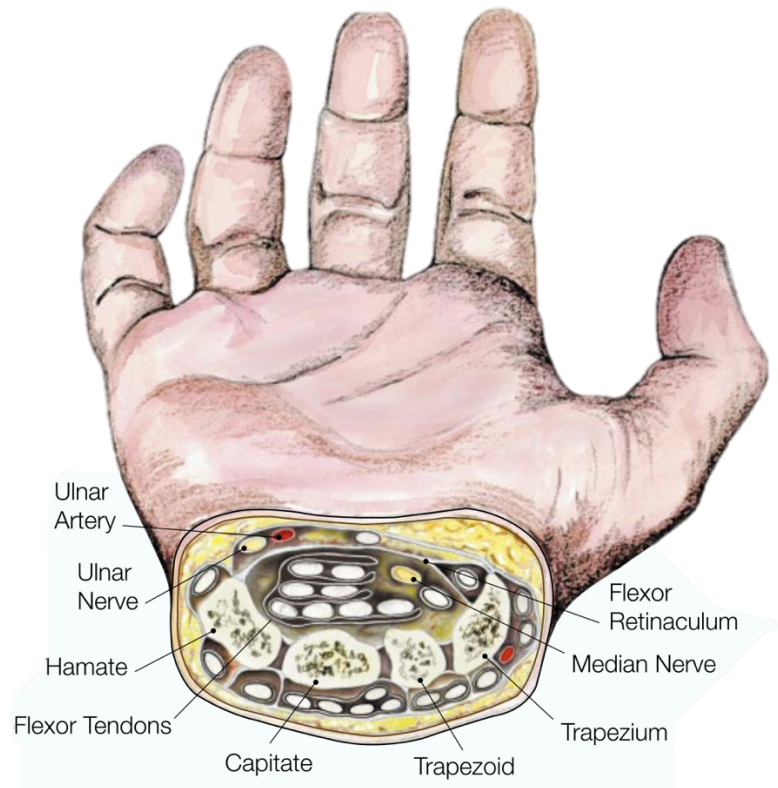
Figure 1. 1. Anatomy of the carpal tunnel (Image from D'Arcy & McGee, 2000).

1.1.1 The Median Nerve

The median nerve is a peripheral nerve with nerve cell bodies originating from the C5-C7 and C8-T1 levels in the spinal cord. The median nerve has both motor and sensory fibres, with motor axons originating in the ventral horn of the spinal cord and sensory axons originating in the dorsal root ganglia (Hochman et al., 2004; Mackinnon, 2002; Rempel et al., 1999; Topp et al., 2006). The nerve itself is composed of myelinated and unmyelinated axons bundled together into nerve fibres that are further bundled together and contained within the endoneurial space. The ratio of myelinated to unmyelinated fibres in the nerve is 1:4 (Mackinnon, 2002). The endoneurial space is enclosed by the perineurium to form a fascicle. Series of fascicles are further bundled together within the epineurium, ultimately forming the nerve (Figure 1.2). Within the perineurium, there are several layers of type I and type II collagen fibrils and elastic fibres, oriented longitudinally, circumferentially and obliquely, giving the nerve mechanical strength and load bearing properties (Topp et al., 2006). The epineurial layer also contains type I and II collagen fibrils and elastic fibres, but also has fibroblasts, mast cells and fat cells (Topp et al., 2006). Fascicles within the epineurium are not tightly attached to the perineurium, allowing for fascicles to slide past each other (Mackinnon, 2002; Rempel et al., 1999; Topp et al., 2006).
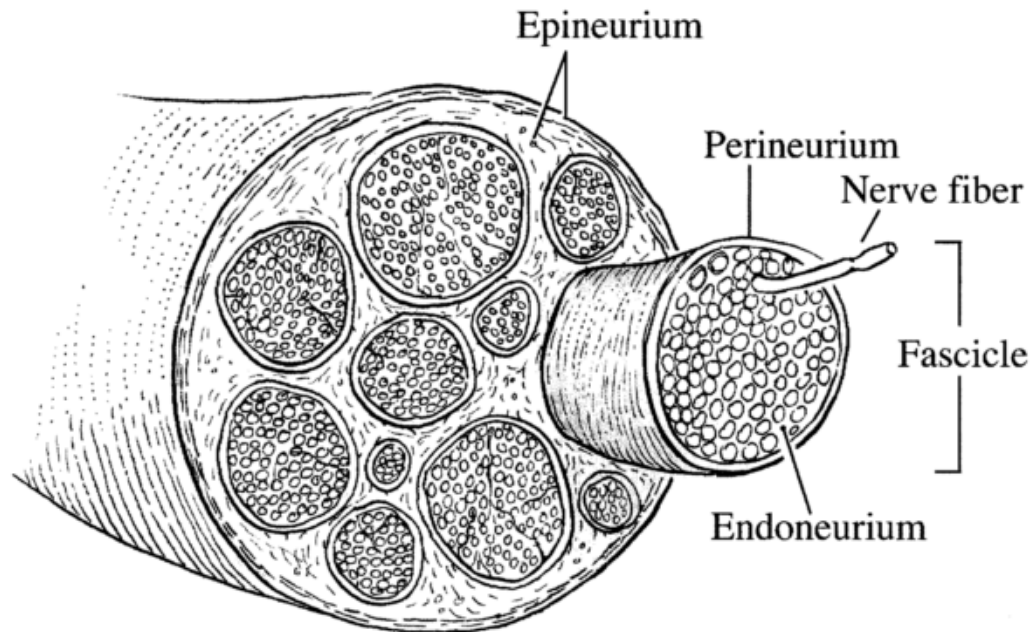
Figure 1. 2. Schematic of a peripheral nerve. Both myelinated fibres and unmyelinated fibres (not shown) are organized into bundles that make up the nerve fibre. Nerve fibres are further bundled together into fascicles, which together create the endoneurial space (endoneurium), enclosed by the perineurium. Within the endoneurial space is endoneurial fluid, capillaries, and collagen fibres (not shown) that run longitudinally between axons (Topp et al., 2006). Several perineurial bundles are brought together by the epineurium, which is made up of fibroblasts, collagen fibres and elastic fibres (not shown). These structures ultimately form the nerve (Image from Hochman & Zilberfarb 2004).

1.1.2 Median Nerve Vasculature

The vascular supply of the median nerve is provided by the radial and ulnar arteries of the arm (Mackinnon, 2002). The radial and ulnar arteries send descending branches from the superficial palmar arch to supply the median nerve through the carpal tunnel. The vasculature of the median nerve is unique in that microvasculature runs through it adjacent to nerve fibres (intraneural), as well as around the nerve itself

5

(extraneural) within a plexus of connective tissue that envelopes the nerve (Lundborg, 1975). Capillaries forming an anastomosis run through the endoneurial space, and arterioles and veins run longitudinally within the epineurium that encloses the nerve fibres (Figure 1.3) (Lundborg, 1975). Blood flow between the anastomoses of the endoneurium and larger vessels within the epineurium (Mackinnon, 2002) has no specific direction, and often changes direction at different segments of the same vessel (Lundborg, 1975). Arterioles in the perineurial space are not able to regulate blood flow since they have poorly developed smooth muscle (Topp et al., 2006). These vessels that pass through the perineurium do so obliquely (Mackinnon, 2002; Perumal et al., 2014) and therefore have a valve-like mechanism (Mackinnon, 2002). Furthermore, there is no lymphatic drainage in the endoneurial space between fascicles; lymphatic capillaries are located only in the epineurium (Mackinnon, 2002; Topp et al., 2006). Overall, blood flow to the epineurium (and subsequent deeper layers) from the radial and ulnar arteries via the superficial palmar arch is supplied through a loose connective tissue that surrounds the nerve (Hochman et al., 2004). There are multiple terms used to refer to this loose connective tissue: the mesoneurium (Hochman et al., 2004; Lundborg, 1975), microvacuolar collagenous dynamic absorbing system (MVCAS) (Guimberteau et al., 2010; Werthel et al., 2014), and loose areolar tissue or sub-synovial connective tissue (Guimberteau et al., 2010). It will herein be referred to as the sub-synovial connective tissue (SSCT).
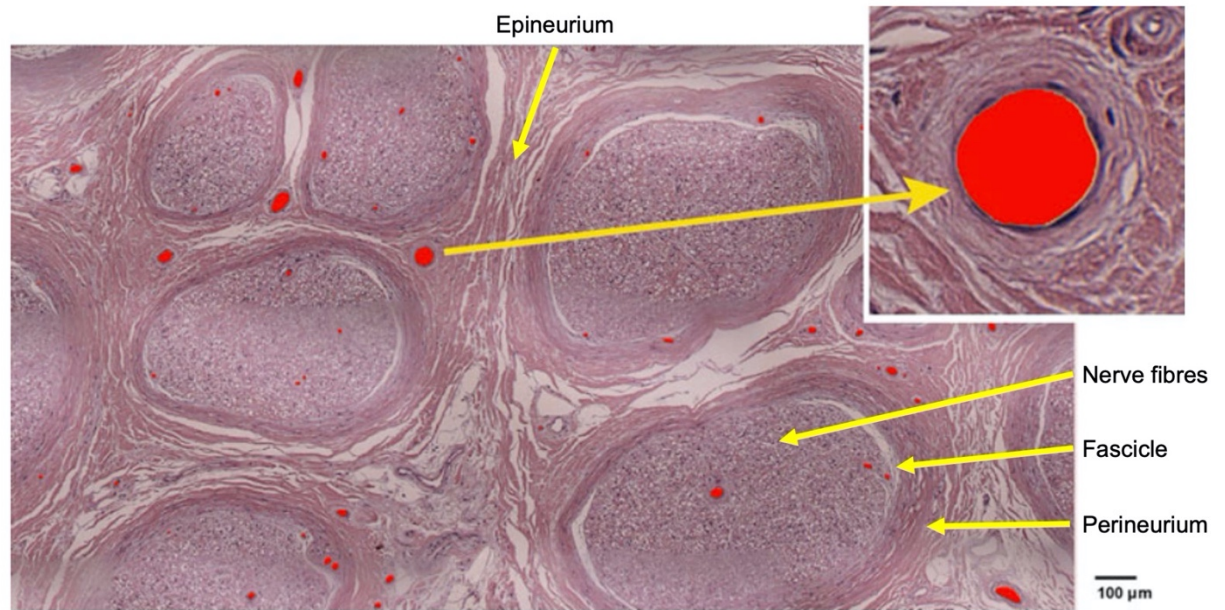
Figure 1. 3. Photomicrograph of a transverse section of the median nerve highlighting intraneural blood vessels (red circles). Intraneural arterial vasculature is visible in between nerve fascicles, and between nerve fibres within the endoneurial space (Image adapted from Perumal & Stringer 2014).

1.1.3 Finger Flexor Tendons

There are nine tendons passing through the carpal tunnel: four tendons of the FDS (digits 2-5), four tendons of the FDP (digits 2-5), and the FPL tendon (digit 1). The tendons are composed of type I collagen fibres which are arranged in a helical arrangement along the tendon, giving rise to their mechanical properties (Myer et al., 2016). The FDP tendons arise from the deep layer of flexor muscles, while the FDS arise from the superficial layer. The FPL also arises from the deep muscle layer. The finger flexor tendons constitute the extrinsic finger flexors, meaning that their muscle bellies are located outside of the hand in the forearm. The FDP tendons insert into the base of the

distal phalanges, while the FDS tendons insert into the shafts of middle phalanges (Allan, 2005). The FPL tendon is enclosed within its own synovial sheath, while the remaining eight tendons are surrounded by the SSCT (Jayaraman et al., 2004; Presazzi et al., 2011). These flexor tendons are also surrounded by the ulnar bursa, providing further cushioning. Both the FDP and FDS receive nutrient supply through a combination of vascular perfusion and synovial diffusion (Myer et al., 2016; Ochiai et al., 1979).

The tendon and the SSCT constitute the gliding unit of the fingers. They move together to produce smooth finger motion, and the SSCT reduces friction during differential finger motion. It is reported that the FDS tendon of the middle finger displaces approximately 20-30 mm during full finger flexion-extension (Kociolek et al., 2015; van Beek et al., 2018). During differential finger motion, the SSCT provides resistance to movement of adjacent tendons, limiting the amount of tendon displacement (Vanhees et al., 2012). This gliding resistance is mainly due to the viscoelastic properties of the SSCT.

1.1.4 Sub-synovial Connective Tissue

The SSCT is a network of multiple layers of collagen bundles (Guimberteau et al., 2010), with smaller vertical collagen fibres interconnecting the bundles (Ettema et al., 2006) (Figure 1.4). It is a thin tissue, with an average thickness of 0.33 ± 0.14 mm (Osamura et al., 2007b). It contains an assortment of hydrophilic chains of proteoglycans and phospholipids, type I, III, IV and V collagen (Ettema et al., 2004), elastin (Jinrok et al., 2004), and a small portion of lipids (Guimberteau et al., 2010). Due to these

components, it has very low permeability and a high affinity for fluid (Osamura et al., 2007b). Its components enable the SSCT to serve its many functions, including shock absorption, lubrication, reducing shear forces, reducing gliding resistance, and acting as a framework for blood and lymphatic vessels (Guimberteau et al., 2010). Within the SSCT, blood and lymphatic vessels are intertwined between its layers and span out in different directions. When the SSCT layers move during finger motion, blood vessels are seen to lie in different planes and therefore experience different displacements (Guimberteau et al., 2010). The SSCT is important in facilitating nerve movement (Guimberteau et al., 2010; Hochman et al., 2004) and differential finger motion of the fingers by allowing for gliding between finger flexor tendons (Osamura et al., 2007a). Because of its unique composure, the SSCT allows the flexor tendons of the hand to have both viscoelastic and synovial fluid lubrication gliding properties (Werthel et al., 2014). Additionally, it has very low permeability (Osamura et al., 2007b) and an affinity for water due to the hydrophilic proteoglycans, allowing it to maintain the fluid environment of the carpal tunnel by absorbing excess fluid. The SSCT ultimately receives its blood supply through vessels originating primarily from the radial and ulnar arteries (Mackinnon, 2002).
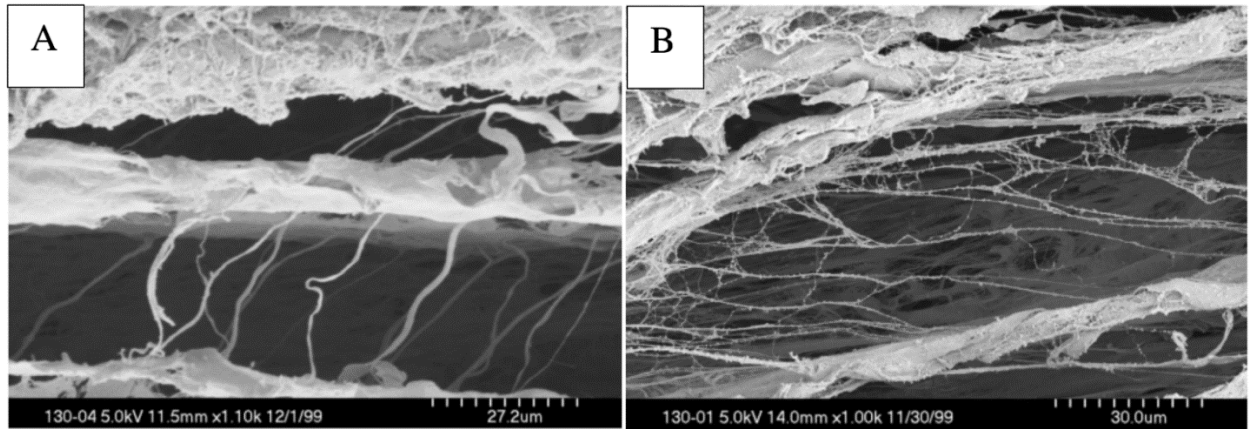
Figure 1. 4. Scanning electron microscopy images of the sub-synovial connective tissue (SSCT). The vertical fibres joining adjacent layers (thick horizontal bundles) are loose in a relaxed state (A) and become stretched as finger flexor tendons move (B) (Images from Ettema et al., 2006).

To allow it to serve its functions in both nerve and tendon motion, as well as in providing framework for blood and lymphatic vessels, the SSCT has a web-like structure with several layers. When the tendons of the fingers glide past one another, the layers of the SSCT "telescope" out, as they are sequentially recruited. Fibrous bundles are recruited layer by layer, with the bundles next to the tendon moving first (Ettema et al., 2006). These layers of the SSCT exhibit viscous properties which influence the displacement of the SSCT fibrils compared to the displacement the adjacent tendon experiences (Ettema et al., 2006; Tat et al., 2015; Zhao et al., 2011). These viscoelastic properties have been observed in cadaveric models where tendon gliding resistance has been reported to increase exponentially with tendon displacement (Zhao et al., 2011). Using ultrasound colour Doppler, Tat et al. (2015) observed less SSCT displacement and lower SSCT velocity compared to the flexor tendon at larger finger excursions and higher movement velocities. Greater frictional work is also associated with higher finger

movement velocities (Tat et al., 2016). These observations were attributed to the viscoelastic properties of the SSCT, where a nonlinear increase in resistance is produced as the fibrils of the SSCT become sequentially stretched (Tat et al., 2015, 2016).

1.2 Carpal Tunnel Syndrome

Carpal tunnel syndrome is the most common peripheral neuropathy. Although its etiology is difficult to ascertain given the multifaceted nature of its development, it is well established that CTS is a compression neuropathy. Patients with CTS have higher carpal tunnel pressure (CTP) compared to healthy individuals (Bauman et al., 1981; Coppieters et al., 2012; Gelberman et al., 1981; Rojviroj et al., 1990; Seradge et al., 1995; Szabo et al., 1989; Werner et al., 1983). Average CTP values range from 10 to 52 mmHg when measured in neutral wrist posture, depending on measurement method. Several biomechanical risk factors have been established through both epidemiological and laboratory investigations, including highly repetitive movements (Bernard et al., 1997; Latko et al., 1999; Nordander et al., 2013; Rempel et al., 1994; Szabo et al., 1989; Thomsen et al., 2002; Werner et al., 1998), forceful exertions (Ferguson et al., 1993; Gabra et al., 2016; Keir et al., 1998; Marquardt et al., 2015; Nathan et al., 2005; Nordander et al., 2013; Rempel et al., 1997; Thomsen et al., 2002; Werner et al., 1983), and non-neutral wrist postures (Babski-Reeves et al., 2003; Bauman et al., 1981; Gelberman et al., 1981; Rojviroj et al., 1990; Szabo et al., 1989; Werner et al., 1983). Exposure to these risk factors have been demonstrated to increase CTP, therefore leading to greater compression on the median nerve. This chronic compression results in a

number of functional, structural and mechanical changes in carpal tunnel tissues which ultimately leads to nerve dysfunction and the associated neurological symptoms that accompany the condition.

1.2.1 Nerve Dysfunction

Carpal tunnel syndrome is primarily diagnosed through clinical evaluation of symptoms and electrodiagnostic testing. Neurological changes that occur in the median nerve are measured through nerve conduction studies (NCS), which serve to quantify the transfer of electrical impulses. Since the median nerve carries both motor and sensory fibres, motor and sensory testing are carried out and results are evaluated together to confirm a diagnosis. The latency (time in milliseconds (ms) from the applied stimulus to the first detected response at the recording site), amplitude (height, in millivolts (mV) or microvolts (μV), from the baseline measure to the peak of the negative phase of the waveform), and conduction velocity (speed of impulse propagation in meters per second (m/s))(Gooch et al., 2007; Preston et al., 2005) of the responses are measured. NCS is conducted by placing a stimulating electrode proximally at the wrist over the median nerve, and measuring the resulting response from a recording electrode either on the abductor pollicis brevis (APB) muscle of the thumb (motor response) or on the finger (sensory response) (Heckel et al., 2015; Preston et al., 2005)(Figure 1.5). Results from NCS are used to diagnose and categorize the severity of the condition (Bland, 2000).
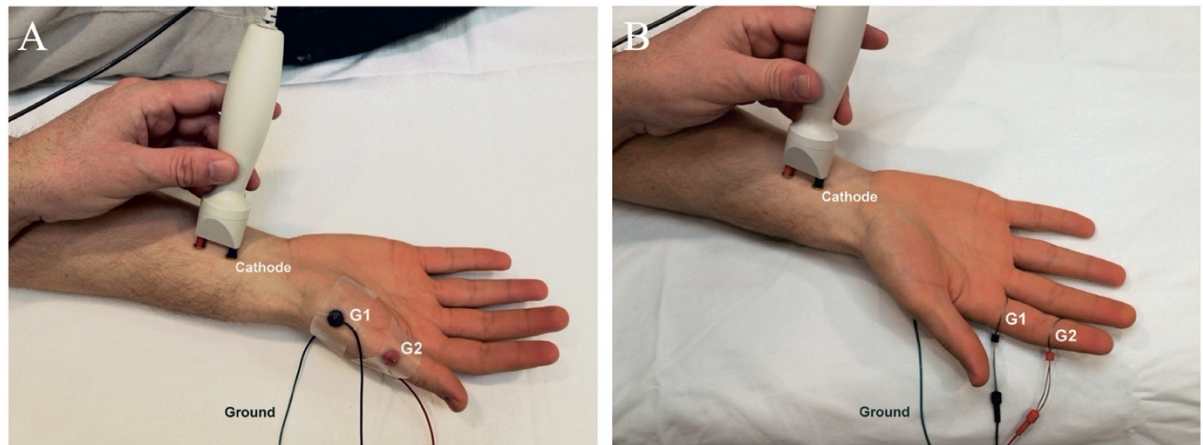
Figure 1. 5. Schematic of nerve conduction study (NCS). A: In motor NCS, the stimulating electrode is placed proximally, while the recording electrode (G1) is placed on the palmar side on the abductor pollicis brevis (APB) muscle of the thumb. B: In sensory NCS, the stimulating electrode is placed proximally while the recording electrode (G1) is placed at the digit (Image from Preston & Shapiro 2005).

1.2.2 Altered Blood Flow

Continuous blood supply to the SSCT and vessels of the nerve is essential to the nerve's healthy functioning. An interruption in blood flow, through either an increase in CTP or through external compression, can alter the blood supply to carpal tunnel tissues. Increased CTP collapses the capillaries within the nerve (Gelberman et al., 1981) and is hypothesized to restrict intrafascicular capillary flow by increasing endoneurial pressure (Lundborg et al., 1983). In animal models, high pressures lead to ischemia (Diao et al., 2005; Powell et al., 1986) and results in impaired nerve function within 30 to 90 minutes (Lundborg, 1975). A pressure of 40-50 mmHg appears to be a critical threshold at which nerve function becomes impaired. At 50 mmHg, motor and sensory responses have been reported to be completely blocked (Gelberman et al., 1983), which may be due to occlusion of epineurial vessels and a significant reduction in intraneural blood flow

velocity (Rydevik et al., 1981). At high pressures (> 80 mmHg) significant axonal

damage is evident (Powell et al., 1986). However, even low pressures can have similar

effects as it causes intraneural and extraneural edema (Tang et al., 2015). Given that the

median nerve lacks lymphatic vessels within the endoneurial space (Mackinnon, 2002;

Rempel et al., 1999), the median nerve is prone to damage through edema. Edema results

in an increase in endoneurial fluid pressure of the nerve (Lundborg et al., 1983), leading

to structural changes of the nerve, most notably, fibrosis of the epineurium and

perineurium (Freeland et al., 2002; Tang et al., 2015). Indeed, even lower pressures (30

mmHg) for a prolonged amount of time results in demyelination of nerves (Powell et al.,

1986). Ischemia results in tissue re-modeling resulting in permanent microstructural and

functional changes. Difference between healthy individuals and patients with CTS

symptoms and/or a positive CTS diagnosis have recently been investigated using

ultrasound. Ultrasound is a relatively low-cost, non-invasive imaging modality that

allows for investigation of biological tissues. Morphological and functional changes in

the median nerve that result from prolonged compression have been visualized using

ultrasound. B-mode ultrasound image evaluations of the carpal tunnel report

morphological changes of the nerve in both shape (Nakamichi et al., 2000), and size

(cross-sectional area (CSA)) (Joy et al., 2011; Kutlar et al., 2017; Mallouhi et al., 2006;

Nakamichi & Tachibana, 2000) indicating nerve swelling. Intraneural blood flow has

been investigated through pulse wave (PW) Doppler, and indicate that intraneural blood

flow is generally higher in individuals experiencing CTS symptoms (Joy et al., 2011;

Wilson et al., 2017) but may vary depending on CTS severity (Evans et al., 2012; Farias

Zuniga et al., 2020). Ischemia has been seen to upregulate fibroblast activity, promoting

atherosclerotic vessel changes (Faller, 1999). Several other vascular pathological changes

of the SSCT have also been noted, including thickening of blood vessel walls leading to

blood flow obstruction (Ettema et al., 2004; Jinrok et al., 2004).

1.2.3 SSCT Injury

There is also histological evidence of increased fibroblast activity and intimal

thickening in the SSCT of patients with CTS (Ettema et al., 2004). Fibrosis of the SSCT

primarily occurs along its border with the tendon (Ettema et al., 2006), indicating that

these changes may be due to shear strain injury between the tendon and SSCT. Shear

injury is proposed to be due to external risk factors, such as repetitive motion or forceful

exertions, where high loads are carried by the interconnecting fibres of the SSCT, causing

them to rupture. These ruptured fibres no longer function to sequentially recruit

horizontal bundles, and then "stick" to the thicker horizontal bundles of the SSCT. Injury

to these fibres induces a non-inflammatory response leading to fibrosis and thickening of

the SSCT (Figure 1.6) (Festen-Schrier et al., 2018). These structural changes to the SSCT

result in increased gliding resistance between finger flexor tendons and the SSCT during

differential finger motion, which can be quantified in-vivo using ultrasound. Ultrasound

has been used to assess tendon and SSCT velocities and the relative displacement

between tissues during repetitive finger movement in CTS patients and healthy controls

(Kociolek et al., 2016; Schrier et al., 2020; Tat et al., 2014, 2013, 2015; van Doesburg et

al., 2012a,b). CTS symptomatic individuals and clinically diagnosed patients exhibit

greater shear strain index (SSI) (a relative measure of excursion between the tendon and SSCT during flexion and extension) (Schrier et al., 2020; Tat et al., 2013; van Doesburg et al., 2012) and greater SSCT thickness than healthy controls (Tat et al., 2015). The effects of partial ischemia on tendon and SSCT motion have also been reported. Tse (2019) demonstrated that 20 minutes of partial ischemia decreases SSCT displacement, while tendon displacement remains relatively unchanged, increasing the chance for injury through shear strain (Tse et al., 2019). Damage to the SSCT can lead to a secondary pathway of median nerve compression; as endothelial cells in the capillaries become distressed, the permeability of the SSCT increases resulting in SSCT edema. This swelling can further compress the median nerve, restricting median nerve blood flow, leading to associated neurophysiological changes.
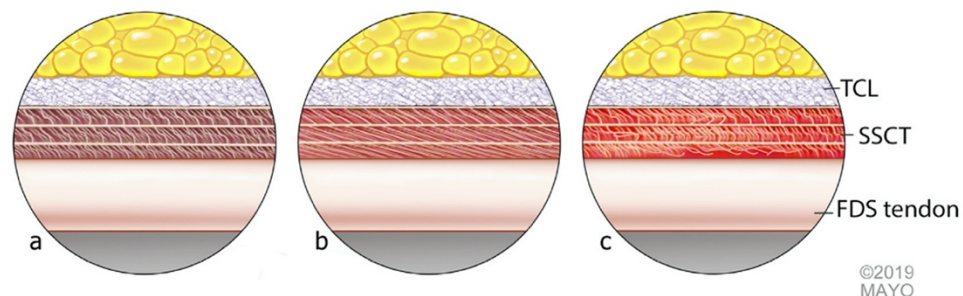
Figure 1. 6. Proposed mechanism of subsynovial connective tissue (SSCT) shear injury leading to SSCT fibrosis and eventual compression of the median nerve resulting in carpal tunnel syndrome. A) In a relaxed state there is no tension on the interconnecting fibres of the SSCT, but during finger motion B) there is progressive recruitment of the layers of the SSCT through stretching of the interconnecting fibres. C) Over time and with repetitive finger motion, damage to the SSCT occurs through breakage of the interconnecting fibres as they are stretched past their limit. This breakage results in the inability of these fibres to assist in recruiting the SSCT layers. A non-inflammatory response occurs which results in fibrosis and thickening of the tissue, further reducing the space within the tunnel and leading to median nerve compression (Image adapted from Schrier et al., 2019). FDS = flexor digitorum superficialis; TCL = transverse carpal ligament.

1.2.4 Change in Tissue Elasticity

Structural changes in tissues that result from damage leading to fibrosis and thickening can also be investigated through measurement of tissue elasticity. A relatively new ultrasound technique called elastography has recently been employed in CTS studies to investigate changes in median nerve and tendon stiffness (Arslan et al., 2018; Ghajarzadeh et al., 2015; Kantarci et al., 2014; S. Lee et al., 2019; Liao et al., 2015; Martin et al., 2017; Ogur et al., 2015; Orman et al., 2013; Tatar et al., 2016; Xin et al., 2017; Yoshii et al., 2017a, 2017b). There are two main methods of US elastography: quasi-static and dynamic. Quasi-static elastography involves using the ultrasound probe to manually provide stress to the tissue, and the resulting strain is estimated from the displacement in the tissue (Gennisson et al., 2013). In contrast, dynamic elastography applies a time-varying force to the tissue, such as shear waves (referred to as shear wave elastography (SWE)), or acoustic radiation force (referred to as Acoustic Radiation Force Impulse Imaging (ARFI)), and measure the propagation of shear waves within the tissue (Gennisson et al., 2013). Since the shear wave speed (m/s), c_s, is related to Young's modulus (E) (kPa) by the equation, $E = 3c_s^2$ (Shiina et al., 2015), the shear wave speed can be used to estimate the tissue's elasticity (Young's modulus) (Kantarci et al., 2014). Studies comparing median nerve stiffness of CTS individuals to healthy controls consistently report greater median nerve stiffness in patients with CTS (Kantarci et al., 2014; Martin & Cartwright, 2017; Orman et al., 2013; Tatar et al., 2016; Yoshii et al., 2017). However, these studies have mainly used quasi-static US elastography (Ghajarzadeh et al., 2015; Liao et al., 2015; Martin et al., 2017; Ogur et al., 2015; Orman

et al., 2013; Tatar et al., 2016; Xin et al., 2017; Yoshii et al., 2017a, 2017b) and less have

used dynamic methods (Arslan et al., 2018; Bortolotto et al., 2017; Kantarci et al., 2014;

Lee et al., 2019; Shen et al., 2013; Wang et al., 2012; Zhang et al., 2017). A study using

SWE reports the elasticity of the median nerve in CTS individuals at 66.7 ± 26.5 kPa,

and 32.0 ± 8.4 kPa in healthy controls (Kantarci et al., 2014). Another study

investigating median nerve stiffness via ARFI elastography report mean shear wave

speeds of 3.64 ± 0.53 m/s, 4.01 ± 0.69 m/s, and 5.06 ± 0.57 m/s in CTS patients with

mild, moderate, and severe CTS respectively, and 2.97 m/s ± 0.41 in healthy controls

(Arslan et al., 2018). However, stiffness of other carpal tunnel tissues such as finger

flexor tendons has not been well investigated even though stiffness of the finger flexor

tendons may increase due to fibrosis of the adjacent SSCT. One investigation that

measured FDS and FDP tendon stiffness in the carpal tunnel on healthy individuals

reported stiffnesses of 2.9 ± 0.2 m/s and 3.2 ± 0.3 m/s for the FDS and FDP, respectively.

Although tendon stiffness can be quantified through shear wave elastography, dynamic

elastography techniques for measuring finger flexor tendon stiffness have only been

validated in cadaveric specimens (Kubo et al., 2017) and in canine Achilles tendon

(Wang et al., 2012).

1.3 Thesis overview

       It is difficult to determine the exact etiology of CTS due to its multifaceted nature

and influence of many internal and external risk factors. However, it is evident from the

literature that vascular factors play a considerable role in the development and

progression of the condition. Additionally, it is clear that the SSCT is an important structure within the carpal tunnel, providing the link between the external environment and the nerve. Exposure to external occupational risk factor such as excessive force, highly repetitive motion, and non-neutral wrist postures, influence internal structures and lead to functional and mechanical changes. Although many of these aspects that may influence CTS development and progression have been investigated individually, it is necessary to investigate how all of these aspects influence each other given the multifaceted nature of the condition. The purpose of this thesis is therefore to improve our understanding of the vascular component to the development and progression to CTS. To achieve this, I have completed a series of three studies aimed at investigating the relationship between blood flow and changes to carpal tunnel tissue function and structure. While the effects of ischemia on median nerve conductivity are well documented, the relationship between local ischemia and the ensuing edema on nerve blood flow and function, and the effects on the other carpal tunnel tissues are less known. Ultrasound allows for non-invasive investigation of intraneural blood flow, and ultrasound elastography provides a new opportunity for quantifying tissue stiffness in-vivo, providing additional information on the structural changes of carpal tunnel tissues. Thus, the purpose of study one was to investigate intraneural blood flow, tendon and SSCT displacement and relative motion in individuals with varying severities of CTS, and to determine the relationship between intraneural blood flow and tendon-SSCT mechanics. Our secondary purpose of study one was to assess the reliability of median nerve CSA measurement to distinguish between CTS severities. My hypotheses for study

one were that intraneural blood flow and tendon-SSCT mechanics would be dependent on severity in clinically diagnosed CTS patients. Study two built off of study one and investigated the predictive ability of ultrasound measures in predicting 6-month follow-up in patients. The aim was to test our hypothesis that intraneural blood flow and tendon mechanics evaluated through ultrasound can predict 6-month disease progression in patients given that changes in intraneural blood flow and tendon mechanics may be early indicators of disease progression. Finally, study three investigated the effects of 30 minutes of blood flow occlusion on median nerve edema, intraneural blood flow, nerve conduction, tissue stiffness and tendon-SSCT mechanics. This study investigated the temporal effects of ischemia and edema and clarified the role of local blood flow on CTS development. This final study allowed me to investigate the role of blood flow occlusion on carpal tunnel tissues, and to compare the observed changes under this condition to what I observed in my clinical populations from study one and two. In this final study, I hypothesized that 30 minutes of partial ischemia via sub-diastolic blood pressure occlusion would result in a number of morphological, functional and mechanical changes in the median nerve, tendons, and SSCT of the carpal tunnel.

Chapter 2: Blood Flow Velocity but Not Tendon Mechanics Relates to Nerve

Function in Carpal Tunnel Syndrome Patients

Amanda Farias Zuniga[1], Amer A. Ghavanini[2,3,4], Gaspar Israelian[3,4], Peter J. Keir[1]

[1]*Department of Kinesiology, McMaster University, Hamilton, Ontario, Canada*
[2]*Canadian Neurologic Center, Mississauga, ON, Canada*
[3]*Department of Medicine, Division of Neurology, University of Toronto, Toronto, ON, Canada*
[4]*Division of Neurology, Trillium Health Partners*

2.1 Abstract

Carpal tunnel syndrome (CTS) develops from chronic compression of the median nerve. Chronic compression results in a number of vascular, structural and functional changes to the carpal tunnel tissues which ultimately manifest in the characteristic symptoms of CTS. The purpose of this study was to investigate the interplay of median nerve function, median nerve hemodynamics, and finger flexor tendon and subsynovial connective tissue (SSCT) mechanics in CTS patients. Thirty-five patients were recruited following nerve conduction study for this double-blinded imaging study. Ultrasound B-mode, pulse-wave Doppler, and colour Doppler images and videos were collected at the proximal carpal tunnel to quantify: (1) median nerve cross-sectional area, (2) intraneural blood flow velocity in 3 wrist postures (neutral (0°), flexion (15°), extension (30°)), and (3) flexor digitorum superficialis and SSCT displacement. Results demonstrate that intraneural blood flow velocity is dependent on median nerve function and wrist posture such that patients with mild CTS are more susceptible to the effects of non-neutral wrist postures. Tendon-SSCT mechanics do not appear to differ based on severity. This study stresses the importance of limiting exposure to non-neutral wrist postures in patients with early signs of the condition.

Key Words: Carpal tunnel syndrome; Nerve conduction studies; Ultrasound; Subsynovial connective tissue; Intraneural blood flow; Median nerve

2.2 Introduction

Carpal tunnel syndrome (CTS) is the most common peripheral neuropathy which results from chronic compression of the median nerve. The confined space of the tunnel makes the tissues within susceptible to compression with the resulting damage leading to altered function and mechanics. Median nerve compression is aggravated by non-neutral wrist postures, often cited as risk factors in CTS [1-6]. Functional changes in the median nerve are often quantified through nerve conduction studies (NCS), which aim to assess the extent of nerve damage by determining conduction velocity, amplitude, and latency of nerve impulses [7,8]. Accordingly, NCS is used to diagnose and classify the severity of CTS [8]. However, it has been recommended that improved CTS detection is needed, especially for symptomatic individuals with negative NCS findings [9]. Several studies have demonstrated increased diagnostic value when combining NCS with ultrasonographic measures, such as measures of median nerve size [9–13] and nerve blood flow [14–17].

Chronically elevated pressure in the carpal tunnel compresses the median nerve and compromises blood flow. High pressure collapses capillaries within the sub-synovial connective tissue (SSCT) [2], which supply blood to the extraneural layer of the nerve and between individual nerve fibres within the median nerve itself (intraneural). Ultimately, compression leads to nerve hypervascularization, which includes increased size and number of blood vessels [18], and/or edema (swelling) that can be quantified through median nerve cross-sectional area (CSA) and intraneural blood flow velocity. Increased median nerve CSA is considered a sign of nerve swelling [11,19] and is

consistently reported to be larger in CTS patients compared to healthy controls

[9,11,19,20]. Intraneural blood flow velocity has been reported to be elevated in

individuals with symptoms of CTS but not diagnosed through NCS [16,21] suggesting

that early signs of CTS may result from altered hemodynamics [15,16]. However, there

appears to be an overall negative relationship between median nerve blood flow velocity

and CTS severity in diagnosed patients, whereby CTS symptomatic and mild cases have

higher blood flow velocities than moderate or severe cases [15]. Non-neutral wrist

postures amplify these effects as non-neutral wrist postures significantly alter intraneural

blood flow velocity in symptomatic individuals depending on wrist posture [21].

Increased carpal tunnel pressure (CTP) also results in impaired mechanics of the

finger flexor tendons occupying the carpal tunnel. The SSCT not only provides a

network for blood and lymphatic vessels, but also reduces gliding resistance between

tendons and the nerve allowing for smooth finger motion [22]. The interconnecting

collagen fibres of the SSCT can be damaged through differential motions between itself

and the tendon, resulting in injury through shear strain. Cumulative shear strain between

finger tendons and the SSCT is postulated as a precursor to CTS development [23,24].

Wrists of CTS-diagnosed individuals show increased fibrosis of the SSCT [25], and CTS-

symptomatic individuals have greater shear strain, as seen by the shear strain index (SSI)

and maximum velocity of the SSCT relative to the tendon, than asymptomatic individuals

[26]. Repetitive finger use is also observed to increase shear strain between the flexor

tendon and SSCT in healthy individuals [27] and CTS patients [28], which may be

exacerbated by non-neutral wrist postures [24]. Tendon mechanics may also be affected

by vascular changes resulting from external compression [29,30], further affirming the role of blood flow on CTS.

Although tendon-connective tissue mechanics and median nerve blood flow have been reported to be altered in clinical populations, the relationship between tendon-SSCT mechanics, intraneural blood flow and CTS severity has not previously been investigated. The relationship between each of these factors have been studied individually, but there is limited knowledge on how hemodynamics, tendon mechanics and CTS severity intersect in CTS patients. A recent study [31] found a linear relationship between intraneural and SSCT blood flow in CTS patients using contrast-enhanced ultrasound. It follows that the median nerve and SSCT are closely linked through their blood supply. There are few studies investigating intraneural blood flow velocity [15,16,21,32,33] and only two investigations to date quantified the relationship between nerve conduction (i.e. clinical severity) and blood flow [14,15]. Furthermore, the effect of non-neutral wrist postures on intraneural blood flow in CTS individuals has not been investigated, although the effect of wrist posture on intraneural blood flow velocity of CTS-symptomatic individuals appears to differ from healthy individuals [21]. The purpose of this study was to quantify median nerve blood flow velocity and tendon mechanics in a clinically diagnosed CTS population with varying severities. A secondary purpose was to quantify median nerve CSA in CTS patients and assess the reliability of median nerve CSA measurement to distinguish between severities. We hypothesized that intraneural blood flow and tendon-SSCT mechanics in CTS patients would be dependent on severity such that intraneural blood flow velocity will follow a negative relationship with CTS severity, and that greater

relative displacement between finger flexor tendon and SSCT will be seen in more severe patients.

2.3 Materials and Methods

This study was double-blinded whereby the data collector and data analyst were blinded to participants' CTS severity. Participants underwent three experimental imaging tests to: (1) to quantify median nerve cross-sectional area (CSA), (2) assess median nerve blood flow velocity in three wrist postures (15° flexion, neutral (0°), 30° extension), and (3) record finger flexor tendon and SSCT motion during a repetitive finger flexion task.

2.3.1 Participants

Symptomatic patients were referred from two neurology clinics following previous referral from their general practitioner and history, neurological examination and electrodiagnostic testing further confirming CTS. Enrolment was offered to consecutive patients, but study participation was voluntary. Exclusion criteria included previous wrist surgery, radial malunion, colles fracture, bifid median nerve, persistent median artery, degenerative joint disease, arthritis of the wrist/hand, hemodialysis, sarcoidosis, and amyloidosis. Patients with hypothyroidism and diabetes mellitus managed through medication were included. Patients of all levels of CTS severity were recruited, with the lead investigator blinded to patient diagnosed severity until completion of data analysis. All data collection was completed in clinic during the fall of 2017. The Hamilton

Integrated Research Ethics Board approved this study and all participants provided informed written consent.

2.3.2 Protocol

2.3.2.1 Nerve Conduction Study

NCS were performed according to the American Association of Electrodiagnostic Medicine guidelines and completed by a Registered EMG Technologist. During the studies, limb temperatures were monitored and warmed if necessary to maintain a temperature of greater than 32 degrees centigrade. Motor NCS were performed in an orthodromic fashion. Sensory studies were performed antidromically and orthodromically. Needle EMG was performed with a disposable monopolar needle. Needle EMG localization was based on [34] and NCS techniques were based on [35]. EMG and NCS excluded other types of peripheral neuromuscular disorders and confirmed median neuropathy at the wrist and thus the diagnosis of carpal tunnel syndrome. Median motor studies were recorded over the motor point of abductor policic brevis (APB). Distal stimulation was performed at 70 mm distance to the motor point measured on a curve line connecting the motor point to mid-volar wrist proximal to the crease of the wrist. Normal distal amplitude of ≥ 6.7 mV and normal distal onset latency of ≤ 4.2 ms were used for median motor studies. Median to digit 2 sensory studies were performed with tab electrodes for recording and with stimulation point at a distance typically 130 mm from the G1 recording electrode. Conduction velocity was calculated by dividing the recording distance over the distal onset latency. Normal distal amplitude

of ≥ 10 µV and normal conduction velocity of ≥ 50 m/sec were used for median to digit 2

sensory studies. For mixed nerve comparison studies, a standard and equal distance of 80

mm was used for both median and ulnar studies with recording over the volar forearm

and stimulation at the palm. Relative delay between the two responses was calculated

based on the latency to peak. A relative delay of ≥ 0.4 ms was considered abnormal.

Rating of severity was based on Bland [8]. Where the motor and sensory responses did

not fit with this severity scale, severity was rated based on the sensory response alone.

2.3.2.2 Ultrasound assessment

Following NCS, patients underwent ultrasound assessment of the carpal tunnel.

During ultrasound image acquisition, participants sat comfortably with their affected hand

supinated and resting in a custom 3D printed splint (Figure 2.1). For patients with

bilateral CTS, the hand with the more severe case was imaged. The custom splint

allowed for standardized wrist and hand postures via a built-in protractor. A Velcro strap

was used to secure the fingers and prevent movement and movement associated muscle

activation during data collection. Sonographic images and videos of the carpal tunnel

area were captured using a high frequency linear array transducer (12L-RS) and

ultrasound system (Vivid Q BT10, GE Healthcare, Milwaukee, WI) optimized to

previously determined settings for each experimental test [21, 27]. A gel standoff wedge

(Aquaflex gel pad, Cone Instruments, Solon, OH) was used between the skin surface and

ultrasound probe in both tasks to allow for image optimization. All ultrasound

assessments and subsequent analysis of images and videos were performed by the same

experimenter who was blinded to each patients' NCS result until the completion of all

data analysis.
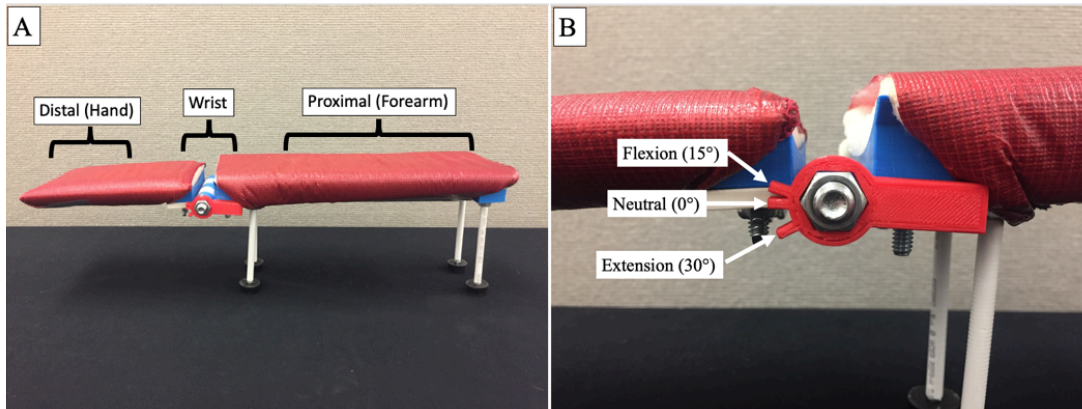
Figure 2. 1: Custom built 3D printed hand and wrist splint (A) with build in protractor (B) used during ultrasound image acquisition. Using the built in protractor, the wrist was positioned into three defined wrist postures, neutral (0°), flexion (15°), and extension (30°).

2.3.3 Sonographic Measurements

2.3.3.1 Median Nerve CSA

Transverse B-mode images of the median nerve were taken on the palmar surface at the carpal tunnel inlet to determine median nerve CSA. The carpal tunnel inlet, at the level of the pisiform, was chosen as it provides the most reliable measurements [36] (Figure 2.2). Two B-mode images were taken at the level of the distal wrist crease in a neutral wrist posture (0°), with the fingers relaxed and semi-flexed.

Greyscale transverse B-mode images were uploaded to ImageJ software (National Institutes of Health, Bethesda, MD) to measure median nerve CSA. Both tracing and ellipse method were used to measure median nerve CSA. In the tracing method, electronic calipers were used to outline the internal rim of the nerve. The ellipse tool was

used to fit an ellipse in the interior rim of the nerve. Values were rounded to the nearest

0.01 mm^2 for both methods. CSA values were averaged from the two images per

participant and used for subsequent analysis.
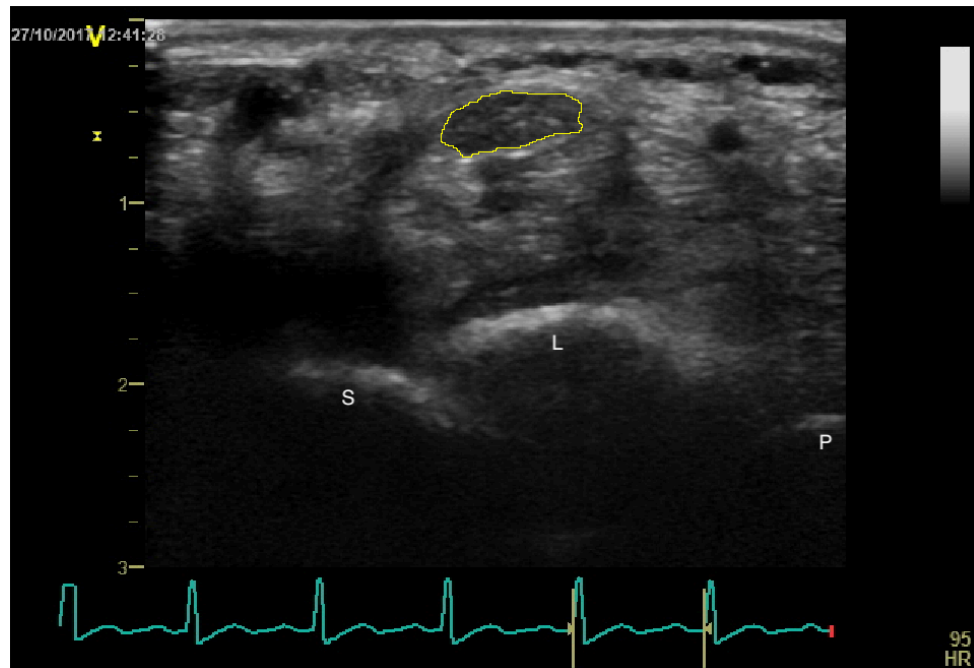
Figure 2. 2: The carpal tunnel inlet is delineated by bony landmarks including the
pisiform (P), lunate (L), and scaphoid (S) bones.

2.3.3.2 Intraneural Blood Flow Velocity

Intraneural blood flow velocity was measured in three wrist postures (15° flexion,

neutral (0°), 30° extension) using pulse wave (PW) Doppler ultrasound in the longitudinal

plane at the proximal wrist crease. PW Doppler videos were acquired according to

established practices [21]. Axial B-mode images allowed for locating the median nerve at

the level of the pisiform and were used to orient the transducer longitudinally. Patients

then rested in each posture to provide steady state values before initiating ultrasonography

collection. Steady state was determined and verified as a consistent velocity signal over a five-second interval. Colour Doppler was used prior to the PW Doppler as a qualitative measure of blood flow. When the colour map was present for the median nerve, the location of greatest colour scale intensity was used to position the 1 mm PW Doppler gate, marking the location of highest blood flow in the median nerve. If the direction of flow was determined from the colour map, a 20° beam steer angle and angle correction factor of 60° was applied. However, if the colour map was not present on the median nerve, the PW Doppler gate was positioned over the median nerve until a signal was obtained and no steer angle or angle correction was used. A wall filter/ low velocity reject of 0.3 cm/s was used, with a colour/ PW frequency of 5 MHz, and a pulse repetition frequency of 0.8 kHz. A 2.5 mm gel standoff wedge was used for image optimization[21]. Two 12 second PW Doppler videos were collected per posture.

High resolution AVI video files were uploaded to MAUI analysis software (Hedgehog Medical Inc., Waterloo, ON) to measure intraneural blood flow velocity. Using MAUI, a pixel-to-scale ratio was first set using the scale on the left hand side of each PW Doppler video. The spectral signal of each PW Doppler velocity trace was analyzed on a frame-by-frame basis and outputted as a CSV file. Peak blood flow velocity (cm/s) was calculated from the CSV file by averaging the peak blood flow values within a 5-second window. Analysis was conducted on two ultrasound videos per posture, and then averaged to result in one mean peak blood flow velocity value per posture for each participant (Figure 2.3).
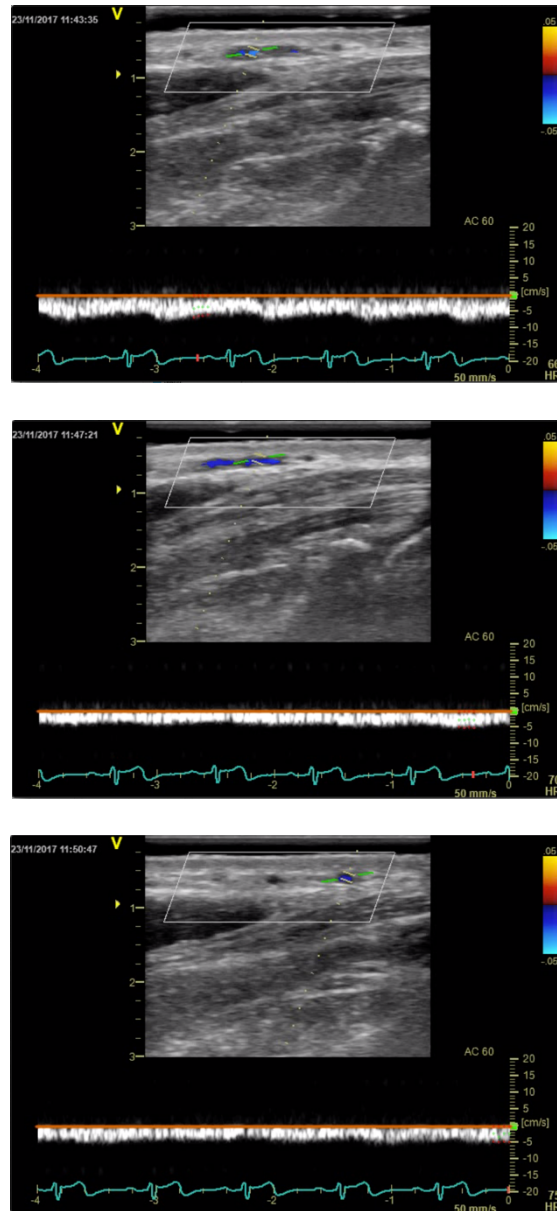
Figure 2. 3: Still images from pulse-wave (PW) Doppler videos from the same patient with their wrist in neutral posture (0°) (top panel), extension (30°) (middle panel), and flexion (15°) (bottom panel). Colour Doppler was first used as a qualitative check of the detection of intraneural blood flow. If a colour map was detected, the 1 mm PW Doppler gate was placed over the area of greatest colour intensity (yellow linear markers). Once this location was determined, a 20° beam steer angle was applied and an angle correction factor of 60° was also applied. Five seconds of consistent blood flow velocity signal was required for measurement. Heart rate (HR) was also collected throughout the protocol (bottom blue trace).

2.3.3.3 Tendon-SSCT motion

Tendon-SSCT motion was recorded through colour Doppler ultrasound videos of the third digit flexor digitorum superficialis (FDS) tendon and its adjacent SSCT. Participants performed 2 sets of 10 repetitions of middle finger flexion-extension with their wrist in a neutral (0°) posture.   Colour Doppler imaging in the longitudinal plane was used while recording tendon movement during the repetitive finger flexion-extension cycles. The ultrasound probe was placed at the proximal wrist crease and electronically steered to 20°, with an aqueous gel standoff wedge to optimize the insonation angle to approximately 60° [26]. Custom handgrips and Velcro straps allowed for isolated middle finger flexion-extension. The FDS tendon and the adjacent SSCT of the third digit were identified through ultrasound with settings adjusted to optimize image quality [26]. This protocol is similar to that previously used [26, 27]. Patients were instructed to perform the task through full range of motion with each repetition. An audible metronome was set to a movement speed of 0.75 Hz and played throughout the trial.

Tendon-connective tissue motion analysis was performed using EchoPac analysis software (General Electric Healthcare, Milwaukee, WI) using methods previously validated in cadaveric specimens [37] and applied to healthy [27] and CTS symptomatic [26] populations. Velocities were obtained by placing three markers collinearly over each tissue (tendon, SSCT). Tissue motion was tracked throughout the entirety of the trial on a frame-by-frame basis. The three velocity traces for each tissue were imported into a custom Matlab program, and were averaged to one representative tissue velocity trace per tissue. This velocity signal was low-pass filtered (4 Hz, 2nd order Butterworth) and

corrected for the angle of insonation (cos θ). Peak tissue displacement was calculated for

each tissue (FDS tendon, SSCT). Peak relative tissue displacements between tendon-

connective tissue displacement were calculated on a point-by-point basis. Shear Strain

Index (SSI) was also calculated [27]. Averages were calculated between the two

ultrasound videos collected and used for subsequent statistical analysis.
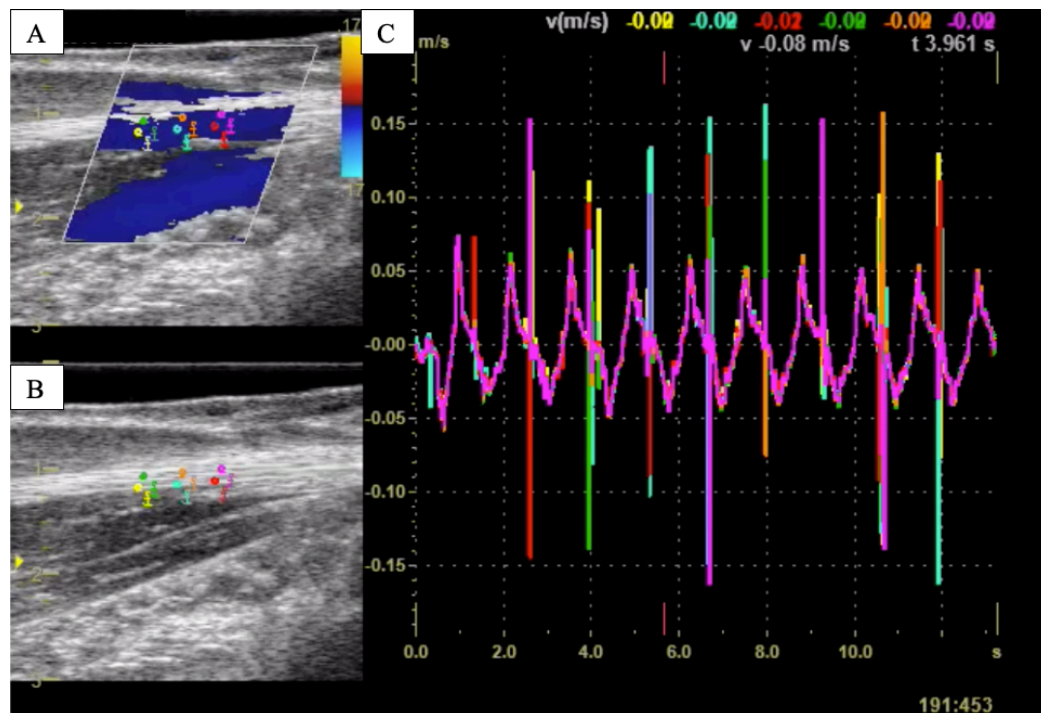
Figure 2. 4: B-mode images with (A) and without (B) colour Doppler map overlay were
used to identify each tissue of interest and place circular regions of interest. B-mode
ultrasound images (A&B) of the flexor digitorum superficialis (FDS) tendon and its
adjacent subsynovial connective tissue (SSCT), and the corresponding velocity traces (C)
as each tissue went through repetitive cycles of flexion and extension. B-mode images
with colour maps (B) were used to determine direction (red = extension, blue = flexion)
and magnitude. Corresponding velocity traces of each region of interest (C) were
obtained through post-processing.

2.3.4 Statistical analysis

Following data analysis, the lead investigator was unblinded to patient CTS severity. Participants were sorted into three severity groups (mild, moderate, severe) defined by the neurologists following standardized guidelines (mild: sensory conduction velocity from index finger to wrist < 40 m/s, motor latency from wrist to abductor pollicis brevis < 4.3 ms; moderate: motor latency 4.3 - 6.5 ms with preserved index finger sensory nerve action potential; severe: motor latency 4.3 - 6.5 ms with absent sensory nerve action potential or motor latency > 6.5 ms) [8]. NCS results including motor and sensory latency (ms), amplitude (mV/μV), and conduction velocity (m/s) were collected from the clinics.

Descriptive statistics (group means and standard deviations (SD)) were calculated for all measures. Normality of all data was assessed using Q-Q plots in R (version 3.5.1) and R Studio (version 1.1.463, Boston, MA; ggPlot function in the "car" package). Confidence bands were constructed on a pointwise basis based on a normal distribution with a 95% confidence interval. All data was required to be centered around the reference line and fall within the confidence bands to satisfy normality. Due to absence of sensory nerve conduction measures in severe cases of CTS, sensory measures from the NCS were not analyzed further. To assess reliability, Intraclass Correlation Coefficient (ICC) and Standard Error of Measurement (SEM) estimates were computed on median nerve CSA values across images (Image 1 vs. Image 2) and between measurement methods (Ellipse vs. Tracing) using a 2-way mixed-effects model. A one-way ANOVA was performed to analyze differences in nerve measures (median nerve motor latency,

motor amplitude, motor nerve conduction velocity, and median nerve CSA) between severity groups. Tukey's HSD post-hoc test was performed to reveal statistically significant differences. In a separate analysis, severity was treated as a continuous variable using motor nerve latency values and a linear regression was performed to predict tendon-SSCT mechanics (peak FDS displacement, peak SSCT displacement, peak relative displacement, SSI) based on motor latency. Outliers were removed and not included in the analysis. These analyses were performed in R (version 3.5.1) and R Studio (version 1.1.463, Boston, MA). Median nerve blood flow velocity was not detected in all patients, nor in all postures for all patients. A total of 3 patients were excluded from the analysis due to not measurable blood flow velocity. In 4 patients, blood flow velocity was not measurable in at least 2 out of 3 postures tested. To allow us to include these 4 patients in our analysis to assess the effects of posture and severity on intraneural blood flow, a random intercept mixed-effects model was performed on peak blood flow velocity as the dependent variable, and posture (15° flexion, neutral (0°), 30° extension), motor latency, and the interaction between posture and motor latency as independent variables (StataIC 14, College Station, TX). Significance was set at $p < .05$.

2.4. Results

2.4.1 Participants

Study participant characteristics are shown in Table 2.1. There were more females (n = 27) than males (n = 8), with females younger (56.6 ± 12.1 years) than males (62.7 ± 8.0 years). More right wrists (n = 21) than left (n = 14) were imaged.

Table 2. 1: Participant characteristics by sex and severity group (n = 35).

	Total	Severity		
		Mild	Moderate	Severe
N	35	13	14	8
Female	27	9	12	6
Male	8	4	2	2
Age (years)	57.7 ± 11.6	56.4 ± 9.1	58.5 ± 14.3	58.3 ± 10.7
Female	56.6 ± 12.1	54.2 ± 8.2	58.7 ± 15.3	56.2 ± 11.1
Male	62.7 ± 8.0	66.0 ± 8.5	57.5 ± 9.2	64.5 ± 9.2

2.4.2 Nerve Conduction Study

NCS results, both motor and sensory, are reported in Table 2 although statistical analysis was only performed on motor responses. Motor latency was statistically different between severity classifications ($F_{(2, 32)} = 29.21$, $p < .001$) with all groups being significantly different and the severe group having the longest latency followed by moderate and mild (mild vs. moderate: $p < .001$; mild vs. severe: $p < .001$; moderate vs. severe: $p = .027$; Table 2). Motor nerve amplitude was significantly different between severity classifications ($F_{(2, 32)} = 3.87$, $p = .031$). Post-hoc tests revealed motor amplitude was statistically greater in mild than the severe group ($p = .024$) but not between mild and moderate ($p = .362$) or moderate and severe ($p = .255$) groups (Table 2). Conduction velocity was statistically significant between severity classifications (F

(2, 23) = 6.31, p < .01). Post-hoc analysis revealed the difference was specifically

between mild and severe (p < .01), but not between mild and moderate (p = .061) or

moderate and severe (p = .512) groups (Table 2.2). In light of these results, motor latency

was used in subsequent analysis of intraneural blood flow and tendon mechanics since it

distinguished between groups.

Table 2. 2: Nerve conduction study (NCS) results for motor and sensory latency, amplitude, and conduction velocity (CV) summarized across severity groups (mean ± standard deviation). *Statistical difference between groups in column. A dagger (†) denotes that the moderate and severe groups contained 3 participants who did not exhibit detectable sensory responses. NR denotes that this measure was not recorded.

Severity	Motor			Sensory		
	Latency (ms)	Amplitude (µV)	CV (m/s)	Latency (ms)	Amplitude (µV)	CV (m/s)
Mild (n=13)	3.83 ± 0.37*	9.70 ± 1.85*	56.87 ± 3.99*	3.48 ± 0.58	24.41 ± 18	31.68 ± 22.36
Moderate (n=14/11†)	5.24 ± 0.73*	8.73 ± 1.85	52.83 ± 3.40	4.31 ± 1.99†	18.67 ± 14.70†	30.54 ± 19.04†
Severe (n=8/5†)	6.08 ± 0.96*	7.43 ± 1.72*	50.90 ± 3.18*	4.82 ± 2.54†	4.54 ± 2.50†	NR

2.4.3 Median nerve Cross-Sectional Area

ICC and SEM estimates demonstrated good to excellent reliability between images (Image 1, Image 2) and methods (Ellipse, Tracing). The Ellipse method for CSA demonstrated excellent reliability (ICC [95% CI] = 0.914 [0.836, 0.956]) and low measurement error (SEM = 1.27 mm^2) while the reliability of the Tracing method was good (ICC [95% CI] = 0.887 [0.787. 0.942]), with slightly higher measurement error (SEM = 1.66 mm^2). Reliability between the two methods was excellent (ICC [95% CI] = 0.939[0.753, 0.978]) and demonstrated low measurement error (SEM = 1.12 mm^2). In light of the reliability results, CSA values obtained from the Ellipse method were used in further analyses.

Median nerve CSA at the distal wrist crease were statistically different between severity classifications (F(2,31) = 12.898, p < .001). Post-hocs revealed that median nerve CSA was statistically greater in severe (15.9 $\pm$ 5.0 mm^2) versus mild (8.8 $\pm$ 2.2 mm^2) and moderate (10.1 $\pm$ 2.7 mm^2) groups (both p < .001), but not between mild and moderate groups (p = .541) (Figure 2.5).
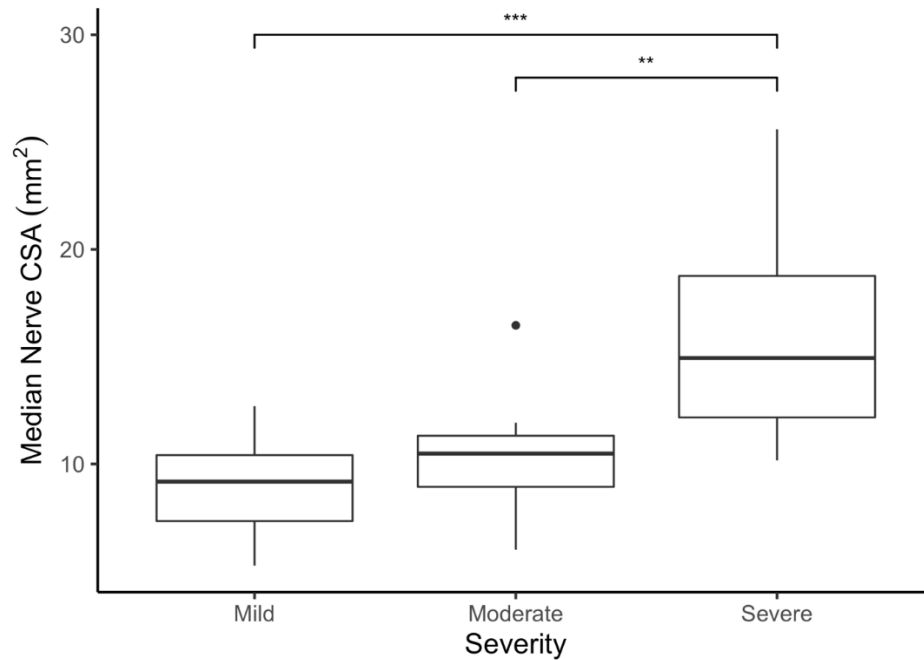
Figure 2. 5: Boxplot of median nerve cross-sectional area (CSA) (mm^2) by severity classification (mild (n = 13), moderate (n = 13), severe (n = 8)). The median (center line), 25th and 75th percentile (horizontal lines of the box) and range (lines extending above and below) are represented. Outlier represented by the black dot. Median nerve CSA differed significantly between mild and severe (p < .001 "***") and between moderate and severe patients (p < .001 "**").

2.4.4 Tissue Displacement

Peak FDS, peak SSCT, relative displacement, and SSI were not significantly associated with motor latency (peak FDS: $R^2 = 0.048$, p = .25; peak SSCT: $R^2 = 0.067$, p = .17; peak relative displacement: $R^2 = 0.$ 002, p = .83; SSI: $R^2 = 0.031$, p = .36), indicating that motor latency did not predict tissue motion (Figure 2.6).
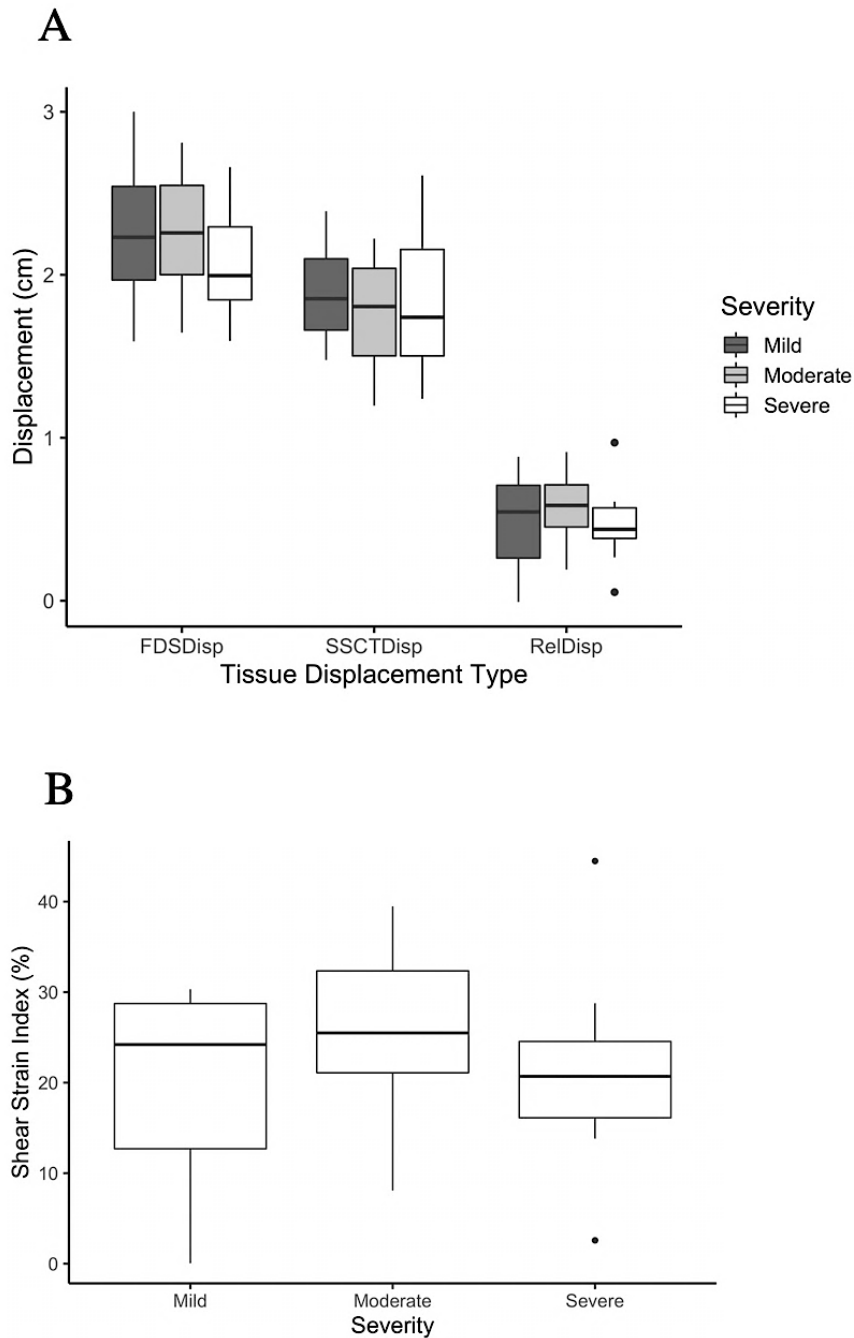
Figure 2. 6: (A) Peak tissue displacement (cm) for FDS, SSCT, and relative FDS-SSCT displacement grouped by motor latency classification. (B) Shear strain index (SSI) by severity group (mild, moderate, severe). Median (center line), 25th and 75th percentile (horizontal lines of the box) and range (bars extending above and below) represented. Outliers are represented by black dots. There were no significant differences between severity groups for any measure of tissue displacement.

2.4.5 Blood Flow Velocity

Intraneural blood flow velocity was detected in 83-86% of participants depending on wrist posture. The overall random intercept mixed effects model approached significance ($p = .0541$), but revealed a significant interaction between posture and motor latency ($p = .023$) in predicting peak blood flow velocity. It was identified that peak blood flow velocities were significantly higher in both non-neutral postures, 15° flexion (2.77 cm/s ± 1.69) ($p = .025$) and 30° extension (2.82 cm/s ± 2.12) ($p = .012$), vs. neutral posture (2.38 cm/s ± 2.07), only at low motor latencies (3-4.5 ms) (Figure 7). There were no differences between 15° flexion vs. 30° extension ($p = .780$).
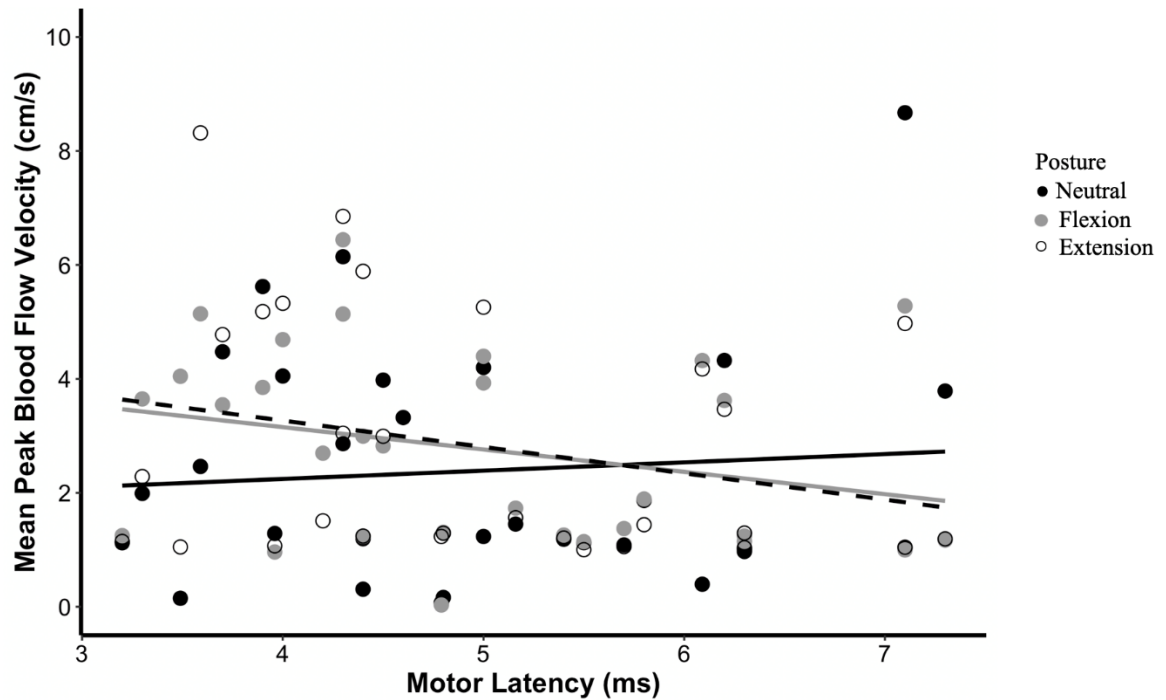
Figure 2. 7: Peak blood flow velocity (cm/s) by posture (30° extension, neutral (0°), and 15° flexion) and motor latency. Participant (individual dots) and overall model fit lines are represented. There was a significant interaction effect on peak blood flow velocity between posture and motor latency, with neutral postures significantly different than deviated postures (flexion and extension) when motor latencies were between 3-4.5 ms, corresponding to mild CTS based on classification from [8].

2.5 Discussion

The purpose of this study was to quantify intraneural blood flow and FDS-SSCT

mechanics in CTS patients with differing clinically diagnosed severities. To fulfill this

purpose, we examined median nerve blood flow, median nerve size, and tendon

mechanics in relation to nerve function in a single patient visit. Our results demonstrate

interrelationships between median nerve hemodynamics and median nerve function. We

found that peak blood flow velocity is significantly higher in non-neutral wrist postures

for patients with mild CTS and that median nerve CSA is significantly larger in severe

CTS patients than those with mild or moderate CTS. Tendon and SSCT mechanics do

not appear to differ based on severity. Our investigation revealed the advantage of using ultrasound measures to identify patients who are susceptible to the effects of non-neutral wrist postures.

Our results indicate that ultrasound measurement of median nerve CSA may distinguish between CTS severities, specifically between mild and severe, and moderate and severe patients. Ultrasound measured median nerve CSA may assist in diagnosing CTS since studies consistently report that median nerve CSA is larger in patients versus control subjects [9,11,19,20,38], and generally becomes larger with increasing severity due to swelling and edema within the nerve [9,14,39,40]. Our results also demonstrate that both ellipse and tracing methods demonstrated good to excellent reliability of median nerve CSA, suggesting that nerve CSA measurements are consistent and reliable regardless of the method chosen, so long as they are done by the same person. This is consistent with reports in sciatic nerve [41] and median nerve in CTS patients [39]. The ellipse method provided slightly more reliable measures of median nerve CSA in our study compared to the tracing method. Overall, ultrasound measured median nerve CSA appears to be a reliable diagnostic tool for CTS.

Tendon-SSCT mechanics did not differ with CTS severity in our sample suggesting that FDS-SSCT mechanics are independent of nerve function and cannot discriminate between patients with differing motor nerve function. Studies investigating tendon-connective tissue mechanics in CTS patients are limited, and this study relates tendon-SSCT motion to median nerve function, specifically motor latency. Patients demonstrated higher SSI than controls performing repetitive finger flexion-extension

motions determined through ultrasound speckle-tracking [28]. Greater SSI has also been

reported in a small sample of CTS symptomatic individuals using Colour Doppler

ultrasound [26]. Our results demonstrated no detectable differences based on median

nerve motor function despite our range of SSI values falling within the reported range for

confirmed patients [28] and symptomatic individuals [26], although there was greater

variability and a larger range of SSI values in this sample. Shear strain between finger

tendons and the SSCT has been suggested as a precursor to CTS development [23,24].

We postulate that we observed no difference in tendon-SSCT mechanics because patients

with clinically diagnosed CTS demonstrate similar tendon-SSCT mechanics regardless of

severity. This suggests that absolute motion of the FDS and SSCT, as well as relative

tendon-SSCT motion, may reach a threshold, and thus may not increase with worsening

of the condition.

The effects of non-neutral wrist posture on median nerve blood flow velocity

appear to be dependent on nerve function, suggesting that median nerve hemodynamics

are closely related to changes due to chronic compression. We found that patients with

motor latency <4.5 ms, classified as having mild CTS [8], were more sensitive to the

effects of non-neutral wrist postures. The intraneural blood flow velocity and median

nerve CSA results from the current study suggest that these nerve hemodynamic

responses are likely due to nerve edema resulting from chronic nerve compression.

Edema develops easily in the intra-and extrafascicular space of nerve, and once present,

cannot be easily drained due to a lack of lymphatic vessels and the presence of the

perineurium barrier [5]. As such, the effects of compression induced edema persist

within the nerve and result in the neurological changes observed in CTS patients [9, 15]. Intraneural blood flow velocity measured at the carpal tunnel inlet has been reported to be elevated in individuals with symptoms of CTS [16,21] suggesting that early signs of CTS may result from altered hemodynamics [15,16]. In a study of CTS patients with various severity, intraneural blood flow velocity was highest in symptomatic individuals who were not confirmed to have CTS through NCS, and decreased as CTS severity increased suggesting that intraneural blood flow is compromised or blocked in more advanced stages [15]. Similar interpretation was reported by El Miedany et al. [14] using Power Doppler ultrasound where an inverse relationship was observed between the Power Doppler signal and NCS classified severity. Our results not only demonstrate that intraneural blood flow velocity decreases with increasing median nerve motor latency, but it demonstrates the relationship between intraneural blood flow, median nerve function and wrist posture. We believe that our results reflect two phenomena. Firstly, in mild patients, the decrease in intraneural blood flow velocity with increasing severity could be a result of increased CTP via edema in the nerve leading to restriction of median nerve blood flow. It has been previously shown that the capillaries contained within the SSCT carrying the blood supply to the median nerve can collapse with increasing pressure [1]. Our results suggest that non-neutral wrist postures further restrict median nerve blood flow. Patients with motor latency <4.5 ms, indicating mild cases, had larger intraneural blood flow velocity in response to non-neutral wrist postures compared to patients who had moderate to severe CTS. We hypothesize that this indicates that non-neutral wrist postures impinge the nerve, and an increase in blood flow is elicited as a response to aid

in repair of the area. Secondly, since this response was not observed in patients with moderate to severe CTS, we believe this reflects significant nerve damage and the absence of the response since an increase in intraneural blood flow would no longer repair the tissue.

It is worth noting that intraneural blood flow velocity was not detectable in approximately 15% of our patients in any given wrist posture. Detection rates of median nerve blood flow using spectral Doppler ultrasound is reported to be approximately 58% in patients [15], and approximately 97% in patients with "highly-likely CTS" [16]. The detection rate achieved in this investigation is closer to that reported by Joy et al., 2011 [16]. Technological differences such as probe frequency can impact detection of low median nerve intraneural blood flow velocities. Differences in methods and cut-off values used for NCS and CTS classification can influence the diagnostic outcome of patients, thus making discussion of underlying neurophysiology between study populations challenging. In this study, NCS test guidelines from the American Association of Electrodiagnostic Medicine [42] and Preston & Shapiro [35] were followed, and Bland [8] was used for CTS classification. In contrast, Evans et al. [15] followed guidelines from the American Association of Electrodiagnostic Medicine [42], while Joy et al. [16] used cut-off values derived from their clinic with guidance from Therimadasamy et al. [43]. Ultrasound is also a highly user-dependent modality. However, in this study one sonographer performed all data collection and analysis, minimizing potential error if multiple sonographers were used. Additionally, the

sonographer was blinded to all NCS results so as to minimize conscious or unconscious bias from NCS results.

A few limitations of this study should be considered when interpreting the results. We did not exclude participants with diabetes mellitus or hypothyroidism from this study to facilitate patient recruitment. In total, 8 of our 35 patients from our sample were diabetic, and a total of 5 out of 35 participants had hypothyroidism. Of those patients, 1 patient had both diabetes and hypothyroidism. These conditions are known to be associated with fluid retention and neurological changes [44,45]. However, patients with these underlying conditions were controlled through medication. Further statistical analysis revealed no significant differences in intraneural blood flow velocity between diabetic vs. non-diabetic, or hypothyroidism patients vs. non-hypothyroidism patients. However, motor latency differed in patients with diabetes vs. those without diabetes and should be noted as a possible limitation. This was a small study with uneven group sizes which may limit generalizability. However, this was an initial foray into combining traditional and novel methods in CTS investigation. Additionally, provocative tests have been demonstrated to increase intraneural blood flow [46] and electrical nerve stimulation has been reported to increase cutaneous blood flow [47]. Since ultrasound examination were performed following physical and electrophysiological examination, it is possible that the intraneural blood flow velocities found in our study are confounded by these tests that preceded our ultrasound measures. However, ultrasound examination was performed 20-30 minutes following baseline testing, allowing sufficient time to return to resting values and low autonomic activation. Finally, systemic blood pressure was not recorded

prior to or during the protocol, so possible fluctuations in blood pressure or differences between hypertensive and non-hypertensive patients are unknown. However, a previous investigation found no influence of systemic blood pressure on median nerve intraneural blood flow [48], and statistical comparison between our patients with and without a history of hypertension revealed no significant difference in intraneural blood flow velocity.

2.6 Conclusions

This study demonstrated that the effects of wrist posture on median nerve blood flow velocity in a CTS population are dependent on severity. Patients with mild CTS are more sensitive to the negative effects of non-neutral wrist postures, suggesting that greater intervention may be needed in these individuals to delay the progression of neurological damage resulting from prolonged, altered nerve hemodynamics. These results suggest that ultrasound assessment of median nerve blood flow can potentially provide earlier, targeted detection of neurological changes, as previously suggested [14]. Ultrasound measures of median nerve CSA aid in CTS diagnosis as median nerve CSA distinguished between CTS severities. This may be particularly advantageous for patients who do not tolerate the sensations associated with NCS. Tendon-connective tissue mechanic differences were not detected between CTS severities in this population, suggesting that changes in tendon-SSCT mechanics do not change with worsening of CTS. Our results suggest that ultrasound may be an asset in CTS diagnosis, and may be a

viable alternative for patients with poor tolerance to stimulation during NCS or patients with unclear NCS results.

2.7 References

[1]   R.H. Gelberman, P. Hergenroeder, A.R. Hargens, G.N. Lundborg, W.H. Akeson, The carpal tunnel syndrome: A study of carpal canal pressures, J. Bone Jt. Surg. 63A (1981) 380–383.

[2]   S. Rojviroj, W. Sirichativapee, W. Kowsuwon, J. Wongwiwattananon, N. Tamnanthong, P. Jeeravipoolvarn, Pressures in the Carpal: A comparison between patients with carpal tunnel syndrome and normal subjects, J. Bone Jt. Surg. 72B (1990) 516–518.

[3]   R.M. Szabo, L.K. Chidgey, Stress carpal tunnel pressures in patients with carpal tunnel syndrome and normal patients, J. Hand Surg. Am. 14 (1989) 624–627.

[4]   T.D. Bauman, R.H. Gelberman, S.J. Mubarak, S.R. Garfin, The acute carpal tunnel syndrome, Clin Orthop Relat Res. 156 (1981) 151–156.

[5]   R. Luchetti, R. Schoenhuber, M. Alfarano, S. Deluca, G. De Cicco, A. Landi, Carpal tunnel syndrome: Correlations between pressure measurement and intraoperative electrophysiological nerve study, Muscle Nerve. 13 (1990) 1164–1168.

[6]   R. Luchetti, R. Schoenhuber, P.A. Nathan, Correlation of segmental carpal tunnel pressures with changes in hand and wrist positions in patients with carpal tunnel syndrome and controls, J. Hand Surg. Am. 23 B (1998) 598–602.

[7]   E. Diao, F. Shao, E. Liebenberg, D.M. Rempel, J.C. Lotz, Carpal tunnel pressure alters median nerve function in a dose-dependent manner: A rabbit model for carpal tunnel syndrome, J Orthop Res. 23 (2005) 218–223.

[8]   J.D. Bland, A neurophysiological grading scale for carpal tunnel syndrome, Muscle

        Nerve. 23 (2000) 1280–1283.

[9]   A.A. Borire, A.R. Hughes, C.J. Lueck, J.G. Colebatch, A.V. Krishnan,

        Sonographic differences in carpal tunnel syndrome with normal and abnormal

        nerve conduction studies, J. Clin. Neurosci. 34 (2016) 77–80.

[10]   D. Pastare, A.K. Therimadasamy, E. Lee, E.P. Wilder-Smith, Sonography versus

        nerve conduction studies in patients referred with a clinical diagnosis of carpal

        tunnel syndrome., J. Clin. Ultrasound. 37 (2009) 389–393.

[11]   Y.M. El Miedany, S.A. Aty, S. Ashour, Ultrasonography versus nerve conduction

        study in patients with carpal tunnel syndrome: Substantive or complementary

        tests?, Rheumatology. 43 (2004) 887–895.

[12]   E.R. Wiesler, G.D. Chloros, M.S. Cartwright, B.P. Smith, J. Rushing, F.O. Walker,

        The use of diagnostic ultrasound in carpal tunnel syndrome, J Hand Surg. 31A

        (2006) 726–732.

[13]   I. Pinilla, C. Martin-Hervas, G. Sordo, S. Santiago, The usefulness of

        ultrasonography in the diagnosis of carpal tunnel syndrome, J. Hand Surg. Eur.

        Vol. 33E (2008) 435–439.

[14]   Y.M. El Miedany, M. El Gaafary, S. Youssef, I. Ahmed, A. Nasr, Ultrasound

        assessment of the median nerve: a biomarker that can help in setting a treat to

        target approach tailored for carpal tunnel syndrome patients, Springerplus. 4 (2015)

        1–10.

[15]   K.D. Evans, S.C. Roll, K.R. Volz, M. Freimer, Relationship between intraneural

vascular flow measured with sonography and carpal tunnel syndrome diagnosis based on electrodiagnostic testing, J Ultrasound Med. 31 (2012) 729–736.

[16]   V. Joy, A.K. Therimadasamy, Y.C. Chan, E.P. Wilder-Smith, Combined Doppler and B-mode sonography in carpal tunnel syndrome, J. Neurol. Sci. 308 (2011) 16–20.

[17]   C. Dejaco, M. Stradner, D. Zauner, W. Seel, N.E. Simmet, A. Klammer, P. Heitzer, K. Brickmann, J. Gretler, F.C. Furst-Moazedi, R. Thonhofer, R. Husic, J. Hermann, W.B. Graninger, S. Quasthoff, Ultrasound for diagnosis of carpal tunnel syndrome: comparison of different methods to determine median nerve volume and value of power Doppler sonography, Ann. Rheum. Dis. 72 (2013) 1934–1939.

[18]   G.N. Lundborg, Structure and Function of the Intraneural Microvessels as Related to Trauma, Edema Formation, and Nerve Function, J. Bone Jt. Surg. 57-A (1975) 938–948.

[19]   K.-I. Nakamichi, S. Tachibana, Cross-Sectional Area in Idiopathic Carpal Tunnel Syndrome : Diagnostic Accuracy, Muscle Nerve. 26 (2002) 798–803.

[20]   K.-I. Nakamichi, S. Tachibana, Enlarged median nerve in idiopathic carpal tunnel syndrome, Muscle Nerve. 23 (2000) 1713–1718.

[21]   K.E. Wilson, J. Tat, P.J. Keir, Effects of Wrist Posture and Fingertip Force on Median Nerve Blood Flow Velocity, BioMed Res. Int. 2017 (2017) 8 pages.

[22]   A.M. Ettema, P.C. Amadio, C. Zhao, L.E. Wold, M.M. O'Byrne, S.L. Moran, K.-N. An, Changes in the functional structure of the tenosynovium in idiopathic carpal tunnel syndrome: a scanning electron microscope study., Plast. Reconstr. Surg. 118

(2006) 1413–22.

[23] M. Vanhees, Y. Morizaki, A.R. Thoreson, D. Larson, C. Zhao, K.-N. An, P.C. Amadio, The effect of displacement on the mechanical properties of human cadaver subsynovial connective tissue, J Orthop Res. 30 (2012) 1732–1737.

[24] Y. Yoshii, C. Zhao, K.D. Zhao, M.E. Zobitz, K.-N. An, P.C. Amadio, The effect of wrist position on the relative motion of tendon, nerve, and subsynovial connective tissue within the carpal tunnel in a human cadaver model, J Orthop Res. 26 (2008) 1153–1158.

[25] O. Jinrok, C. Zhao, P.C. Amadio, K.-N. An, M.E. Zobitz, L.E. Wold, Vascular pathologic changes in the flexor tenosynovium (subsynovial connective tissue) in idiopathic carpal tunnel syndrome, J. Orthop. Res. 22 (2004) 1310–1315.

[26] J. Tat, K.E. Wilson, P.J. Keir, Pathological changes in the subsynovial connective tissue increase with self-reported carpal tunnel syndrome symptoms, Clin. Biomech. 30 (2015) 360–365.

[27] J. Tat, A.M. Kociolek, P.J. Keir, Repetitive differential finger motion increases shear strain between the flexor tendon and subsynovial connective tissue, J Orthop Res. 31 (2013) 1533–1539.

[28] M.H.M. van Doesburg, Y. Yoshii, J. Henderson, H.R. Villarraga, S.L. Moran, P.C. Amadio, Speckle-tracking sonographic assessment of longitudinal motion of the flexor tendon and subsynovial tissue in carpal tunnel syndrome, J Ultrasound Med. 31 (2012) 1091–1098.

[29] Y. Yoshii, C. Zhao, J. Henderson, K.D. Zhao, K.-N. An, P.C. Amadio, Velocity-

dependent changes in the relative motion of the subsynovial connective tissue in the human carpal tunnel, J Orthop Res. 29 (2011) 62–66.

[30]   C.T.F. Tse, P.J. Keir, External Compression and Partial Ischemia Decrease Human Finger Flexor Tendon and Subsynovial Connective Tissue Relative Motion, J. Orthop. Res. (2019) 1–7.

[31]   M. Motomiya, T. Funakoshi, K. Ishizaka, M. Nishida, Y. Matsui, N. Iwasaki, Blood Flow Changes in Subsynovial Connective Tissue on Contrast-Enhanced Ultrasonography in Patients With Carpal Tunnel Syndrome Before and After Surgical Decompression, J Ultrasound Med. 37 (2018) 1597–1604.

[32]   A.A. Borire, L.H. Visser, L. Padua, J.G. Colebatch, W. Huynh, N.G. Simon, M.C. Kiernan, A.V. Krishnan, Utility of maximum perfusion intensity as an ultrasonographic marker of intraneural blood flow, Muscle Nerve. 55 (2017) 77–83.

[33]   K.D. Evans, K.R. Volz, C. Hutmire, S.C. Roll, Morhphologic Characterization of Intraneural Flow Associated With Median Nerve Pathology, J. Diagnostic Med. Sonogr. 28 (2012) 11–19.

[34]   A.A. Leis, V.C. Trapani, Atlas of Electromyography, Oxford University Press, Oxford, 2000.

[35]   D.C. Preston, B. Shapiro, Electromyography and Neuromuscular Disorders: Clinical Electrophysiologic Correlations, Elsevier, 2005.

[36]   A.D. Junck, E.. Escobedo, B.M. Lipa, M. Cronan, C. Anthonisen, E. Poltavskiy, H. Bang, J.J. Han, Reliability Assessment of Various Sonographic Techniques for

Evaluating Carpal Tunnel Syndrome., J Ultrasound Med. 34 (2015) 2077–88.

[37] J. Tat, A.M. Kociolek, P.J. Keir, Validation of Color Doppler Sonography for Evaluating Relative Displacement Between the Flexor Tendon and Subsynovial Connective Tissue, J Ultrasound Med. 34 (2015) 679–687.

[38] C.B. Gonzalez-Suarez, B.C. Fidel, J.T.C. Cabrera, F.C. Dela Cruz, M.V.T. Gesmundo, C.F.G. Regala, R. Saratan, C.G. Suarez, K. Grimmer, Diagnostic Accuracy of Ultrasound Parameters in Carpal Tunnel Syndrome: Additional Criteria for Diagnosis, J. Ultrasound Med. (2019).

[39] L. Moran, M. Perez, A. Esteban, J. Bellon, B. Arranz, M. Del Cerro, Sonographic measurement of cross-sectional area of the median nerve in the diagnosis of carpal tunnel syndrome: Correlation with nerve conduction studies, J. Clin. Ultrasound. 37 (2009) 125–131.

[40] I.. Tatar, A. Kurt, N.G. Yavasoglu, B. Hekimoglu, Carpal tunnel syndrome : elastosonographic strain ratio and cross- sectional area evaluation for the diagnosis and disease severity ., Med Ultrason. 18 (2016) 305–311.

[41] H. Sarafraz, M.R. Hadian, N.A. Yazdi, G. Olyaei, H. Bagheri, Test-retest reliability of nerve and muscle morphometric characteristics utilizing ultrasound imaging in individuals with unilateral sciatica and controls, Chiropr. Man. Therap. 26 (2018) 1–10.

[42] S. Chen, M. Andary, R. Buschbacher, D. Del Toro, B. Smith, Y. So, K. Zimmermann, T.R. Dillingham, Electrodiagnostic reference values for upper and lower limb nerve conduction studies in adult populations, Muscle Nerve. (2016)

371–377. https://doi.org/10.1002/mus.25203.

[43]   A.K. Therimadasamy, E. Li, E.P. Wilder-Smith, Can studies of the second lumbrical interossei and its premotor potential reduce the number of tests for carpal tunnel syndrome?, Muscle and Nerve. 36 (2007) 491–496. https://doi.org/10.1002/mus.20850.

[44]   A.A. Borire, T. Issar, N.C. Kwai, L.H. Visser, N.G. Simon, A.M. Poynten, M.C. Kiernan, A.V. Krishnan, Correlation between markers of peripheral nerve function and structure in type 1 diabetes, Diabetes. Metab. Res. Rev. 34 (2018) 1–8.

[45]   A.A. Borire, R. Arnold, B.A. Pussell, N.C. Kwai, L.H. Visser, N.G. Simon, M.C. Kiernan, A.V. Krishnan, Effects of hemodialysis on intraneural blood flow in end-stage kidney disease, Muscle and Nerve. 57 (2018) 287–293.

[46]   E.S. Ng, K.W. Ng, E.P. Wilder-Smith, Provocation tests in doppler ultrasonography for carpal tunnel syndrome, Muscle and Nerve. 47 (2013) 116–117.

[47]   F.L. Cramp, G.R. McCullough, A.S. Lowe, D.M. Walsh, Transcutaneous electric nerve stimulation: The effect of intensity on local and distal cutaneous blood flow and skin temperature in healthy subjects, Arch. Phys. Med. Rehabil. 83 (2002) 5–9. https://doi.org/10.1053/apmr.2002.27478.

[48]   S.G. Ehmke, The Effect of Force, Posture, and Repetitive Wrist Motion on Intraneural Blood Flow in the Median Nerve, McMaster University, 2015.

Chapter 3: Ultrasound Examination Predicts 6-Month Progression in Carpal Tunnel Syndrome Patients

Amanda Farias Zuniga[1], Amer A. Ghavanini[2,3,4], Gaspar Israelian[3,4], Peter J. Keir[1]

[1]*Department of Kinesiology, McMaster University, Hamilton, Ontario, Canada*
[2]*Canadian Neurologic Center, Mississauga, ON, Canada*
[3]*Department of Medicine, Division of Neurology, University of Toronto, Toronto, ON, Canada*
[4]*Division of Neurology, Trillium Health Partners*

3.1 Abstract

Carpal tunnel syndrome (CTS) is a peripheral neuropathy resulting from chronic median nerve compression. Chronic compression leads to neurological changes that are quantified through nerve conduction studies (NCS). Although NCS represent the gold standard in CTS assessment, they provide limited prognostic value. Several studies have identified ultrasound as a tool in diagnosing and potentially predicting the progression of CTS in patients. The purpose of this study was to evaluate the predictive value of ultrasound examination in CTS patients. Twenty patients recruited at their first visit with the neurologist completed two NCS and ultrasound examinations approximately 6-months apart. Ultrasound examination consisted of B-mode, pulse-wave Doppler and colour Doppler ultrasound videos and images to quantify median nerve cross-sectional area, intraneural blood flow velocity in 3 wrist postures (15° flexion, neutral, and 30° extension), and displacement of the flexor digitorum superficialis (FDS) tendon and the adjacent subsynovial connective tissue (SSCT) of the middle finger during repetitive finger flexion-extension cycles. A questionnaire was administered to assess the work-relatedness of CTS. Linear regression analyses revealed that intraneural blood flow velocity ($R^2 = 0.36$, $p = 0.03$), assessed in wrist flexion, and relative FDS-SSCT displacement ($R^2 = 0.27$, $p = 0.04$) and shear strain index ($R^2 = 0.28$, $p = 0.04$) were significant predictors of nerve sensory and motor changes at 6-months. Results suggest the possibility of using a battery of ultrasound measures as viable markers to predict median nerve functional changes within 6 months.

3.2 Introduction

Carpal tunnel syndrome (CTS) is a peripheral neuropathy arising from chronic median nerve compression. CTS prevalence in the general population is approximately 8%, higher in those in laborious jobs[1]. CTS is increasingly occupationally related. A recent report showed a significant increase in the annual cases that CTS was compensated as an occupational disease over the past decade[2]. Exposure to force, repetition, awkward postures and vibration are significant risk factors for CTS[3–8]. Mechanistically, repetitive differential finger motion increases shear strain between the flexor digitorum superficialis tendon (FDS) and its adjacent subsynovial connective tissue (SSCT) in participants with and without symptoms of CTS[9,10]. Cumulative shear strain is believed to precede CTS development[11,12], causing fibrosis and scarring within the carpal tunnel, ultimately resulting in greater nerve compression and altered local blood flow[13].

Symptoms and nerve conduction studies (NCS) are currently the standard to diagnose CTS. NCS assesses the ability of the nerve to conduct electrical impulses, characterizing the amplitude, conduction velocity and latency of the impulses[14,15]. These outcomes reflect the neurophysiological integrity of the median nerve, representing axonal integrity and degree of myelination[16]. NCS results also categorize severity[15]. However, it is difficult to predict the progression of CTS and determine which patients will require future surgery. Severity has not been found to be the most predictive indicator for CTS progression[17], and does not provide significant predictive value for return to work and post-operative hand function[18].

There is support for ultrasound in CTS diagnosis[19–27]. Ultrasound findings, particularly median nerve cross-sectional area (CSA), are significantly correlated with NCS. A moderate to very strong relationship has been reported between median CSA and severity classification determined by NCS[21,25,26,28]. Using median nerve CSAs to create 9 diagnostic categories, Ziswiler et al.[23] found a strong negative association between CSA and sensory nerve conduction velocity (ρ=-0.65, p<0.001), where conduction velocity decreased by 2.0 m/s per mm^2 increase in CSA. A moderate positive correlation was also observed between CSA and distal motor latency (ρ=0.50, p<0.001). The relationship between median nerve intraneural blood flow, collected through ultrasound, and NCS has also been demonstrated[29,30]. El Miedany et al.[29] reported a strong negative relationship between intraneural flow and NCS severity (r=-0.737), and Joy et al.[30] reported statistically significant positive relationships between all NCS parameters (distal motor latency, sensory peak latency) and intraneural blood flow velocity (r=0.362-0.264).

There is some evidence for the predictive value of ultrasound in CTS patients. In particular, El Miedany and colleagues[29] followed 233 subjects from baseline through a 6-month period during their treatment which consisted of conservative (i.e. injections, splints, and exercise) and surgical treatments. Their baseline measures included NCS, and ultrasound outcomes including median nerve CSA, flattening ratio (FR), and Power Doppler (PD) signal to assess vascularity. PD signals were graded from 0 to 3, with 0 representing no PD signal, and 3 representing three single or more than two confluent vessels present. Their multivariate regression analysis demonstrated that a baseline

median nerve CSA of <14.0 mm^2 and a PD score of >2 at baseline were associated with improvement at 6 months. Receiver operating characteristic (ROC) curves also demonstrated that increased median nerve vascularity had good prognostic value[29]. These results suggest baseline ultrasound measures provide insight into 6-month treatment outcomes.

There are challenges in predicting CTS progression from NCS and symptoms; ultrasound may provide a solution. The purpose of this investigation was to evaluate the predictive value of ultrasound assessment. We also investigated if work history and history of hand use, both work- and non-work-related, would aid in predicting CTS progression given the work-relatedness of CTS. We hypothesized that intraneural blood flow velocity and tendon-connective tissue mechanics would be most predictive of neurological findings at 6-month follow-up.

3.3 Methods

3.3.1 Experimental Design and Setup

This clinical, double-blinded study consisted of an initial visit and a 6 month follow-up. Ultrasound imaging was used to quantify median nerve CSA, intraneural blood flow velocity and tissue motion *in vivo* at both visits. NCS was also conducted at both visits as the universally applied reference "gold" standard. Data from outcome measures collected at the initial visit were used to predict NCS outcomes at the follow-up visit with the aim to develop diagnostic criteria based on ultrasound findings to provide level II evidence.

Results from the initial visit have been reported previously[31]. The initial visit was completed between October 2016 and January 2017, and follow-up visits were completed an average of 186 days later (range: 143 – 251 days) between April and July 2017. Consecutive patients were recruited at the initial visit, however, study participation was voluntary. Between the two visits, patients received the standard of care treatment consisting of a wrist splint. The initial visit occurred after an initial NCS, either on the day of the patient's initial appointment with the neurologist or at a later date. NCS was repeated at the 6-month follow-up visit. During both visits, patients participated in an ultrasound examination where B-mode, pulse wave (PW) Doppler imaging, and colour Doppler imaging were performed. Each session was 30-45 minutes long. Protocols at both visits were identical and were performed by the same experimenter who was blinded to patient NCS results throughout ultrasound collection and analysis.

3.3.2 Participants

Participants were recruited for this study if they participated in the initial visit[31] and had not undergone surgery for the condition within 6-months. Patients with hypothyroidism and diabetes mellitus managed through medication were included. Patients with all levels of CTS severity were recruited. If the patient was diagnosed with bilateral CTS, the same hand that was previously imaged at the initial visit was imaged for this study. This study was approved by the Hamilton Integrated Research Ethics Board and all participants provided informed written consent prior to study participation. Participant information including age and sex were also collected.

3.3.3 Nerve Conduction Study

The study protocol at both the initial visit and the 6-month follow-up visit were

identical (Farias Zuniga et al., 2020)[31]. Briefly, a Registered EMG Technologist

conducted NCS following guidelines from the American Association of Electrodiagnostic

Medicine. Limb temperatures were monitored throughout NCS and warmed if necessary

to maintain a temperature over 32°C. Motor NCS were performed orthodromically, while

sensory studies were performed antidromically and orthodromically. Needle EMG was

performed with a disposable monopolar needle, and localization was based on Leis &

Trapani[32] and NCS techniques were based on Preston & Shapiro[33]. Other peripheral

neuromuscular disorders were excluded through EMG and NCS. Noted median

neuropathy at the wrist confirmed diagnosis of carpal tunnel syndrome. Rating of CTS

severity was based on Bland[8]. Where the motor and sensory responses did not fit with

this severity scale, severity was rated based on the sensory response alone.

3.3.4 Ultrasound Protocol

Complete details for the ultrasound protocol can be found in our baseline study[31].

Participants were seated comfortably with their affected hand supinated and resting in a

custom 3D printed hand and wrist splint to keep the hand, wrist and forearm in place and

allow for standardized postures via a built-in protractor. A Velcro strap secured the

fingers and prevented unwanted movement. A high frequency linear array transducer

(12L-RS) and ultrasound system (Vivid Q BT10, GE Healthcare, Milwaukee, WI) was

optimized to predetermined settings for each experimental test[9,31,34]. A gel standoff wedge (Aquaflex gel pad, Cone Instruments, Solon, OH) was used between the skin surface and ultrasound probe for image optimization.

The protocol collected sonographic images and videos in three experimental tasks. In the first experimental task, two transverse B-mode images were taken to determine median nerve CSA with the probe on the palmar surface at the carpal tunnel inlet with the wrist in neutral (0°) posture and the fingers relaxed (semi-flexed). In the second task, PW Doppler ultrasound was used to image median nerve intraneural blood flow. PW Doppler videos were collected with the wrist in three postures: 15° flexion, neutral (0°), and 30° extension. The ultrasound probe was oriented in the longitudinal plane and placed in line with the proximal wrist crease. PW Doppler settings were optimized to established settings[31,34] using duplex mode. Two 12-second PW Doppler videos were collected per posture. In the third task, colour Doppler imaging was used to obtain videos of the FDS tendon of the third digit and its adjacent SSCT during repetitive finger flexion-extension of the third digit. Custom 3D printed handgrips with Velcro straps were used to isolate the third digit during the repetitive motion protocol. The repetitive motion trial consisted of 2 sets of 10 repetitions of finger flexion-extension cycles of the third digit with the wrist in neutral (0°) posture. An audible metronome was set to the movement speed of 0.75 Hz to help participants maintain a consistent rhythm as well as standardizing movement speed. The ultrasound probe was placed at the proximal wrist crease, and established colour Doppler imaging settings were used[9,35].

3.3.5 Workplace Questionnaire

To gain insight into work- and non-work-relatedness of CTS in our population, we developed a questionnaire to gain information on workplace and leisure practices. The questionnaire (Appendix E) combined a series of questions from the QPSNordic: General Nordic Questionnaire for psychological and social factors at work[36], and a self-administered questionnaire for handwork[37]. The questionnaire asked general questions including total number of years of employment, the nature of work (or past work, if retired) and the type and amount (hours/week) of non-work-related hand activity. Non-work-related hand use was defined as any hand activity that did not pertain to their job and was not associated with paid work. This included leisurely activities, chores, hobbies, and exercise. Frequency and intensity of current and past hand use in their workplace and during leisure time was assessed on a 0 to 10 scale. Participants completed the questionnaire at their initial visit prior to the experimental protocol.

3.3.6 Data Analysis

Following completion of ultrasound data analysis, the lead investigator was unblinded to the neurological results. Participants were sorted into three severity groups (mild, moderate, severe) defined by the neurologists following standardized guidelines (mild: sensory conduction velocity from index finger to wrist <40 m/s, motor latency from wrist to abductor pollicis brevis <4.3 ms; moderate: motor latency 4.3-6.5 ms with preserved index finger sensory nerve action potential; severe: motor latency 4.3-6.5 ms with absent sensory nerve action potential or motor latency >6.5 ms)[15]. NCS results

including motor and sensory latency (ms), amplitude (mV/μV), and conduction velocity

(CV) (m/s) were collected from the clinics.

B-mode images were uploaded to ImageJ software (National Institutes of Health,

Bethesda, MD) and the tracing tool was used to trace the median nerve border and

measure median nerve CSA. Values were rounded to the nearest 0.01 mm^2. Analysis

was performed on the two B-mode images collected and averaged to result in one median

nerve CSA value per participant, per session.

From the PW Doppler imaging, high resolution AVI video files were uploaded to

the Measurements from Arterial Ultrasound Imaging (MAUI) analysis software

(Hedgehog Medical Inc., Waterloo, ON) to determine the average peak blood flow

velocity within a 5 second window. Analysis was conducted on the two PW Doppler

ultrasound video collected, and then averaged to provide one peak blood flow velocity

(cm/s) value per posture, per participant, per session.

EchoPac analysis software (General Electric Healthcare, Milwaukee, WI) was

used to analyze FDS and SSCT tissue motion during the repetitive motion trials. The

middle 8 out of 10 repetitions were analyzed. FDS and SSCT velocities were obtained by

placing three markers collinearly over each tissue. Tissue motion was tracked on a

frame-by-frame basis throughout the entirety of the video. From this, the three velocity

traces for each tissue were imported into a custom Matlab program where they were

averaged to create one representative tissue velocity trace per tissue. This velocity signal

was low-pass filtered (4 Hz, 2nd order Butterworth) and corrected for the angle of

insonation (cosθ). Peak tissue displacement was calculated for each tissue separately

(FDS and SSCT). Peak relative tissue displacements between tendon-connective tissue

displacement were calculated as the difference between peak FDS displacement and peak

SSCT displacement. Shear Strain Index (SSI)[9] was also calculated as the ratio between

peak relative displacement (peak FDS displacement – peak SSCT displacement) and peak

FDS displacement multiplied by 100%.

Data from the questionnaires collected at the initial visit were extracted and

compiled. Participant industry of work were summarized to look for similarities among

participants. Work- and non-work-related hand frequency, and work- and non-work-

related hand intensity ratings were averaged.

To determine the predictive ability of baseline ultrasound measures on progression

over 6 months, linear regressions were performed for each baseline measure on predicting

nerve conduction, specifically distal motor latency, motor amplitude, sensory CV, and

sensory amplitude. Given the limited sample size, regressions were performed

independently for each measure rather than entering them all into a multiple linear

regression model. In each linear regression model, the dependent variable was the NCS

outcome from the follow-up visit (distal motor latency or motor amplitude or sensory CV

or sensory amplitude). Independent variables for each regression were the following

from the initial visit: motor latency, motor amplitude, sensory CV, sensory amplitude,

peak FDS displacement, peak SSCT displacement, peak relative displacement, SSI,

median nerve CSA, peak blood flow velocity (in flexion, neutral, and extension), number

of work years, work-related hand frequency, non-work-related hand frequency, work-

related hand intensity, non-work-related hand intensity. All statistical analyses were

performed in R (version 3.5.1) and R Studio (version 1.1.463, Boston, MA) and significance was set at p<0.05.

3.4 Results

3.4.1 Participant Characteristics

Participant characteristics are shown in Table 1. Thirty-five patients were recruited at the initial visit to participate in the study. Of these patients, 21 returned for a follow-up visit approximately 6 months later. More patients with moderate CTS returned for their follow-up visit than those diagnosed with either mild or severe CTS. Seven patients did not return because they underwent surgery within the 6-month window. Of these 7, two patients had mild CTS, one had moderate CTS, and 4 had severe CTS. The remaining 7 patients declined further participation in the study.

Table 3. 1: Participant characteristics by sex and severity group for the follow-up visits (n = 21).

	Follow-up Visit
N	21
Male	4
Female	17
Age	57.5 ± 12.4
Male	57.8 ± 6.3
Female	57.5 ± 13.5
Severity (N)	
Mild	7
Moderate	10
Severe	4

3.4.2 Nerve Conduction Study

Given that NCS is currently the main diagnostic tool for CTS, we investigated the change in NCS parameters over the 6-month period. In this sample of 21 patients, motor latency generally improved (decreased) in 63% of participants over 6 months (Figure 1). On average, motor latency in this population improved by 0.55 ms, from 5.02 ms at the initial visit to 4.47 ms at the follow-up visit (Figure 1a). Mean motor amplitude also improved by 0.43 mV, from a group average of 9.21 mV at the initial visit to an average of 9.64 mV at follow-up (Figure 1b). Average sensory CV worsened, decreasing from 38.3 m/s at the initial visit to 37.1 m/s at follow-up (Figure 1c). Sensory amplitude slightly declined from 18.5 μV at baseline to 17.3 μV at follow-up (Figure 1d).
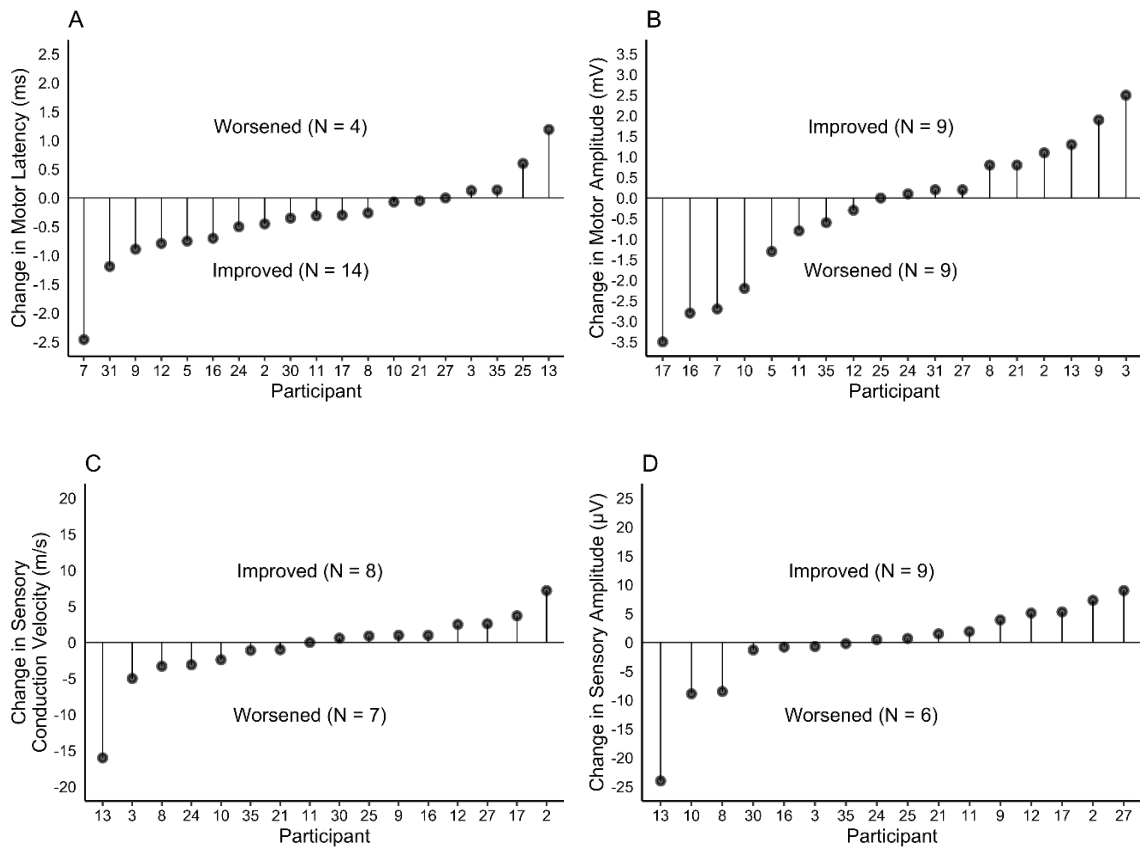
Figure 3. 1: Absolute change in distal motor latency (A), motor amplitude (B), sensory conduction velocity (C) and sensory amplitude (D) between initial and follow-up visits for each participant. Change indicating improvement or worsening of that outcome are represented in indicated areas above or below the x-axis. Participants without values are not displayed.

3.4.3 Workplace Characteristics

Participants reported a total of 26-30 years of work experience. At the time of their initial visit, 2 patients were unemployed and 5 patients were retired. Their professions (or past professions, if retired) ranged greatly from military personnel, to health care workers, to homemaker. When currently employed patients were asked about the frequency of repetitive handwork at their current job on a 0 to 10 scale, with 0 indicating "handles idle most of the time" and 10 indicating "rapid steady

exertion/motion, no pauses, difficulty keeping up", the average response was 5. When

asked about the intensity of handwork in their current workplace on a 0 to 10 scale, with 0

indicating "none" and 10 indicating "extreme", the average response was 4. For non-

work related hand frequency and intensity, the average responses were 5 and 4,

respectively.

3.4.4 Tendon-Connective Tissue Motion

Peak FDS and peak SSCT displacement, peak relative FDS-SSCT displacement

and SSI outcomes did not greatly differ between sessions (Figure 2). Peak FDS

displacement increased from 21.7±4.1 mm at the initial visit to 22.2±3.8 mm at follow-up

(Figure 2a). Peak SSCT displacement decreased from initial to follow-up, from 18.4±3.9

mm to 17.6±5.0 mm (Figure 2b). These changes were reflected in an increase in peak

relative displacement from 5.1±2.5 mm at the initial visit to 5.9±4.0 mm at follow-up

(Figure 2c). Additionally, SSI increased by 2.4% between initial to follow-up

measurements from 22.8±10.4% to 25.2±15.4% (Figure 2d). However, there was

considerable variability observable when each participant was visualized across sessions.
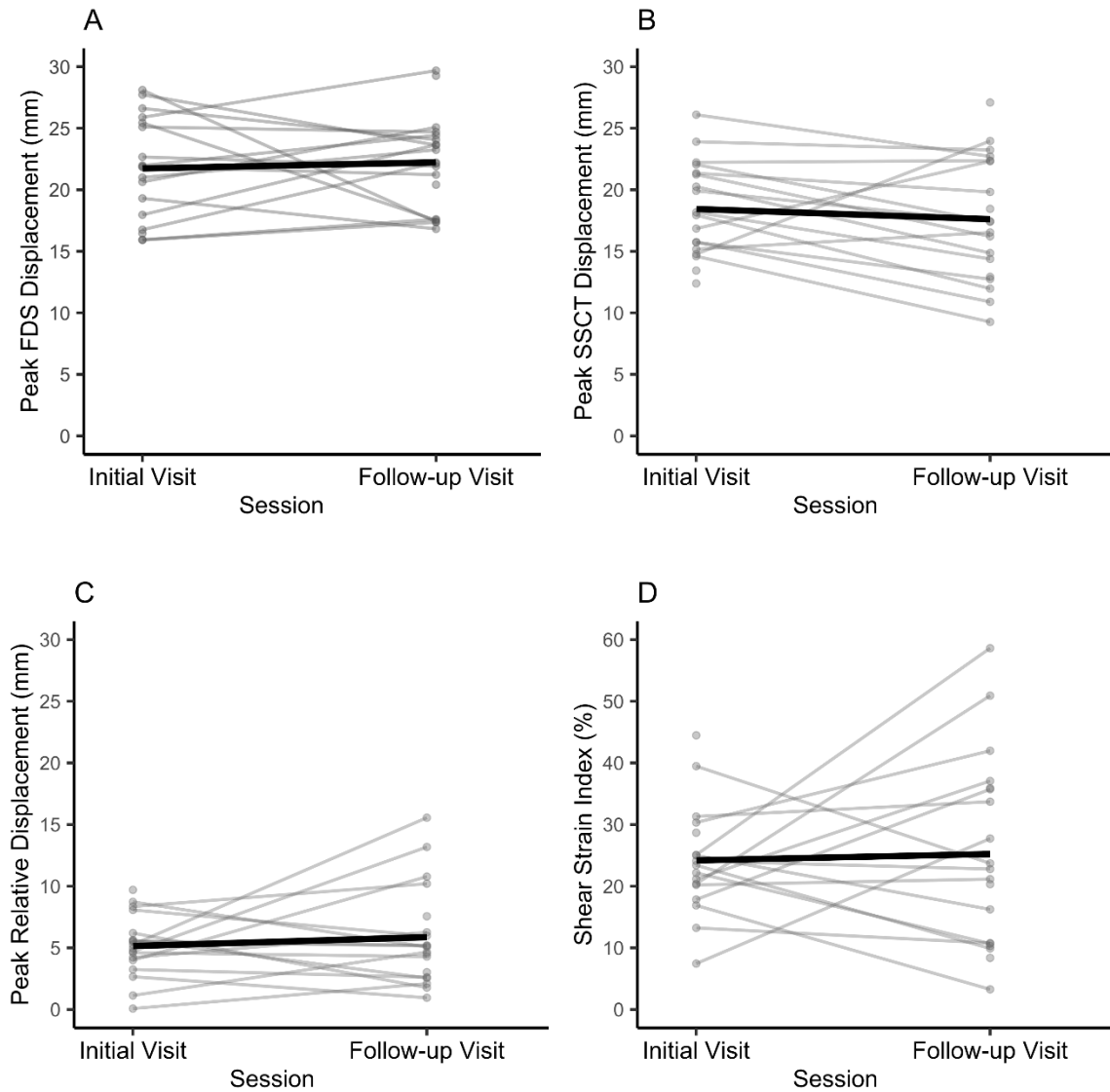
Figure 3. 2: Peak flexor digitorum superficialis (FDS), peak sub-synovial connective tissue (SSCT), peak relative displacement and shear strain index (SSI) during repetitive finger flexion-extension motions. Each participant is represented by grey points and an accompanying grey line demonstrating their change in outcome between initial visit and the follow-up visit. Black lines represent the group mean. On average, peak FDS displacement increased while peak SSCT displacement decreased, resulting in an overall increase in peak relative displacement by approximately 0.8 mm and increase in SSI by approximately 2.4%. Note that some participants did not have points at either the initial or follow-up visit which was attributable to poor image quality that did not make image analysis possible.

3.4.5 Median Nerve CSA

Median nerve CSA increased between the initial visit and follow up visit. At the initial visit, average CSA was 10.41±5.16 mm^2, while at follow-up the average group CSA was 12.09±6.16 mm^2 (Figure 3).
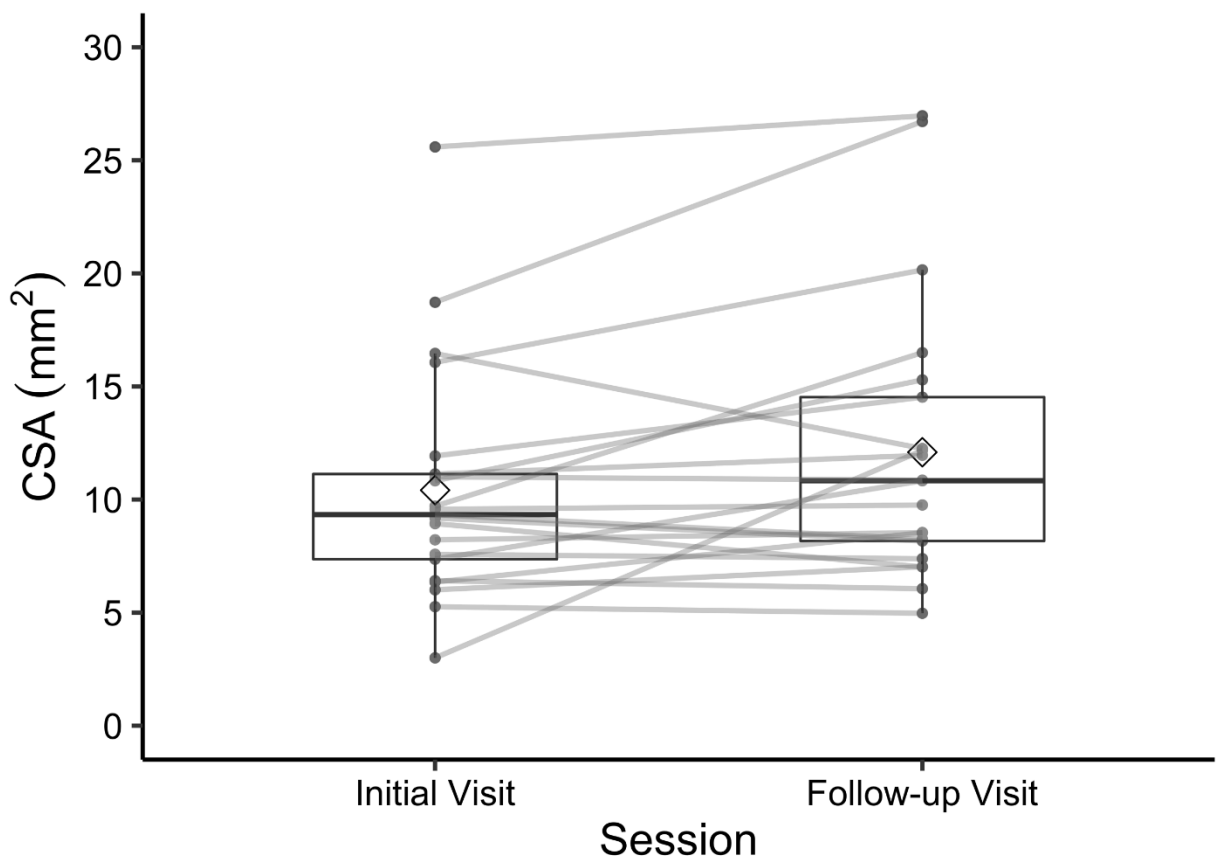
Figure 3. 3: Boxplot demonstrating median nerve cross-sectional area (CSA) (mm^2) at the initial visit and follow-up visit 6-months later. The median (center line), mean (center open diamond), 25th and 75th percentiles (upper and lower horizontal lines of the box, respectively), and range no larger than 1.5 times the interquartile range between the first and third quartile (lines extending above and below) are represented. Each participant is represented by individual grey points, and grey lines connect their initial and follow-up CSAs to demonstrate their change in median nerve CSA. On average, median nerve CSA increased from 10.4±5.2 mm^2 at the initial visit to 12.1±6.2 mm^2 at follow-up.

3.4.6 Median Nerve Blood Flow Velocity

Changes in intraneural blood flow velocity were observed at the 6-month follow-up visit, primarily evident at a neutral wrist posture (0°). At the initial visit, the average intraneural blood flow velocity was 2.54±2.22 cm/s, while at follow-up it was 3.53±1.85 cm/s. In wrist extension (30°), intraneural blood flow velocity was an average of 2.40±1.61 cm/s at the initial visit and 2.67±1.92 cm/s at the follow-up visit. When measured in a flexed wrist posture (15°), intraneural blood flow velocity was 2.70±1.44 cm/s at the initial visit and 3.09±2.17 cm/s at the 6-month follow-up visit (Figure 4).
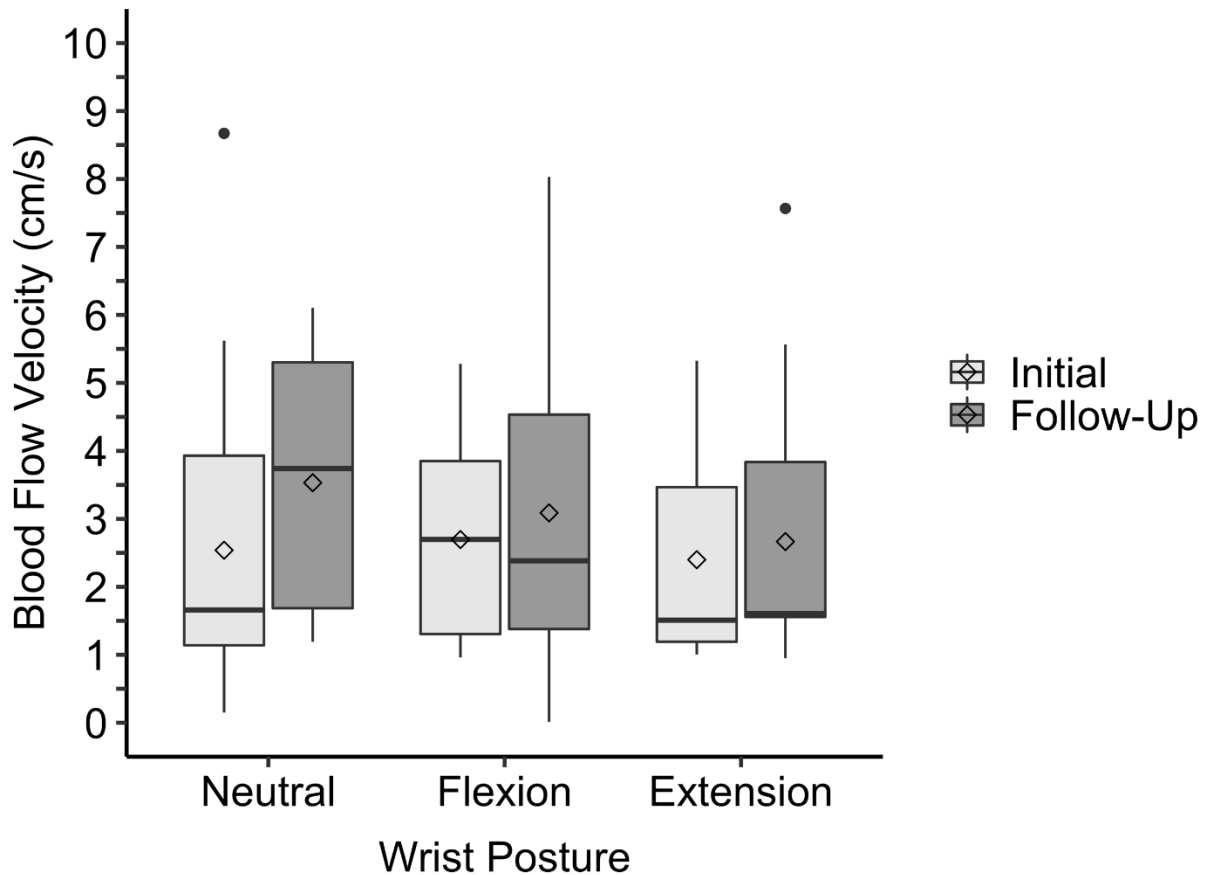
Figure 3. 4: Boxplots of intraneural blood flow velocity (cm/s) of the median nerve measured at neutral (0°), flexion (15°) and extension (30°) wrist postures, at both initial (light grey) and follow-up (dark grey) visits. Mean (open diamonds), median (center line), 25th and 75th percentile (upper and lower horizontal lines of the box, respectively), and range no larger than 1.5 times the interquartile range between the first and third quartile (lines extending above and below) are displayed. Outliers are represented by black dots. Intraneural blood flow velocity generally increased between initial and follow-up visit when measured at all wrist postures. The greatest increase was observed for the neutral wrist posture, where intraneural blood flow velocity increased from 2.54±2.22 cm/s to 3.53±1.85 cm/s. When measured at 30° of wrist extension, intraneural blood flow velocity increased from 2.40±1.61 cm/s to 2.67±1.92 cm/s between visits. At 15° of wrist flexion, blood flow velocity increased from 2.70±1.44 cm/s to 3.09±2.17 cm/s at the 6-month follow-up.

3.4.7 Regression analysis

The linear regression analyses revealed that motor latency ($F(1,17)=15.97$, $p<0.001$) , peak relative displacement ($F(1, 14)=5.126$, $p=0.04$), and SSI ($F(1, 14)=5.387$, $p=0.04$) measured at the initial visit significantly predicted motor latency at 6-months follow-up (Figure 5a-c). Motor latency measured at the initial visit accounted for 48% of the explained variability in motor latency at the follow-up visit. Peak relative displacement measured at the initial visit explained 27% of the variability, and SSI from the initial visit accounted for 28% of the variability in motor latency at the follow-up visit. Sensory CV at the follow-up visit was significantly predicted by sensory CV at the initial visit ($F(1,14)=19.78$, $p<0.001$)(Figure 5d), intraneural blood flow velocity measured in wrist flexion at the initial visit ($F(1,11)=6.282$, $p=0.03$) (Figure 5e), and non-work-related hand intensity ($F(1,12)=6.584$, $p<0.02$) (Figure 6a). Sensory CV was the best predictor of follow-up sensory CV, accounting for 59% of the variability. Intraneural blood flow velocity in flexion at the initial visit accounted for 36% of the variability, while non-work-related hand intensity at the initial visit accounted for 35% of the variability in follow-up sensory CV. Sensory amplitude at follow-up was significantly predicted by initial sensory amplitude ($F(1,14)=19.97$, $p<0.001$) (Figure 5f), accounting for 59% of the variability, while non work-related hand intensity significantly ($F(1,12)=5.487$, $p=0.04$) (Figure 6b) accounted for 31% of the variability. No other independent variables assessed statistically significantly explained the variability in follow-up motor latency, sensory latency or sensory amplitude. None of the independent variables assessed significantly explained the variability in follow-up motor amplitude.
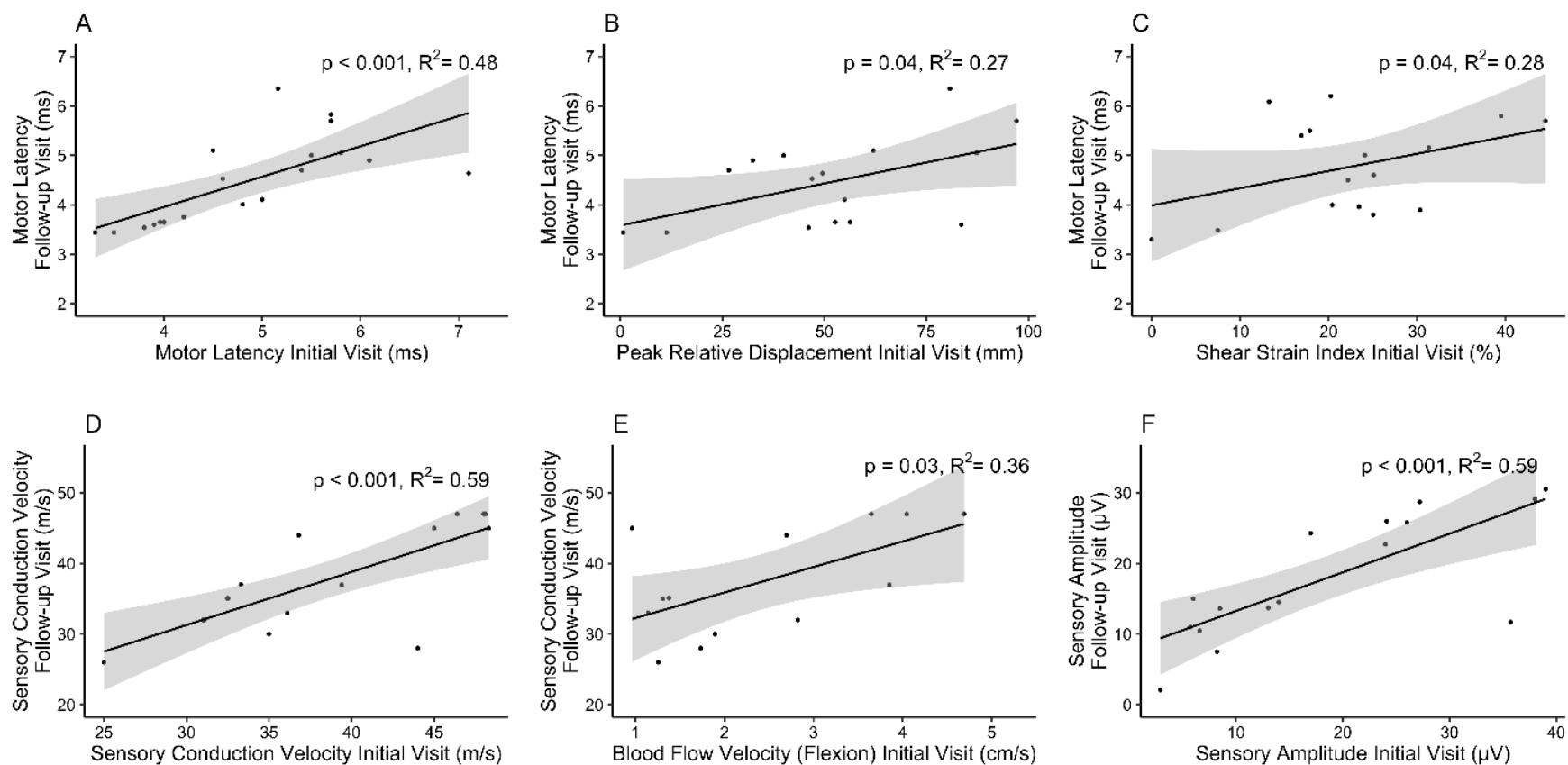
Figure 3. 5: Linear regression analysis results predicting the variability in follow-up nerve conduction study (NCS) outcomes. Motor latency measured at the 6-month follow-up visit was significantly predicted by (A) initial motor latency, (B) initial peak relative FDS-SSCT displacement, and (C) initial shear strain index (SSI). Sensory conduction velocity (CV) at follow-up was significantly predicted by sensory CV at the initial visit (D) and intraneural blood flow velocity at the initial visit when measured in a wrist flexion position (E). Sensory amplitude at follow-up was predicted by sensory amplitude at the initial visit (F). Data points, regression line and the 95% confidence interval (grey shading) are shown.
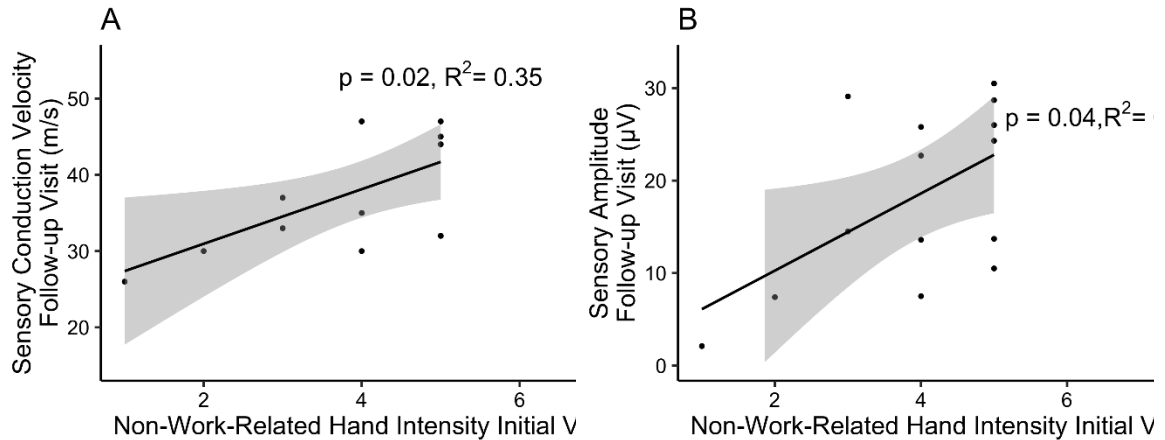
Figure 3. 6: Linear regression analysis results predicting the variability in follow-up nerve conduction study (NCS) outcomes from self-reported non-work-related hand intensity. Non-work-related hand intensity was rated on a 10 point scale, with 0 representing "none" and 10 representing "extreme". Sensory conduction velocity at follow-up was significantly predicted by non-work-related hand intensity at the initial visit (A). Sensory amplitude at follow-up was significantly predicted by non-work-related hand intensity at the initial visit (B). Data points, regression line and the 95% confidence interval (grey shading) are shown.

3.5 Discussion

Carpal tunnel syndrome is a multifaceted condition resulting from prolonged compression of the median nerve, resulting in measurable neurological changes. However, determining if and to what extent a patient's condition will progress continues to be difficult to ascertain. The intention of this investigation was to evaluate the ability of ultrasound examination at initial assessment to predict the 6-month evolution of CTS. Our outcome measures were NCS results, median nerve CSA, intraneural blood flow velocity, and tendon-connective tissue displacement. We also administered a questionnaire to capture the number of work years, and work- and non-work-related hand

use. We hypothesized that intraneural blood flow velocity and tendon-connective tissue mechanics would be predictive of neurological CTS findings at 6 months follow-up. This hypothesis was partly confirmed, although our data suggests that tendon-SSCT mechanics and intraneural hemodynamics predict separate, albeit related, neurological findings.

Relative FDS-SSCT motion and SSI were statistically significant predictors of median nerve motor latency, accounting for 27% and 28% of the variability, respectively. This suggests that tendon-SSCT mechanics may provide prognostic value for motor changes, and that those with higher relative FDS-SSCT displacement and SSI may be more likely to suffer greater motor nerve fibre damage over time. It has been reported that patients[38] and CTS symptomatic individuals[10] exhibit higher SSI than controls. Shear strain is the main pathomechanical theory for SSCT injury, where increased shear results in injury to the interconnecting fibres between the parallel bundles of collagen of the SSCT[13]. This injury is progressive[11] and leads to eventual fibrosis and thickening, particularly at the tendon border[13], further narrowing the carpal tunnel space and compressing the median nerve. The median nerve is susceptible to compression as the endothelial cells of the nerve increase in permeability leading to epineural and intraneural edema, altering intraneural blood flow and oxygen supply[39–41]. This leads to changes in nerve function of the nerve such as slowed conduction, and eventual permanent axonal damage if not reversed[39,41]. Our data suggests that quantifying tendon-SSCT mechanics at baseline may allow prediction the progression of nerve damage.

We found that intraneural blood flow velocity of the median nerve at 15° of wrist flexion predicted 36% of median nerve sensory CV variability. This is similar to

previous work that found median nerve blood flow was prognostic of 6-month sensory latency[29]. However, we only found this in wrist flexion. In our sample, those with lower blood flow velocities at the initial visit had lower sensory CV 6 months later, indicating sensory decline and more severe CTS. These results support previous studies suggesting a U-shaped relationship between electrodiagnostic results and blood flow velocity in CTS patients, where blood flow velocity is highest in individuals with symptoms but electrodiagnostically negative CTS, and lowest in those with severe confirmed CTS[29,31,42]. This likely reflects the impact of chronic insult to the nerve, resulting in a loss of perfusion and circulatory disturbances[41] which lead to altered nerve function[39,41].

Interestingly, non-work-related hand intensity was a statistically significant predictor of both sensory CV and amplitude, accounting for 35% of the variability in sensory CV and 31% in sensory amplitude. Those reporting higher non-work-related hand intensity at baseline had higher sensory CV and sensory amplitudes at follow-up. Number of work years was not a significant predictor. Although these results appear surprising, it is worth noting that "hand intensity" in the questionnaire was fairly subjective and based on patient interpretation. Additionally, hand use intensity is not currently considered a risk factor for CTS development. Biomechanical risk factors, such as repetitive hand use, forceful exertions, and non-neutral hand postures, have been clearly linked to CTS development[3–7]. However, we are restricted from establishing a clear relationship to the work-relatedness of CTS as we did not directly quantify exposure to biomechanical risk factors.

Although the purpose of this investigation was to explore the predictive ability of ultrasound outcomes, we also included NCS outcomes in our regression models since NCS is considered the gold standard in CTS assessment. Nerve conduction study findings at baseline best predicted follow-up NCS findings, with sensory amplitude and CV being the best overall predictors, followed by motor latency. Baseline sensory amplitude and sensory CV accounted for 59% of the variability in sensory amplitude at follow-up, and baseline motor latency accounted for 48% of follow-up motor latency. We believe these results can be explained by the generally modest changes in NCS parameters between initial and follow-up visits. The majority of patients did not experience significant improvement or decline in their NCS outcomes that would change their CTS severity categorization. Given that this sample was prescribed a conservative treatment (i.e. wrist splint), this is still encouraging as it demonstrates that conservative treatments can be effective at stalling further deterioration of nerve function. It is also possible that the 6-month period between visits was insufficient to capture declines in neurophysiological state that results from chronic nerve compression, particularly in this sample with conservative treatment.

There are some considerations when interpreting the results of this investigation and generalizing it to the clinical population. Our sample size restricted our statistical approach and did not allow us to run a multiple regression analysis to determine the single best predictor for 6-month follow-up NCS. In total, 7 patients elected to have carpal tunnel release surgery within the 6-month period and were excluded. However, this study was an initial investigation into the predictive value of these sets of outcome

measures in CTS patients. Second, there is currently no questionnaire to capture the relationship between hand use and CTS. We chose to use the QPSNordic: General Nordic Questionnaire[36] and supplemented it with select items from the questionnaire for handwork[37]. The questionnaire from Haines et al.[37] was developed for individuals with Dupuytren's contracture, and neither questionnaire has been validated in CTS patients. The questionnaire used in this study may not have accurately captured the impact of hand work in this population.

Our results point towards the advantage of using an array of ultrasound outcome measures as viable markers to predict median nerve functional changes in 6 months. We found that tendon-SSCT mechanics and intraneural blood flow velocity were the best ultrasound outcomes to predict median nerve motor and sensory changes 6 months later. Our results may also highlight the importance of repeat testing and repeated follow-ups to track CTS progression. Although our results demonstrate that ultrasound can provide prognostic value, our statistical results show that they account for a small proportion of neurophysiological changes. Future studies should explore ultrasound in the prognosis of CTS cases with a larger cohort. Determining the predictive ability of ultrasound examination can help develop "biomarkers" of the condition and improve the detection, treatment and management of CTS.

3.6 References

1.   Luckhaupt S, Dahlhamer J. 2013. Prevalence and work-relatedness of carpal tunnel
      syndrome in the working population, United States, 2010 national health interview
      survey. Am. J. Ind. Med. 56(6):615–624.

2.   Roquelaure Y, Chazelle E, Gautier L, et al. 2017. Time trends in incidence and
      prevalence of carpal tunnel syndrome over eight years according to multiple data
      sources: Pays de la Loire study. Scand. J. Work. Environ. Heal. 43(1):75–85.

3.   Keir PJ, Farias Zuniga A, Mulla DM, Somasundram KG. 2019. Relationships and
      Mechanisms Between Occupational Risk Factors and Distal Upper Extremity
      Disorders. Hum. Factors. [Epub ahead of print].

4.   Barcenilla A, March LM, Chen JS, Sambrook PN. 2012. Carpal tunnel syndrome
      and its relationship to occupation: A meta-analysis. Rheumatology 51(2):250–261.

5.   Kozak A, Schedlbauer G, Wirth T, et al. 2015. Association between work-related
      biomechanical risk factors and the occurrence of carpal tunnel syndrome: an
      overview of systematic reviews and a meta-analysis of current research. BMC
      Musculoskelet. Disord. 16(231):1–19.

6.   Roquelaure Y, Garlantézec R, Evanoff BA, et al. 2020. Personal, biomechanical,
      psychosocial, and organizational risk factors for carpal tunnel syndrome: a
      structural equation modeling approach. Pain 161(4):749–757.

7.   Harris-Adamson C, Eisen EA, Neophytou A, et al. 2016. Biomechanical and
      psychosocial exposures are independent risk factors for carpal tunnel syndrome:
      assessment of confounding using causal diagrams. Occup Env. Med 73(11):727–

734.

8.   Rempel DM, Gerr F, Harris-Adamson C, et al. 2015. Personal and workplace factors and median nerve function in a pooled study of 2396 US workers. J Occup Env. Med 57(1).

9.   Tat J, Kociolek AM, Keir PJ. 2013. Repetitive differential finger motion increases shear strain between the flexor tendon and subsynovial connective tissue. J Orthop Res 31(10):1533–1539.

10.   Tat J, Wilson KE, Keir PJ. 2015. Pathological changes in the subsynovial connective tissue increase with self-reported carpal tunnel syndrome symptoms. Clin. Biomech. 30(4):360–365.

11.   Vanhees M, Morizaki Y, Thoreson AR, et al. 2012. The effect of displacement on the mechanical properties of human cadaver subsynovial connective tissue. J Orthop Res 30(11):1732–1737.

12.   Yoshii Y, Zhao C, Zhao KD, et al. 2008. The effect of wrist position on the relative motion of tendon, nerve, and subsynovial connective tissue within the carpal tunnel in a human cadaver model. J Orthop Res 26(8):1153–1158.

13.   Ettema AM, Amadio PC, Zhao C, et al. 2006. Changes in the functional structure of the tenosynovium in idiopathic carpal tunnel syndrome: a scanning electron microscope study. Plast. Reconstr. Surg. 118(6):1413–22.

14.   Diao E, Shao F, Liebenberg E, et al. 2005. Carpal tunnel pressure alters median nerve function in a dose-dependent manner: A rabbit model for carpal tunnel syndrome. J Orthop Res 23(1):218–223.

15.   Bland JD. 2000. A neurophysiological grading scale for carpal tunnel syndrome. Muscle Nerve 23(8):1280–1283.

16.   Gooch CL, Weimer LH. 2007. The Electrodiagnosis of Neuropathy: Basic Principles and Common Pitfalls. Neurol. Clin. 25(1):1–28.

17.   Padua L, Padua R, Aprile I, et al. 2001. Multiperspective follow-up of untreated carpal tunnel syndrome: A multicenter study. Neurology 56(11):1459–1466.

18.   Braun RM, Jackson WJ. 1994. Electrical studies as a prognostic factor in the surgical treatment of carpal tunnel syndrome. J. Hand Surg. Am. 19(A):893–900.

19.   Azami A, Maleki N, Anari H, Iranparvar M. 2014. The diagnostic value of ultrasound compared with nerve conduction velocity in carpal tunnel syndrome. Int. J. Rheum. Dis. 17:612–620.

20.   El Miedany YM, Aty SA, Ashour S. 2004. Ultrasonography versus nerve conduction study in patients with carpal tunnel syndrome: Substantive or complementary tests? Rheumatology 43(7):887–895.

21.   Karadaĝ YS, Karadaĝ Ö, Çiçekli E, et al. 2010. Severity of Carpal tunnel syndrome assessed with high frequency ultrasonography. Rheumatol. Int. 30(6):761–765.

22.   Kutlar N, Bayrak A., Bayrak İ., et al. 2017. Diagnosing carpal tunnel syndrome with Doppler ultrasonography: a comparison of ultrasonographic measurements and electrophysiological severity. Neurol. Res. 39(2):126–132.

23.   Ziswiler H-R, Reichenbach S, Vögelin E, et al. 2005. Diagnostic value of sonography in patients with suspected carpal tunnel syndrome: A prospective

study. Arthritis Rheum. 52(1):304–311.

24.   Wiesler ER, Chloros GD, Cartwright MS, et al. 2006. The use of diagnostic

ultrasound in carpal tunnel syndrome. J Hand Surg 31A(1):726–732.

25.   Padua L, Pazzaglia C, Caliandro P, et al. 2008. Carpal tunnel syndrome:

Ultrasound, neurophysiology, clinical and patient-oriented assessment. Clin.

Neurophysiol. 119(9):2064–2069.

26.   Lee C., Kim T., Yoon E., Dhong E. 2005. Correlation of high-resolution

ultrasonographic findings with the clinical symptoms and electrodiagnostic data in

carpal tunnel syndrome. Ann. Plast. Surg. 54(1):20–23.

27.   Fujimoto K, Kanchiku T, Kido K, et al. 2015. Diagnosis of Severe Carpal Tunnel

Syndrome Using Nerve Conduction Study and Ultrasonography. Ultrasound Med.

Biol. 41(10):2575–2580.

28.   Pulikkottil BJ, Schub M, Kadow TR, et al. 2016. Correlating Median Nerve Cross-

sectional Area With Nerve Conduction Studies. J. Hand Surg. Am. 41(10):958–

962.

29.   El Miedany YM, El Gaafary M, Youssef S, et al. 2015. Ultrasound assessment of

the median nerve: a biomarker that can help in setting a treat to target approach

tailored for carpal tunnel syndrome patients. Springerplus 4(1):1–10.

30.   Joy V, Therimadasamy AK, Chan YC, Wilder-Smith EP. 2011. Combined Doppler

and B-mode sonography in carpal tunnel syndrome. J. Neurol. Sci. 308:16–20.

31.   Farias Zuniga A, Ghavanini AA, Israelian G, Keir PJ. 2020. Blood flow velocity

but not tendon mechanics relates to nerve function in carpal tunnel syndrome

patients. J. Neurol. Sci. 411(116694).

32.   Leis AA, Trapani VC. 2000. Atlas of Electromyography. Oxford: Oxford University Press.

33.   Preston DC, Shapiro B. 2005. Electromyography and Neuromuscular Disorders: Clinical Electrophysiologic Correlations. Elsevier. 459–472 p.

34.   Wilson KE, Tat J, Keir PJ. 2017. Effects of Wrist Posture and Fingertip Force on Median Nerve Blood Flow Velocity. BioMed Res. Int. 2017:8 pages.

35.   Tat J, Kociolek AM, Keir PJ. 2015. Validation of Color Doppler Sonography for Evaluating Relative Displacement Between the Flexor Tendon and Subsynovial Connective Tissue. J Ultrasound Med 34(4):679–687.

36.   Lindström K, Elo A-L, Skogstad A, et al. 2000. User's Guide for the QPSNordic: General Nordic Questionnaire for psychological and social factors at work. Nordic Council of Ministers.

37.   Haines A, Levis C, Goldsmith CH, et al. 2017. Dupuytren's contracture and handwork: A case-control study. Am. J. Ind. Med. 60(8):724–733.

38.   Van Doesburg MHM, Yoshii Y, Henderson J, et al. 2012. Speckle-tracking sonographic assessment of longitudinal motion of the flexor tendon and subsynovial tissue in carpal tunnel syndrome. J Ultrasound Med 31(7):1091–1098.

39.   Freeland A., Tucci M., Barbieri R., et al. 2002. Biochemical Evaluation of Serum and Flexor Tenosynovium in Carpal Tunnel Syndrome. Microsurgery 22:378–385.

40.   Lundborg GN, Myers R, Powell H. 1983. Nerve compression injury and increased endoneurial fluid pressure : a " miniature compartment syndrome ". J. Neurol.

Neurosurg. Psychiatry 46:1119–1124.

41.   Sunderland S. 1976. The nerve lesion in the carpal tunnel syndrome. J. Neurol.

Neurosurg. Psychiatry 39(7):615–626.

42.   Evans KD, Roll SC, Volz KR, Freimer M. 2012. Relationship between intraneural

vascular flow measured with sonography and carpal tunnel syndrome diagnosis

based on electrodiagnostic testing. J Ultrasound Med 31:729–736.

Chapter 4: Thirty minutes of Sub-Diastolic Blood Flow Occlusion Alters Carpal Tunnel Tissue Function and Mechanics

Amanda Farias Zuniga (MSc), Peter J. Keir* (PhD)

Department of Kinesiology, McMaster University, Hamilton, ON, Canada

*Corresponding Author:

Peter J. Keir, PhD
McMaster University
Department of Kinesiology
Ivor Wynne Centre, Room 212
1280 Main Street West
Hamilton, ON, Canada, L8S4K1
Telephone: 905-525-9140 ext. 23543
Email: pjkeir@mcmaster.ca

Word Count: 5,462

4.1 Abstract

There is evidence that carpal tunnel syndrome (CTS) development is driven by vascular factors, specifically resulting from ischemia and edema. The purpose of this study was to investigate the vascular hypothesis of CTS development by quantifying the temporal effects of 30 minutes of sub-diastolic brachial blood flow occlusion on median nerve edema, intraneural blood flow velocity, nerve function as measured through nerve conduction study (NCS), tendon-connective tissue mechanics, and carpal tunnel tissue stiffness. Forty healthy volunteers underwent 30 minutes of sub-diastolic brachial occlusion while NCS and ultrasound examination were performed consecutively every 5-minutes. Motor latency ($p < 0.001$), sensory conduction velocity ($p < 0.001$), sensory amplitude ($p = 0.04$), nerve blood flow ($p < 0.001$), peak relative FDS-SSCT displacement ($p = 0.02$) and shear strain ($p = 0.04$) were significantly affected by partial ischemia. Our results highlight the dependency of carpal tunnel tissue function on adequate blood flow.

4.2 Introduction

Carpal tunnel syndrome (CTS) is a peripheral neuropathy of the median nerve at the wrist, that ultimately results in dysfunction of the sensory and motor fibres of the nerve. The underlying pathophysiology of CTS is not well understood due to complexity of causes, risk factors and presentation of symptoms, resulting in many cases of CTS to be considered idiopathic. Several mechanisms have been proposed including increased external compression on the nerve, increased hydrostatic pressure or carpal tunnel pressure (CTP), and the disruption of blood flow. There is significant evidence that altered nerve perfusion due to ischemia of the capillaries that supply the median nerve is a significant mechanism in CTS development (Diao et al., 2005; Gelberman et al., 1983; Lundborg et al., 1982; Rydevik et al., 1981; Sunderland, 1976; Szabo et al., 1983).

Circulation to the carpal tunnel is supplied by the radial and ulnar arteries in the forearm, which divide into small vessels that ultimately supply the nerve's internal (intraneural) and external (extraneural) microvasculature. Disruptions in normal circulation can threaten the function of carpal tunnel tissues, such as with chronic compression through elevated CTP, which is common in CTS. Chronic compression alters carpal tunnel hemodynamics as elevated CTP compress intra- and extraneural microvessels. This leads to ischemia (inadequate blood supply)(Rydevik et al., 1981) and edema (accumulation of fluid) (Lundborg et al., 1983), and result in deterioration of nerve function (Diao et al., 2005; Gelberman et al., 1983; Lundborg, 1975). The median nerve is prone to damage through edema as it lacks lymphatic vessels within the endoneurial space (Mackinnon, 2002; Rempel et al., 1999). This cascade of events is evident in

recent *in vivo* ultrasound studies that have investigated median nerve intraneural blood flow (Borire et al., 2017; Evans et al., 2012; Farias Zuniga et al., 2020; Joy et al., 2011; Wilson et al., 2017) and edema (Borire et al., 2016; Mallouhi et al., 2006; Nakamichi et al., 2000, 2002). High intraneural blood flow is considered pathologic as it is more detectable (Borire et al., 2017) and higher in symptomatic patients (Joy et al., 2011; Wilson et al., 2017). It is also typically higher in milder cases (Evans et al., 2012; Farias Zuniga et al., 2020), indicating elevated intraneural blood flow may be a compensatory response to ischemia in early stages of the condition. Median nerve edema, measured as an increase in nerve cross-sectional area (CSA), is also characteristic of individuals with CTS (Borire et al., 2016; El Miedany et al., 2004; Nakamichi et al., 2000, 2002), and increases with CTS severity (Borire et al., 2016; El Miedany et al., 2015; Farias Zuniga et al., 2020; Moran et al., 2009; Tatar et al., 2016). These observations are hypothesized to be the manifestation of cascading events in response to nerve ischemia, ultimately resulting in measurable neurological changes and symptoms of CTS.

Ischemia of the nerve and the resulting nerve edema generates an increase in endoneurial fluid pressure of the nerve (Lundborg et al., 1983). This leads to structural changes including fibrosis of the epineurium (outer layer) and perineurium (inner layer) of the nerve (Powell et al., 1986). Changes in nerve function are measurable through nerve conduction studies (NCS). NCS on CTS patients demonstrate changes in nerve conduction velocity and both the amplitude and latency of motor and sensory responses (Bland, 2000; Gooch et al., 2007) indicating median nerve dysfunction. Neurological

changes manifest in the characteristic symptoms of CTS such as pain, numbness and tingling, and can affect typical hand function.

Changes in the microcirculation of carpal tunnel tissues has also been shown to lead to chronic fibroblast invasion (Gupta et al., 2004), fibrosis and thickening of the epineurium (Faller, 1999; Mackinnon, 2002), and accumulation of scar tissue (Faller, 1999; Gupta et al., 2004). This leads to changes in its elastic properties (Ghajarzadeh et al., 2015) such that the nerve becomes stiffer (Orman et al., 2013). Ultrasound elastography is a relatively new imaging modality that quantifies tissue elasticity. Ultrasound elastography studies consistently report increased median nerve stiffness in CTS patients compared to healthy controls (Arslan et al., 2018; Ghajarzadeh et al., 2015; Kantarci et al., 2014; Kubo et al., 2017; Liao et al., 2015; Martin et al., 2017; Orman et al., 2013; Shen et al., 2013; Tatar et al., 2016; Wang et al., 2012; Xin et al., 2017; Yoshii et al., 2017b, 2017a). Changes in nerve stiffness have been proposed to precede changes in nerve size (Kantarci et al., 2014), reflecting the degenerative changes in the nerve (Miyamoto et al., 2014). Thus, elastography may be useful in identifying individuals in early stages of CTS, prior to neurophysiological changes.

The connective tissue within the carpal tunnel, known as the subsynovial connective tissue (SSCT), is important to vascular integrity, mechanical ability, and protection of tissues in the tunnel. The SSCT provides a collagenous network to support blood and lymphatic vessels that supply the median nerve and tunnel space (Guimberteau et al., 2010), absorbs mechanical stress within the carpal tunnel (Filius et al., 2014; Vanhees et al., 2012), and reduces gliding friction between the finger flexor tendons

during finger motion (Guimberteau et al., 2010). Recent work from our laboratory suggests that acute partial ischemia via brachial cuff occlusion has a significant effect on SSCT mechanics (Tse et al., 2019). Using colour Doppler sonography, local partial ischemia was found to decrease SSCT displacement during repetitive finger flexion-extension motion. These results demonstrate an interconnectedness between local blood supply and the ability of the SSCT to perform its functions. Indeed, a common histological finding in CTS patients is fibrosis of the SSCT (Ettema et al., 2004) along with vascular proliferation, hypertrophy, obstruction and wall thickening of the vessels that are integrated within the SSCT matrix (Jinrok et al., 2004).

The importance of regulating adequate and continuous blood supply to the carpal tunnel is evident from the literature. It has been demonstrated that inadequate blood flow affects both the structure and function of the median nerve and the surrounding tissues including the tendons and SSCT. Although the acute and prolonged effects of decreased blood supply on carpal tunnel tissue structure and function have been investigated individually, the effects of occlusion on these outcomes have not been investigated simultaneously. The temporal effects of ischemia have been reported almost only in seminal studies on intraneural blood vessels (Rydevik et al., 1981) and peripheral nerve sensory and motor conduction (Gelberman et al., 1983). Additionally, while ultrasound elastography has been employed to investigate median nerve stiffness, stiffness of the finger flexor tendons, which may change due to fibrosis of the SSCT, have not been well investigated.

The purpose of this study was to quantify the temporal effects of 30 minutes of sub-diastolic brachial blood flow occlusion on median nerve edema, intraneural blood flow velocity, nerve function as measured through NCS, tendon mechanics, and finger flexor tendon stiffness. It was hypothesized that 30 minutes of sub-diastolic blood pressure occlusion would result in: (i) median nerve edema, quantified by an increase in median nerve CSA; (ii) a decrease in intraneural blood flow velocity; (iii) relative displacement and shear strain between the finger flexor tendon and its adjacent SSCT; (iv) increased tendon stiffness; and (v) changes in NCS measures, such as an increase in motor latency, decrease in sensory conduction velocity, and decrease in motor and sensory amplitude, indicating nerve conduction impairment.

4.3 Materials and Methods

4.3.1 Participants

Forty healthy participants with no upper extremity disorders in the past year were recruited from the university population. Informed, written consent was obtained prior to data collection. Exclusion criteria for all participants include diagnosis of CTS, and any symptoms of CTS including pain, numbness or tingling in the hand. Participants were screened for symptoms of CTS using the Levine's CTS Questionnaire (Levine et al., 1993)(Appendix G) and Katz Hand Diagrams (Katz et al., 1990)(Appendix F) and were required to score "0" indicating no symptoms of CTS to participate. This study was approved by the Hamilton Integrated Research Ethics Board.

4.3.2 Protocol

Once written, informed consent was obtained, participants were required to rest seated for approximately 5 minutes and baseline blood pressure was collected using an automatic blood pressure cuff (Dinamap 100 V2, GE Healthcare, Milwaukee, WI). Blood pressure was collected 3 times and averaged to obtain one representative blood pressure. If one measurement was not within 10% of the previous measurement, a fourth measurement was taken and the erroneous measurement was removed from the average calculation. The calculated average blood pressure was then used to calculate 80% of the diastolic blood pressure (DBP), which was subsequently used as the level of inflation for the sphygmomanometer for the brachial occlusion part of the protocol.

The assessment was then performed on the right wrist and arm while the participant was supine, with the right shoulder abducted to 45°, elbow approximately between 0°-5° of flexion, and the forearm supinated. A custom splint fastened to a fixed surface immobilized the wrist and maintained each posture without impeding wrist and finger movement. The protocol began with baseline measurements of all outcome variables, starting with NCS followed by ultrasound assessment. A sonographic system (RS80A with Prestige, Samsung Medison, Seoul, South Korea) equipped with an 18 MHz linear probe (LA4-18B) was used to examine the median nerve, SSCT and FDS tendon and flexor digitorum profundus (FDP) tendon. Ultrasound assessment consisted of a battery of tests including: 1) B-mode images to quantify median nerve CSA; 2) pulse wave (PW) Doppler to quantify intraneural blood flow velocity; 3) shear wave elastography (SWE) to quantify finger flexor tendon stiffness; 4) and colour Doppler to

quantify FDS and SSCT individual displacements and relative displacement. For all

ultrasound tests, except for the fourth test, participants remained static, laying supine with

their arm and hand placed into the custom splint, with their hand and fingers were relaxed

and wrist in neutral position (0°). In the fourth test, participants were asked to move only

their middle finger through repetitive flexion-extension cycles. Following baseline data

collection, a manual cuff was secured around the upper right arm and inflated to 80% of

the participant's resting DBP. Brachial artery occlusion was applied for 30 minutes

during which NCS and ultrasound assessments cycled through every five minutes (Figure

4.1).
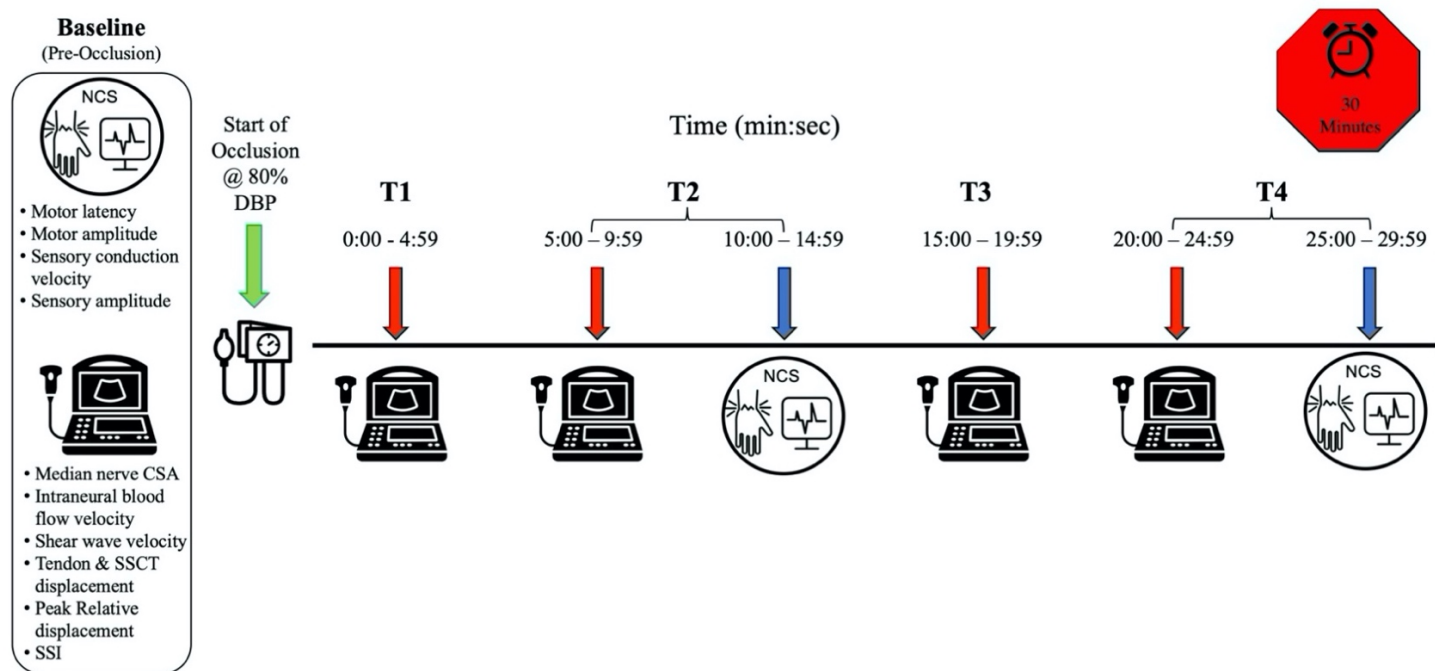
Figure 4. 1. Overview of protocol. Ultrasound and nerve conduction study (NCS) examination were done at baseline (pre-occlusion) and at 5-minute windows after the start of occlusion at 80% of diastolic blood pressure (DBP). Due to methodological constraints, simultaneous collection of ultrasound and NCS measurements were not possible, so they were performed consecutively. Within each ultrasound window, 4 ultrasound measures were collected in the same order each time: (1) axial B-mode images (for median nerve cross-sectional area (CSA)), (2) pulse-wave Doppler (for intraneural blood flow velocity), (3) shear wave elastography (for tendon stiffness), and (4) colour Doppler (for tendon-connective tissue motion). Within each NCS window, orthodromic motor and sensory nerve stimulation were performed, always starting with motor stimulation. Outcome measures for NCS included motor latency and amplitude, and sensory conduction velocity and amplitude. For the purpose of graphical representations of the results, the second ultrasound collection window plus the first NCS collection window will be referred to as T2 (timepoint 2), and the fourth ultrasound collection window plus the second NCS collection window will be referred to as T4 (timepoint 4).

4.3.3 Nerve Conduction Study

Median nerve NCS was completed following guidelines from the American Association of Electrodiagnostic Medicine (Jablecki et al., 1993) with techniques based on (Preston et al., 2005). Electromyography was recorded using 9 mm diameter Ag-AgCl surface electrodes. For motor NCS, the active electrode (G1) was placed on the thumb over the abductor pollicis brevis motor point, and the reference electrode (G2) was placed distally over the tendon at the first metacarpophalangeal joint. Nerve stimulation was delivered with a constant current stimulator (DS7AH; Digitimer, Welwyn Garden City, UK) using a square wave pulse (200 μs pulse width). Stimulation occurred 70 mm from the motor point measured on a curved line connecting the motor point to the wrist proximal to the wrist crease. The median nerve was also stimulated distally just superior to the elbow. For sensory NCS, electrodes were cut down to 2 cm × 2cm squares and placed on the proximal and middle phalanges of the index finger, with the G1 electrode placed proximally. Stimulation was applied from a distance of approximately 130 mm and 275 mm from the G1 electrode. Distances between cathode and G1 electrode were measured and recorded for all participants and used in the calculation of sensory conduction velocity. The stimulation site was traced on to the participant using a water-resistant marker to maintain consistency of placement during the occlusion portion of the protocol. Motor and sensory NCS were performed in an orthodromic fashion. A wet ground was placed around the right forearm away from all collection sites. Measurements were amplified (× 1000), band pass filtered (20 Hz – 2.5 kHz)(Model 2024F; Intronix Technologie Corporation, Bolton, ON, Canada). All signals were

digitized at 5 kHz (Cambridge Electronic Design, Cambridge, UK) and analyzed with commercial software (Signal, version 6.02, Cambridge Electronic Design).

4.3.4 Ultrasound

4.3.4.1 B-mode imaging

The probe was first placed in an axial orientation on the palmar wrist surface and positioned at the carpal tunnel inlet at the level of the pisiform. Two B-mode images were captured at this level for further measurement of the median nerve CSA similar to previous protocols (Farias Zuniga et al., 2020) (Figure 4.2). With the transducer in this position, the perimeter of the transducer was traced onto the palmar surface of the participant's forearm using a water-resistant marker. This outline acted as a guide for obtaining images from this location once brachial occlusion began.
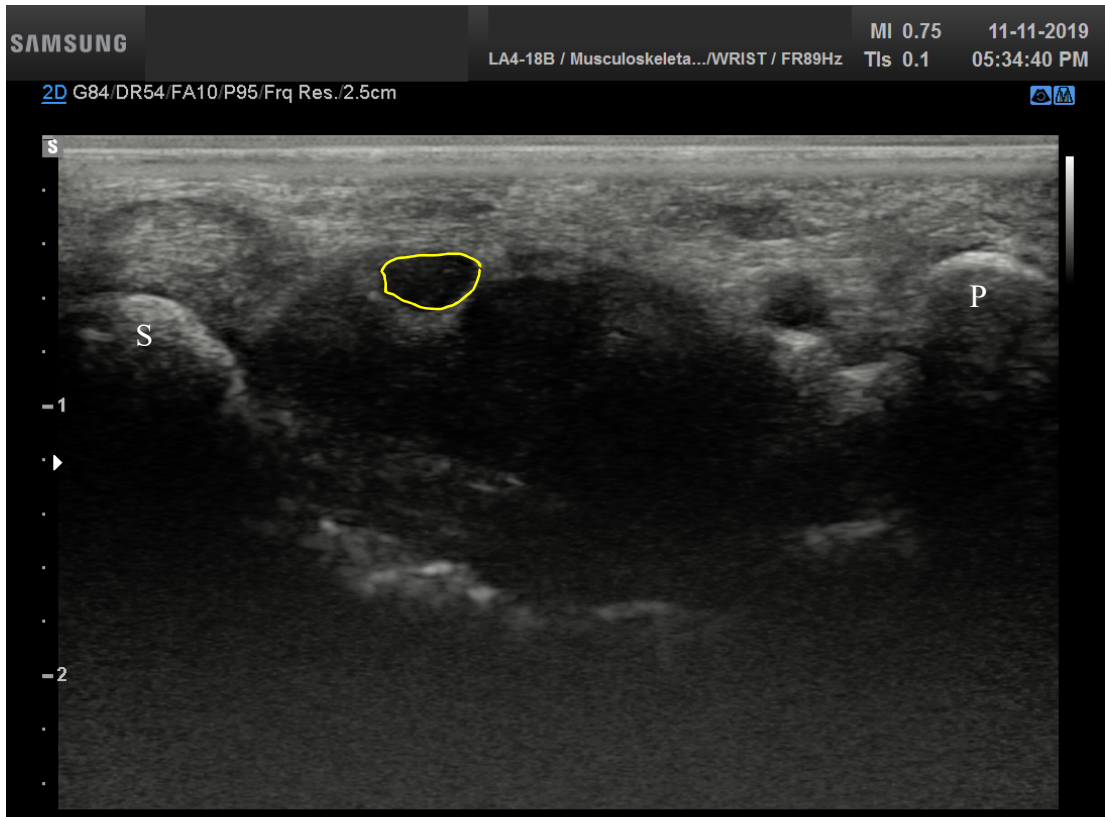
Figure 4. 2. B-mode image of the median nerve (outlined in yellow) and surrounding anatomical landmarks at the carpal tunnel inlet, including the scaphoid (S) and pisiform (P) carpal bones.

4.3.4.2 Pulse-wave Doppler imaging

Once the median nerve at the carpal tunnel inlet was identified, the probe was rotated and placed longitudinally at the carpal tunnel inlet. PW Doppler with a custom setting optimized for low velocities was used to evaluate median nerve intraneural blood flow following previously established methodology (Ehmke et al. 2020; Farias Zuniga et al. 2020; Wilson et al. 2017) . Colour Doppler was first used to locate the point of maximal intraneural blood flow along the nerve identified by the intensity of the color scale. Once the highest area of blood flow on color Doppler was identified, the PW

Doppler window (1 mm) was positioned over this area to obtain the blood flow pattern in duplex mode. The colour map was also used to determine the direction of flow, where a 20° beam steer and angle correction factor of 60° was subsequently applied. If no colour map was present, then the PW Doppler window was placed over the nerve until a consistent signal was achieved. Five seconds of "steady state" values were required to ensure stability of the signal. Steady state was defined as a consistent intraneural blood flow velocity signal. In this case, no beam steer or angle correction was applied. Two 12-s PW Doppler videos were collected (Figure 4.3). A 2.5 mm gel standoff wedge (Aquaflex gel pad, Cone Instruments, Solon, OH) was used between the skin surface and ultrasound probe for image optimization. The gel standoff wedge was also outlined onto the participant's wrist.
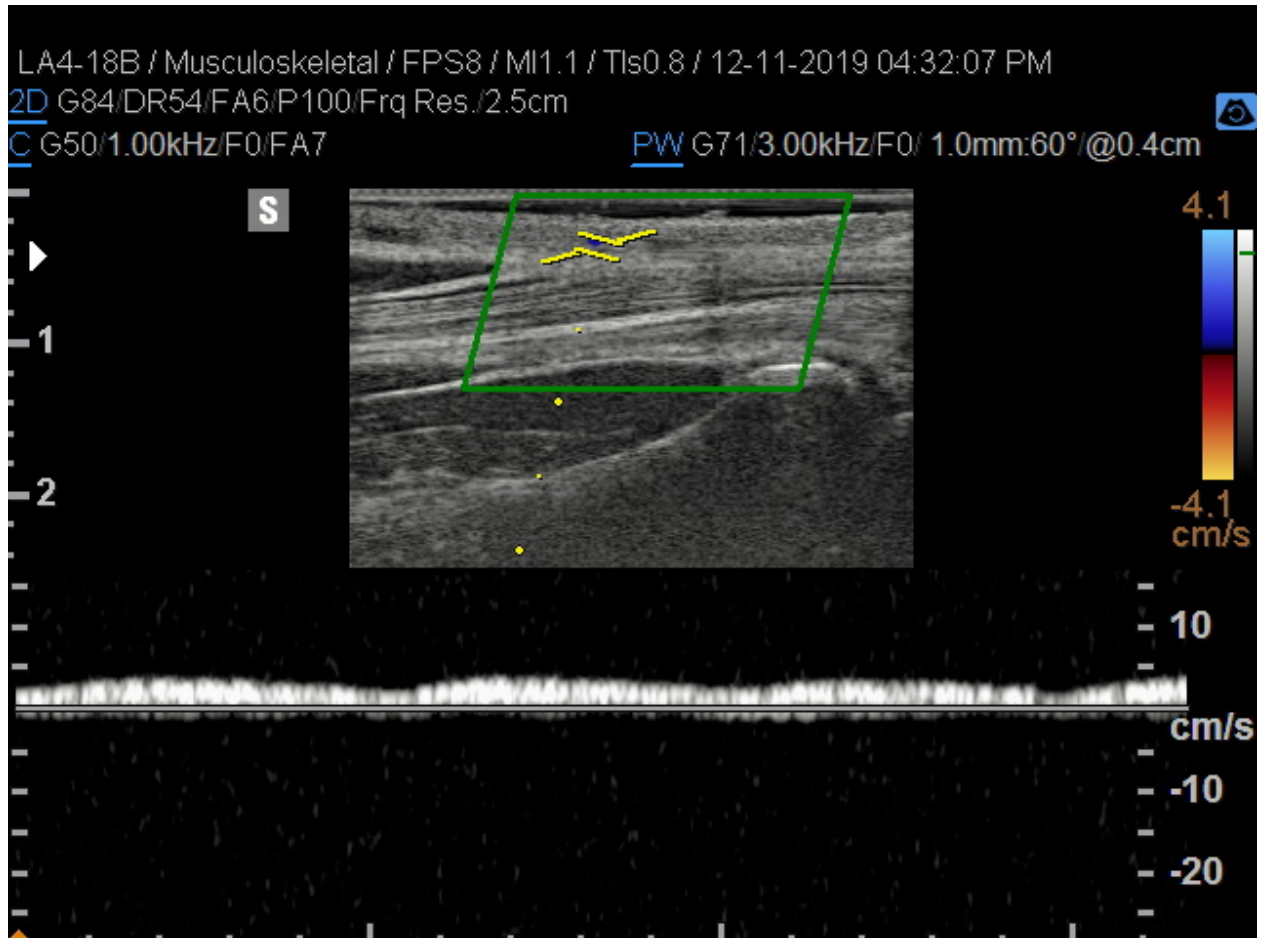
Figure 4. 3. Pulse-wave (PW) Doppler signal (white trace) of median nerve intraneural blood flow velocity (cm/s) collected in duplex mode. Colour Doppler was first used to detect directional blood flow. If a colour map was present (as shown above) a 20° beam steer and angle correction factor of 60° was applied and the PW Doppler gate (1 mm) was placed over the area of the greatest colour intensity (yellow region of interest marker).

4.3.4.3 Shear wave elastography

Tendon stiffness was then assessed using SWE with a 9 MHz linear probe (LA2-9A). The probe was placed over the proximal carpal tunnel at the point where the FDS and FDP tendons join (Figure 4.4). To avoid effects of compression, the transducer was

placed onto the skin with light contact and a generous amount of gel was used. The

machine's software allowed placement of a region of interest (ROI) box, which was

placed over the FDS and FDP tendons of the middle finger within the carpal tunnel.

Since it was not possible to change the shape or dimensions of the ROI box, it was not

possible to isolate for one tendon specifically or to isolate for the median nerve. Once

prompted, the machine displayed the shear wave velocity in m/s within the ROI which

was recorded and saved. Two measurements were taken, being careful not to move or

compress the transducer between collections. The transducer was also outlined onto the

participant's skin.
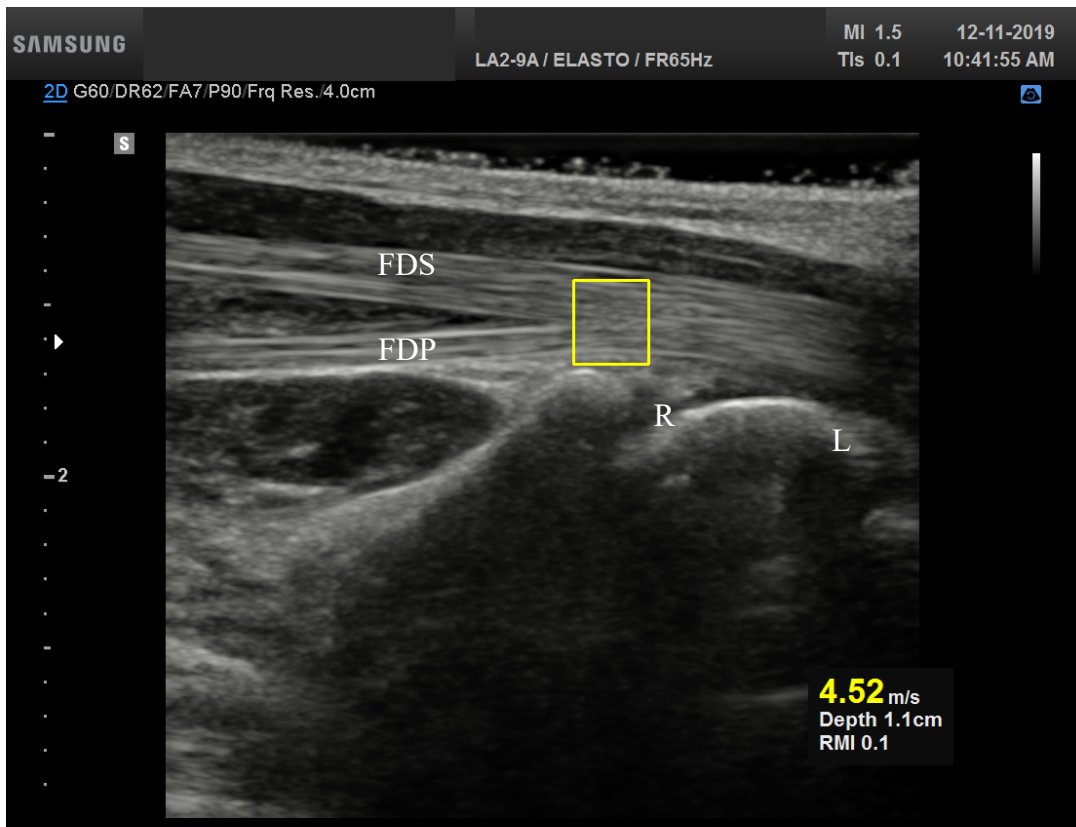
Figure 4. 4. Image of shear wave velocity measurement of carpal tunnel tendons using shear wave elastography (SWE). To obtain a shear wave velocity value for the tissue, a region of interest (ROI) box was placed over the area where both the flexor digitorum superficialis (FDS) and flexor digitorum profundus (FDP) tendons joint as they enter the carpal tunnel, and the shear wave velocity was displayed in m/s. The tip of the radius bone (R) and the lunate bone (L) were also used as anatomical guides. The image was saved and the shear wave velocity value were extracted.

4.3.4.4 Colour Doppler imaging

To examine FDS-SSCT motion, a 12 MHz linear array transducer (12L-RS) and ultrasound system (Vivid Q BT10, GE Healthcare, Milwaukee, WI) were optimized to predetermined colour Doppler settings (Farias Zuniga et al., 2020; Tat et al., 2013, 2015b). The transducer was positioned longitudinally at the distal wrist crease and electronically steered to 20°. A gel standoff wedge was used to optimize the angle of

insonation to approximately 60°. To identify the middle finger FDS tendons from other

tendons in the ultrasound image, participants performed flexion-extension movements

with their middle finger. Once the tendon and its adjacent SSCT were identified in the

image, the position of the transducer was traced onto the participant's wrist. Custom 3D

printed hand grips and Velcro straps were then used to then secure all other fingers and

allow movement of only the middle finger. Participants were instructed to perform

repetitive finger flexion-extension cycles with their middle finger, moving through their

full range of motion with each repetition. They were instructed to follow the audible

metronome which was set at 0.75 Hz to guide their movement speed. Participants

performed 2 sets of 10 repetitions of middle finger flexion-extension while colour

Doppler videos were recorded to capture middle finger FDS and its adjacent SSCT

motion.

4.3.5 Additional Measures

Although not part of our primary outcome variables, peripheral oxygen saturation

(SpO_2) and ratings of perceived discomfort (RPD) were also collected throughout the

protocol to monitor subject discomfort. A pulse oximeter (Homiee, Shenzhen, China)

was placed on the participant's right index finger, and SpO_2 was recorded at baseline and

at the beginning of every ultrasound collection block. Participants were asked to indicate

their RPD on a visual analog with a scale ranging between 0 (no discomfort) to 10

(intolerable discomfort). Perceived discomfort was collected at baseline and at the end of

every ultrasound collection block through the occlusion protocol.

4.3.6 Data Analysis

All NCS signals were analyzed using commercial software (Signal, version 6.02, Cambridge Electronic Design). Motor onset latency at the wrist and elbow were calculated as the time in milliseconds (ms) between the time of the stimulation pulse and the start of the leading edge of the motor response. The latency at the wrist was subtracted from the latency at the elbow to yield the motor onset latency response of the median nerve. Sensory onset latency was calculated in a similar fashion as the time (ms) between the stimulation pulse and the start of the leading edge of the sensory response. Sensory conduction velocity (m/s) was then calculated by dividing the measured distance between the stimulation site and recording electrode by the sensory latency. A custom script in Signal software calculated the maximum motor and sensory amplitude at each frame in the trial, and the maximum amplitude from each trial was extracted. Ultrasound images and videos were exported from the sonographic system for further analysis. To obtain median nerve CSA measurements, B-mode images were imported into ImageJ software (National Institutes of Health, Bethesda, MD) and the tracing tool was used (Figure 4.2). Measurements were completed by an independent rater and image order was randomized to avoid potential order bias when tracing the nerve. The inside border of the median nerve was traced and values were rounded to the nearest 0.01 mm^2. Since two B-mode images were taken at each timepoint, analysis was performed on both images and then averaged to result in one median nerve CSA value per time point. PW Doppler videos were exported as high resolution AVI video files and imported to the Measurements from Arterial Ultrasound Imaging (MAUI) analysis software (Hedgehog

Medical Inc., Waterloo, ON)(Figure 4.3). Average peak blood flow velocity within a 5

second window was determined from each video. Since two videos were collected at

each timepoint, both videos were analyzed and then averaged to yield one peak blood

flow velocity value (cm/s) per timepoint. Shear wave velocity (m/s) values from SWE

were extracted from the saved images (Figure 4.4). For each time point, the mean of two

collected values provided a single representative shear wave velocity. FDS tendon and

SSCT tissue motion from the repetitive motion trials were analyzed offline using EchoPac

analysis software (General Electric Healthcare, Milwaukee, WI) following previously

established processes (Tat et al. 2015a,b). FDS and SSCT velocities were extracted from

the colour Doppler videos by placing three markers collinearly over each tissue of

interest. Tissue motion was tracked on a frame-by-frame basis throughout the video to

ensure the markers captured the motion of the tissues of interest at all times. From this

analysis, tissue velocities were produced for each marker, which were then imported into

a custom Python program for further analysis. Tissue velocities from the three markers

were averaged to yield one representative tissue velocity for FDS and SSCT. Artifacts

were detected and removed, and the signal was low-pass filtered (4 Hz, 2nd order

Butterworth) and corrected for the angle of insonation ($\cos\theta$). Velocities were integrated

on a point-by-point basis to calculate displacement for each tissue. Peak tissue

displacement was calculated for the FDS and SSCT separately. Peak relative FDS-SSCT

displacement ("peak relative displacement") was calculated point-by-point as the

difference between peak FDS and SSCT displacement at each flexion-extension cycle.

Shear strain index (SSI) was calculated as the difference between peak FDS displacement

and peak SSCT displacement divided by the peak FDS displacement, multiplied by 100%.

4.3.7 Statistical Analysis

Descriptive statistics (mean ± standard deviation (SD)) were calculated for all measures at each timepoint. Outliers were identified and excluded from analysis if they exceeded physiological limits reported in the literature. Linear mixed effects analysis was performed in R (version 3.5.1) and R Studio (version 1.1.463, Boston, MA) using the lme4 package (Bates et al., 2012) to analyze the relationship between time and each outcome variable (median nerve CSA, intraneural blood flow velocity, motor latency, motor amplitude, sensory conduction velocity, sensory amplitude, shear wave velocity, peak FDS displacement, peak SSCT displacement, peak relative displacement, SSI). Time was treated as a categorical variable given that collection of each outcome variable was collected within blocks. The effects of occlusion were assessed by comparing each timepoint (T1-T4) to the baseline measurement. Time was entered as a fixed effect, and subject as a random effect. For all outcome variables, the full data set (N = 40) was included in the statistical analysis. For all tissue motion variables (FDS displacement, SSCT displacement, peak relative displacement and SSI) a subset of the data (N = 11) was included in the statistical analysis. P-values were obtained using lmerTest function in the "car" package (Kuznetsova et al., 2017). Significance was set a $p < 0.05$.

4.4 Results

A total of forty participants (20 males, 20 females; age = 23.3 ± 4.1 years) participated in the study. Participants were normotensive with a mean systolic blood pressure of 116.6 ± 11.7 mm Hg, and mean diastolic blood pressure of 66.9 ± 6.8 mm Hg. The average pressure used for cuff inflation was 53.5 ± 5.6 mm Hg.

The effect of occlusion time on all outcome variables is shown in Figure 4.5. Statistical analysis using linear mixed effects models revealed significant effects of occlusion on both NCS and ultrasound measures including: motor latency, sensory conduction velocity, sensory amplitude, intraneural blood flow velocity, peak relative displacement, and SSI. Occlusion did not significantly affect median nerve CSA or tissue stiffness. Occlusion had significant effects on NCS outcomes, where motor latency and sensory conduction velocity were significantly different at T2 ($p < 0.001$) and T4 ($p < 0.001$). Sensory amplitude was significantly different at T4 ($p = 0.04$). Intraneural blood flow velocity was statistically significant at all timepoints following the onset of occlusion ($p < 0.001$). Peak relative displacement ($p = 0.02$) was significantly different T2, and SSI ($p = 0.04$) was significant at T2 and T3. The effects of brachial occlusion on each outcome variable is described further.
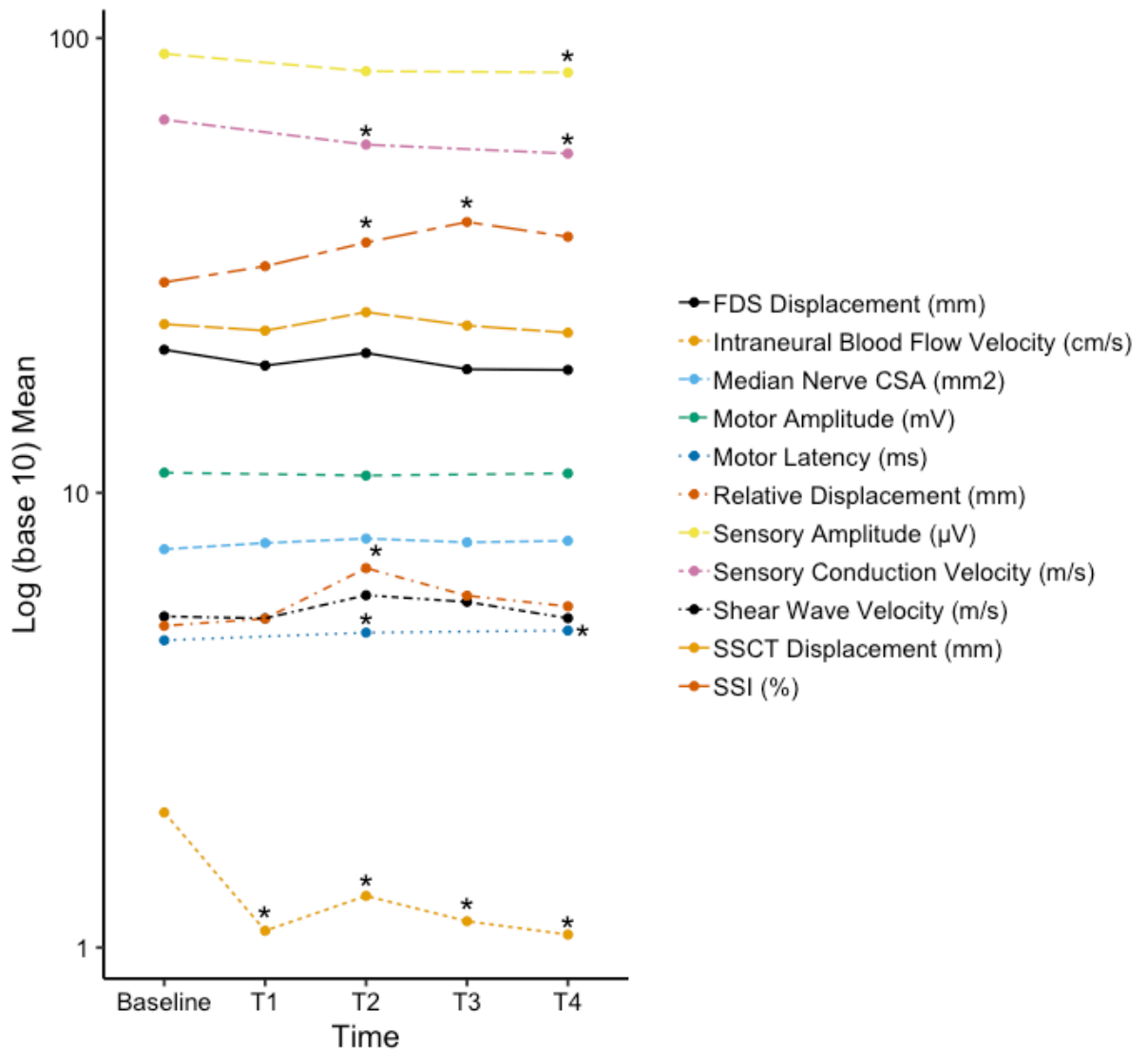
Figure 4. 5. Mean effect of occlusion on all nerve conduction study (NCS) and ultrasound outcome measures. Data was log transformed (base 10) for visual representation and plotted against occlusion timepoints on the x-axis. Occlusion time is represented by blocks (T1-T4) as indicated in the study protocol above (Figure 4.1). Brachial occlusion significantly affected motor latency, sensory conduction velocity, sensory amplitude, intraneural blood flow velocity, peak relative displacement and shear strain index (SSI). Significance ($p < 0.05$) is denoted by (*). All timepoints (T1-T4) of each outcome variable were compared to that variable's value at Baseline.

4.4.1 Nerve Conduction Study Outcomes

Motor latency, sensory conduction velocity and sensory amplitude significantly changed with brachial occlusion at 80% DBP. Motor latency was significantly longer after 10 minutes of occlusion (T2) ($p < 0.001$) and after 25 minutes of occlusion (T4) ($p < 0.001$) compared to baseline (Figure 4.6a). At baseline, mean motor latency was 4.74 ± 0.57 ms and increased to 4.92 ± 0.55 ms at T2. Motor latency remained elevated at T4, with a mean motor latency of 4.98 ± 0.50 ms. Sensory conduction velocity was significantly lower after 10 minutes (T2) ($p < 0.001$) and 25 minutes (T4) ($p < 0.001$) of occlusion (Figure 4.6b). Sensory conduction velocity at baseline was 66.2 ± 9.77 m/s and significantly decreased following occlusion to 58.3 ± 8.81 m/s at T2. Sensory amplitude at baseline was 92.3 ± 31.1 μV and significantly decreased after 25 minutes of occlusion (T4) ($p = 0.04$) to 84.0 ± 32.9 μV (Figure 4.6c). Motor amplitude was not significantly affected by occlusion time.
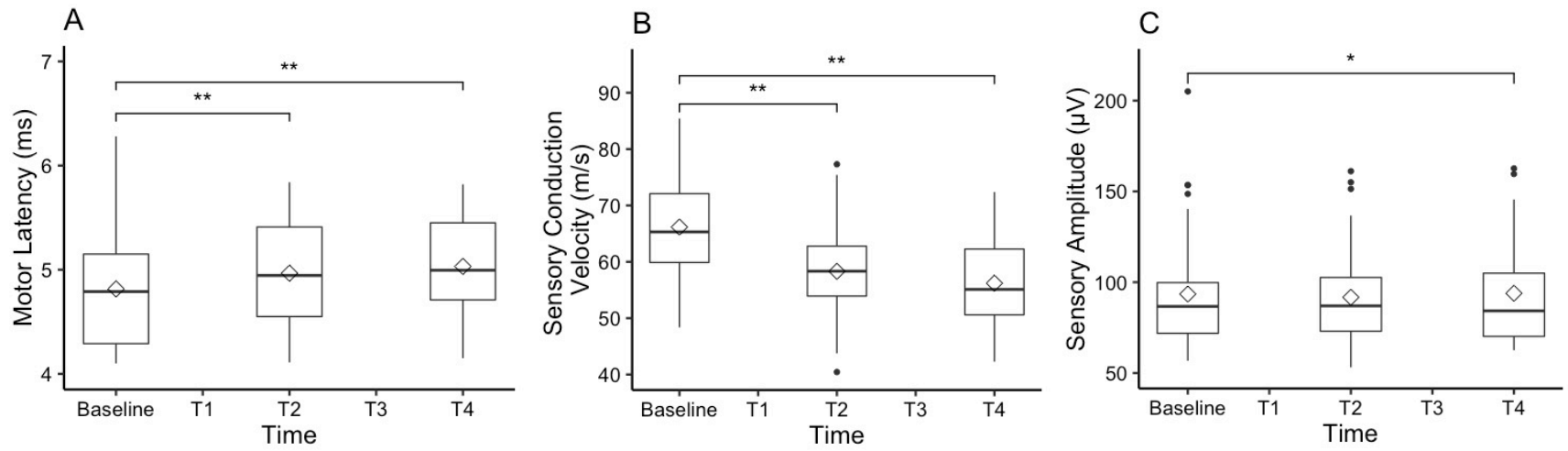
Figure 4. 6. Boxplots of median nerve motor latency (ms), sensory conduction velocity (m/s) and sensory amplitude (μV) at baseline and over occlusion time (T1-T4; see Figure 4.1 for description of timepoint blocks). Mean (open diamonds), median (center line), 25th and 75th percentile (upper and lower horizontal lines of the box, respectively), and range no larger than 1.5 times the interquartile range between the first and third quartile (lines extending above and below) are displayed. Outliers are represented by black dots. A: Motor latency was significantly different from baseline at T2 ($p < 0.001$ "**") and T4 ($p < 0.001$ "**"). B: Sensory conduction velocity was significantly different from baseline at T2 ($p < 0.001$ "**") and T4 ($p < 0.001$ "**"). C: Sensory amplitude was significantly different from baseline at T4 ($p = 0.04$ "*").

4.4.2 Ultrasound Outcomes

4.4.2.1 Intraneural Blood Flow Velocity

Intraneural blood flow velocity was significantly affected upon immediate occlusion of brachial blood flow ($p < 0.001$, Figure 4.7). At baseline, prior to brachial occlusion, mean intraneural blood flow velocity was 1.98 ± 1.80 cm/s. Upon occlusion, intraneural blood flow velocity decreased to 1.09 ± 0.68 cm/s immediately (T1), and remained significantly lower compared to baseline at all remaining timepoints. Intraneural blood flow velocity was 1.30 ± 0.93 cm/s at T2, 1.14 ± 0.71 cm/s at T3, and 1.07 ± 0.98 cm/s at T4.
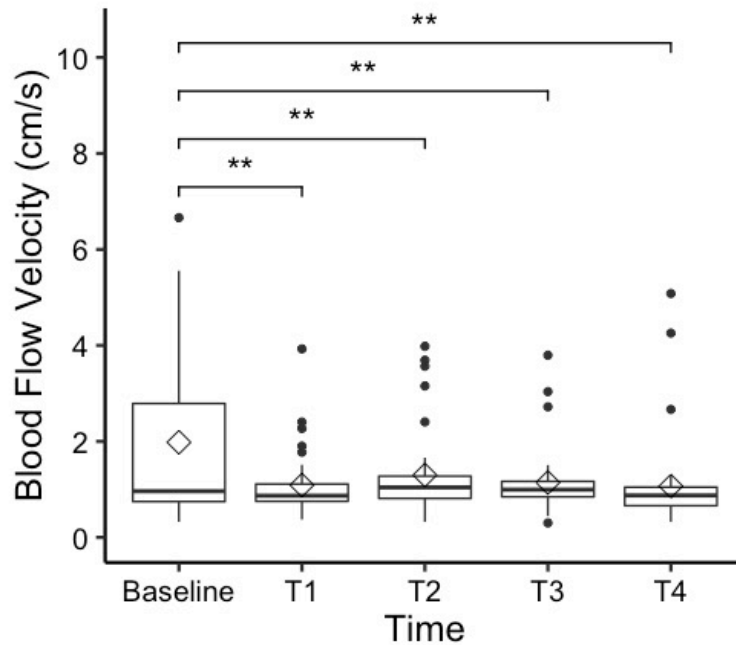
Figure 4. 7. Boxplots of median nerve intraneural blood flow velocity (cm/s) at baseline and over occlusion time (T1-T4; see Figure 4.1 for description of timepoint blocks). Mean (open diamonds), median (center line), 25th and 75th percentile (upper and lower horizontal lines of the box, respectively), and range no larger than 1.5 times the interquartile range between the first and third quartile (lines extending above and below) are displayed. Outliers are represented by black dots. Intraneural blood flow velocity was significantly (p < 0.001 "**") different at all timepoints (T1-T4) compared to baseline.

4.4.2.2 Tissue Displacement

Statistical analysis revealed a significant effect of brachial occlusion on peak relative displacement (Figure 4.8a) and SSI (Figure 4.8b). At baseline, mean peak relative displacement was 5.1 ± 1.9 mm, and increased significantly (p = 0.02) after 10 minutes of occlusion (T2) to 6.8 ± 2.9 mm. Peak relative displacement was not significantly different from baseline at any other timepoint.   Shear strain index was 29.0 ± 14.6 % at baseline and increased significantly (p = 0.03) to 35.5 ± 15.5 % at T2 after

five minutes of occlusion, and to 39.4 ± 24.0 % after 10 minutes of occlusion (p = 0.03).

SSI was not significantly different at any other timepoints compared to baseline.

Individual tissue displacements (FDS and SSCT) were not affected by occlusion time.
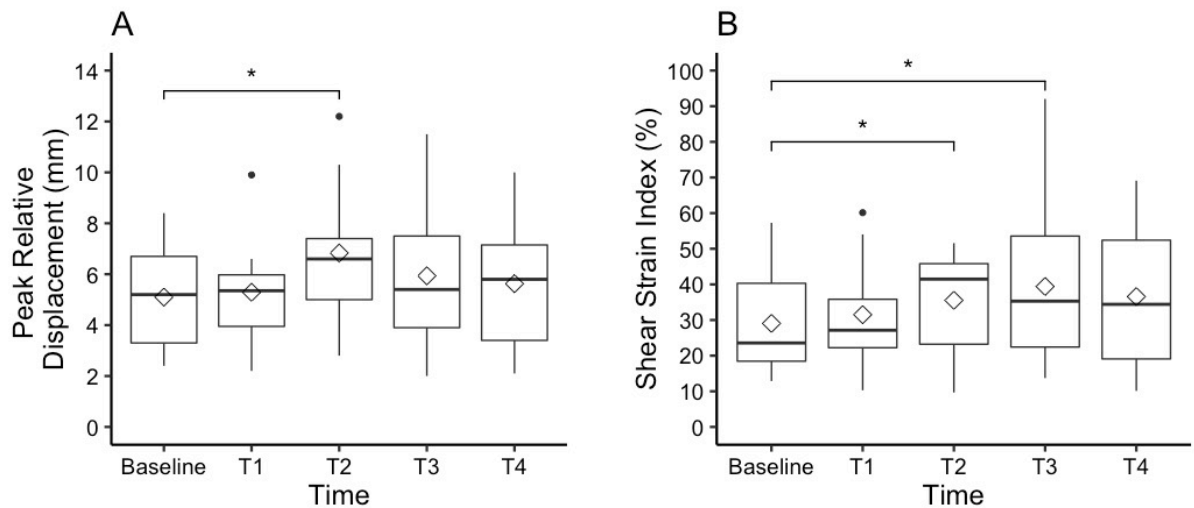
Figure 4. 8. Boxplots of (A) peak relative displacement (mm) and (B) shear strain index (SSI)(%) at baseline and over occlusion time (T1-T4; see Figure 4.1 for description of timepoint blocks). Mean (open diamonds), median (center line), 25th and 75th percentile (upper and lower horizontal lines of the box, respectively), and range no larger than 1.5 times the interquartile range between the first and third quartile (lines extending above and below) are displayed. Outliers are represented by black dots. Peak relative displacement (p = 0.02 "*") between the flexor digitorum superficialis (FDS) and the subsynovial connective tissue (SSCT) was significantly different from baseline at T2. SSI (p = 0.03 "*") was significantly different from baseline at T2 and T3.

4.4.3 Additional Measures

SpO$_2$ and RPD remained relatively stable throughout the protocol. All SpO$_2$ were

above an average of 96% throughout the protocol, and all RPD were a 4 or less

corresponding to "mild to moderate" discomfort.

4.5 Discussion

In this study, the effects of compromised blood flow on median nerve function was tested as a model of CTS development due to vascular factors. The purpose of this study was to investigate the effects of 30 minutes of sub-diastolic brachial occlusion on the function and structure of carpal tunnel tissues. We quantified the effects of blood flow occlusion on median nerve edema, tissue stiffness, intraneural blood flow velocity, FDS and SSCT displacement and relative displacement, and motor and sensory changes as measured through NCS. Brachial occlusion at 80% DBP had significant effects on median nerve conduction, median nerve intraneural blood flow and FDS-SSCT mechanics. Median nerve motor latency and sensory conduction velocity were significantly affected after 10 minutes of occlusion, and sensory amplitude was significantly affected after 25 minutes of occlusion. Intraneural blood flow velocity was affected immediately once brachial occlusion was applied and the effects persisted throughout the 30 minutes of occlusion. Peak relative displacement and SSI of the FDS and SSCT were significantly higher after 5-10 minutes of occlusion. Overall, this occlusion model may be used in future investigations as a way to induce "temporary CTS" in healthy individuals, with minimal discomfort to participants.

Our results support the hypothesis that vascular mechanisms are responsible for CTS development (Lundborg et al., 1983; Sugimoto et al., 1994; Sunderland, 1976). Brachial occlusion at 80% DBP drove significant neurophysiological changes and a decline in intraneural blood flow velocity. The effects of blood flow occlusion on median

nerve function and intraneural blood flow have been documented in both human and animal models. Gelberman and colleagues (1983) measured motor and sensory latencies of the median nerve after 30-240 minutes of compression at increasing pressures, and found that motor and sensory responses were significantly affected at 40-50 mm Hg (Gelberman et al., 1983). In rat tibial nerves, nerve microcirculation was significantly decreased or completely stopped between 50-70 mm Hg (Rydevik et al., 1981). The average cuff pressure used in our protocol was 53.5 ± 5.6 mm Hg, and we observed significant changes in motor and sensory at this level of cuff occlusion. Sensory deficits were most predominant, with sensory conduction velocity decreasing by 12% from baseline, and sensory amplitude decreasing by 9%. Additionally, we observed a significant and immediate decline in intraneural blood flow velocity at the onset of brachial occlusion, which remained low throughout the entirety of the protocol. Together, these results suggest that brachial occlusion resulted in decreased intraneural blood flow, which led to measurable changes in nerve function. Sensory nerve fibres were more affected by this transient nerve ischemia, which was expected since sensory fibres are more susceptible to damage (Kilmer et al., 2002). In the literature, prolonged compression has been reported to lead to increased endoneurial fluid pressure (Lundborg et al., 1983), resulting in median nerve edema and swelling. We did not observe a significant change in median nerve CSA, indicating that significant nerve swelling did not occur during this 30-minute protocol. This suggests that the observed effects were due to ischemia and not to the additional effects of edema. It is possible that if our protocol

continued beyond 30 minutes we may have seen nerve edema begin, and further deficits in nerve conduction would have been recorded. As an additional measure, we also evaluated SpO_2 throughout the protocol via a pulse oximeter. We observed no significant declines in SpO_2 during the occlusion protocol. This seems to indicate that the vascular dynamics within the carpal tunnel are important even if the nerve is receiving adequate oxygen supply.

We also saw a significant increase in peak relative FDS-SSCT displacement and SSI, indicative of increased shear strain between the finger flexor tendons and SSCT. Tendon-SSCT relative displacement is consistently reported to be higher in CTS symptomatic or confirmed patients (Filius et al., 2015; Tat et al., 2015b; van Doesburg et al., 2012), reflecting abnormal gliding of the SSCT. SSI in patients or CTS symptomatic individuals has been reported to be 30 – 79% (Farias Zuniga et al., 2020; Filius et al., 2015; Schrier et al., 2020; Tat et al., 2015b; van Doesburg et al., 2012). In our investigation, SSI reached an average peak value of 39.4% after 10 minutes of occlusion in our healthy population, thus comparable to CTS symptomatic individuals and patients. This demonstrates the high dependency of the SSCT on local perfusion to maintain normal functioning.

Although we saw significant changes in median nerve function and tendon-SSCT mechanics, we did not observe significant changes in tendon stiffness. Overall, tendon stiffness did not change from baseline throughout the occlusion protocol as we had hypothesized, likely due to the acute nature of this protocol. Changes in tissue stiffness

are a result of fibrosis, thickening and the accumulation of scar tissue (Faller, 1999; Gupta et al., 2004), processes which take many months, if not years, to develop.

Due to methodological constraints, there are some limitations to these study results and interpretation. It was not possible to collect both ultrasound and NCS outcomes simultaneously due to the limited anatomical space available at the wrist. Since the median nerve was of interest for all of our outcome variables, it was not possible to have both the nerve stimulation bar and the ultrasound probe in the same location for simultaneous measurement. To accommodate we chose to alternate between NCS and ultrasound collection over the 30 minutes of occlusion. As such, we assumed in some of our interpretation that changes in NCS and ultrasound outcomes were occurring concurrently although these measures were not taken at the same time. A second consideration is that limb temperature was not measured throughout the protocol. Limb temperature is known to affect NCS outcomes such as conduction velocity since limb temperature affects ion channel function, acetylcholinesterase activity, and muscle contractility (Gooch & Weimer 2007). However, the study was performed in a temperature controlled indoor setting, so limb temperature was assumed to not change significantly throughout the duration of the protocol or between participants. Finally, there is a possibility that there was an influence from external autonomic activation due to NCS that were performed both before baseline ultrasound measures and throughout the experimental protocol which may have affected our intraneural blood flow velocity measurements (Borire et al., 2018).

4.6 Conclusion

Our results indicate that carpal tunnel tissue function is highly dependent on local blood flow, and supports ischemia as a significant mechanism in median nerve dysfunction and CTS development. We observed that 30 minutes of partial ischemia via brachial occlusion at 80% DBP induces significant functional and mechanical changes to the carpal tunnel tissues, specifically to the median nerve and SSCT. Our results show that the SSCT is a very important structure within the carpal tunnel and is significantly affected by inadequate blood flow. We observed that partial ischemia affected both the function of the SSCT itself, and the flow of blood through the SSCT to the nerve. The SSCT is the main linking element between finger function and nerve function, and is therefore the keystone for healthy hand function. These results indicate the importance of maintaining adequate blood supply to the carpal tunnel. This means that individuals with compromised blood flow may be at higher risk of developing CTS, such as individuals with atherosclerosis, or in workplaces requiring overhead work and prolonged static contractions of the upper extremity. Additionally, many of the observed outcomes in this investigation align with reported outcomes in CTS patients.

4.8 References

Arslan H, Yavuz A, İlgen F, Aycan A, Ozgokce M, Akdeniz H. The efficiency of
acoustic radiation force impulse (ARFI) elastography in the diagnosis and staging of
carpal tunnel syndrome. J Med Ultrason 2018;1–7.

Bates D, Maechler M, Bolker B, Walker S, Christensen RH., Singmann H, Dai B, Scheipl
F, Grothendieck G, Green P, Fox J. Package "lme4". CRAN. R Found Stat Comput
Vienna, Austria 2012;

Bland JD. A neurophysiological grading scale for carpal tunnel syndrome. Muscle Nerve
2000;23:1280–1283.

Borire AA, Arnold R, Pussell BA, Kwai NC, Visser LH, Simon NG, Kiernan MC,
Krishnan AV. Effects of hemodialysis on intraneural blood flow in end-stage kidney
disease. Muscle and Nerve 2018;57:287–293.

Borire AA, Hughes AR, Lueck CJ, Colebatch JG, Krishnan AV. Sonographic differences
in carpal tunnel syndrome with normal and abnormal nerve conduction studies. J
Clin Neurosci 2016;34:77–80.

Borire AA, Visser LH, Padua L, Colebatch JG, Huynh W, Simon NG, Kiernan MC,
Krishnan AV. Utility of maximum perfusion intensity as an ultrasonographic marker
of intraneural blood flow. Muscle Nerve 2017;55:77–83.

Diao E, Shao F, Liebenberg E, Rempel DM, Lotz JC. Carpal tunnel pressure alters
median nerve function in a dose-dependent manner: A rabbit model for carpal tunnel
syndrome. J Orthop Res 2005;23:218–223.

El Miedany YM, Aty SA, Ashour S. Ultrasonography versus nerve conduction study in patients with carpal tunnel syndrome: Substantive or complementary tests? Rheumatology 2004;43:887–895.

El Miedany YM, El Gaafary M, Youssef S, Ahmed I, Nasr A. Ultrasound assessment of the median nerve: a biomarker that can help in setting a treat to target approach tailored for carpal tunnel syndrome patients. Springerplus 2015;4:1–10.

Ettema AM, Amadio PC, Zhao C, Wold LE, An KN. A histological and immunohistochemical study of the subsynovial connective tissue in idiopathic carpal tunnel syndrome. J Bone Jt Surg 2004;86:1458–1466.

Evans KD, Roll SC, Volz KR, Freimer M. Relationship between intraneural vascular flow measured with sonography and carpal tunnel syndrome diagnosis based on electrodiagnostic testing. J Ultrasound Med 2012;31:729–736.

Faller DV. Endothelial cell responses to hypoxic stress. Clin Exp Pharmacol Physiol 1999;26:74–84.

Farias Zuniga A, Ghavanini AA, Israelian G, Keir PJ. Blood flow velocity but not tendon mechanics relates to nerve function in carpal tunnel syndrome patients. J Neurol Sci Elsevier, 2020;411.

Filius A, Thoreson AR, Wang Y, Passe SM, Zhao C, An K-N, Amadio PC. The effect of tendon excursion velocity on longitudinal median nerve displacement: Differences between carpal tunnel syndrome patients and controls. J Orthop Res 2015;33:483–487.

Filius A, Thoreson AR, Yang TH, Vanhees M, An KN, Zhao C, Amadio PC. The effect of low- and high-velocity tendon excursion on the mechanical properties of human cadaver subsynovial connective tissue. J Orthop Res 2014;32:123–128.

Gelberman RH, Szabo RM, Williamson RV., Hargens AR, Yaru NC, Minteer-Convery MA. Tissue pressure threshold for peripheral nerve viability. Clin Orthop Relat Res 1983;No. 178:285–291.

Ghajarzadeh M, Dadgostar M, Sarraf P, Emami-Razavi S., Miri S, Malek M. Application of ultrasound elastography for determining carpal tunnel syndrome severity. Jpn J Radiol 2015;33:273–278.

Gooch CL, Weimer LH. The Electrodiagnosis of Neuropathy: Basic Principles and Common Pitfalls. Neurol Clin 2007;25:1–28.

Guimberteau JC, Delage JP, McGrouther DA, Wong JKF. The microvacuolar system: how connective tissue sliding works. J Hand Surg Eur Vol 2010;35:614–622.

Gupta R, Rowshan K, Chao T, Mozaffar T, Steward O. Chronic nerve compression induces local demyelination and remyelination in a rat model of carpal tunnel syndrome. Exp Neurol 2004;187:500–508.

Jablecki CK, Andary MT, So YT, Wilkins DE, Williams FH. Literature review of the usefulness of nerve conduction studies and electromyography for the evaluation of patients with carpal tunnel syndrome. Muscle Nerve 1993;16:1392–1414.

Jinrok O, Zhao C, Amadio PC, An K-N, Zobitz ME, Wold LE. Vascular pathologic changes in the flexor tenosynovium (subsynovial connective tissue) in idiopathic

carpal tunnel syndrome. J Orthop Res 2004;22:1310–1315.

Joy V, Therimadasamy AK, Chan YC, Wilder-Smith EP. Combined Doppler and B-mode
    sonography in carpal tunnel syndrome. J Neurol Sci 2011;308:16–20.

Kantarci F, Ustabasioglu FE, Delil S, Olgun DC, Korkmazer B, Dikici AS, Tutar O,
    Nalbantoglu M, Uzun N, Mihmanli I. Median nerve stiffness measurement by shear
    wave elastography: A potential sonographic method in the diagnosis of carpal tunnel
    syndrome. Eur Radiol 2014;24:434–440.

Katz JN, Stirrat CR. A self-administered hand diagram for the diagnosis of carpal tunnel
    syndrome. J Hand Surg Am 1990;15:360–363.

Kilmer DD, Davis BA. Electrodiagnosis in carpal tunnel syndrome. Hand Clin
    2002;18:243–255.

Kubo K, Zhou B, Cheng Y-S, Yang T-H, Qiang B, An K-N, Moran SL, Amadio PC,
    Zhang X, Zhao C. Ultrasound elastography for carpal tunnel pressure measurement:
    A cadaveric validation study. J Orthop Res 2017;1–7.

Kuznetsova A, Brockhoff PB, Christensen RH. lmerTest Package: Tests in Linear Mixed
    Effects Models. J Stat Softw 2017;82:1–26.

Levine DW, Simmons BP, Koris MJ, Daltroy LH, Hohl G., Fossel AH, Katz JN. A self-
    administered questionnaire for the assessment of severity of symptoms and
    functional status in carpal tunnel syndrome. Class Pap Orthop 1993;75:1585–1592.

Liao Y, Lee W, Lee M, Chen W, Chiou H-J, Kuo T-T, Yeh C-K. Carpal Tunnel
    Syndrome : US Strain Imaging for Diagnosis. Radiology 2015;275:205–214.

Lundborg GN. Structure and Function of the Intraneural Microvessels as Related to Trauma, Edema Formation, and Nerve Function. J Bone Jt Surg 1975;57-A:938–948.

Lundborg GN, Gelberman RH, Minteer-Convery M, Lee YF, Hargens AR. Median nerve compression in the carpal tunnel—Functional response to experimentally induced controlled pressure. J Hand Surg Am 1982;7:252–259.

Lundborg GN, Myers R, Powell H. Nerve compression injury and increased endoneurial fluid pressure : a " miniature compartment syndrome ". J Neurol Neurosurg Psychiatry 1983;46:1119–1124.

Mackinnon SE. Pathophysiology of nerve compression. Hand Clin 2002;18:231–241.

Mallouhi A, Pültzl P, Trieb T, Piza H, Bodner G. Predictors of carpal tunnel syndrome: Accuracy of gray-scale and color doppler sonography. Am J Roentgenol 2006;186:1240–1245.

Martin MJ, Cartwright MS. A Pilot Study of Strain Elastography in the Diagnosis of Carpal Tunnel Syndrome. J Clin Neurophysiol 2017;34:114–118.

Miyamoto H, Halpern EJ, Kastlunger M, Gabl M, Arora R, Bellmann-Weiler R, Feuchtner GM, Jaschke WR, Klauser AS. Carpal Tunnel Syndrome : Diagnosis by Means of Median Nerve Elasticity — Improved Diagnostic Accuracy of US with Sonoelastography. Radiology 2014;270:481–486.

Moran L, Perez M, Esteban A, Bellon J, Arranz B, Del Cerro M. Sonographic measurement of cross-sectional area of the median nerve in the diagnosis of carpal

tunnel syndrome: Correlation with nerve conduction studies. J Clin Ultrasound 2009;37:125–131.

Nakamichi K-I, Tachibana S. Enlarged median nerve in idiopathic carpal tunnel syndrome. Muscle Nerve 2000;23:1713–1718.

Nakamichi K-I, Tachibana S. Cross-Sectional Area in Idiopathic Carpal Tunnel Syndrome : Diagnostic Accuracy. Muscle Nerve 2002;26:798–803.

Orman G, Ozben S, Huseyinoglu N, Duymus M, Orman KG. Ultrasound Elastographic Evaluation in the Diagnosis of Carpal Tunnel Syndrome: Initial Findings. Ultrasound Med Biol 2013;39:1184–1189.

Powell HC, Myers RR. Pathology of experimental nerve compression. Lab Invest 1986;55:91—100.

Preston DC, Shapiro B. Electromyography and Neuromuscular Disorders: Clinical Electrophysiologic Correlations. Elsevier, 2005.

Rempel DM, Dahlin L, Lundborg GN. Pathophysiology of nerve compression syndromes: response of peripheral nerves to loading. J Bone Joint Surg Am 1999;81:1600–10.

Rydevik B, Lundborg G, Bagge U. Effects of graded compression on intraneural blood flow: An in vivo study on rabbit tibial nerve. J Hand Surg Am 1981;6:3–12.

Schrier VJMM, Evers S, Geske JR, Kremers WK, Villarraga HR, Selles RW, Hovius SER, Gelfman R, Amadio PC. Relative Motion of the Connective Tissue in Carpal Tunnel Syndrome: The Relation with Disease Severity and Clinical Outcome.

Ultrasound Med Biol 2020;00:1–9.

Shen ZL, Geoffrey Vince D, Li Z-M. In Vivo Study of Transverse Carpal Ligament Stiffness Using Acoustic Radiation Force Impulse (ARFI) Imaging. PLoS One 2013;8:1–11.

Sugimoto H, Miyaji N, Ohsawa T. Carpal Tunnel Syndrome: Evaluation of Median Nerve Circulation with Dynamic Contrast-enhanced MR Imaging. Radiology 1994;190:459–466.

Sunderland S. The nerve lesion in the carpal tunnel syndrome. J Neurol Neurosurg Psychiatry 1976;39:615–626.

Szabo RM, Gelberman RH, Williamson RV, Hargens AR. Effects of increased systemic blood pressure on the tissue fluid pressure threshold of peripheral nerve. J Orthop Res 1983;1:172–178.

Tat J, Kociolek AM, Keir PJ. Repetitive differential finger motion increases shear strain between the flexor tendon and subsynovial connective tissue. J Orthop Res 2013;31:1533–1539.

Tat J, Kociolek AM, Keir PJ. Validation of Color Doppler Sonography for Evaluating Relative Displacement Between the Flexor Tendon and Subsynovial Connective Tissue. J Ultrasound Med 2015a;34:679–687.

Tat J, Wilson KE, Keir PJ. Pathological changes in the subsynovial connective tissue increase with self-reported carpal tunnel syndrome symptoms. Clin Biomech 2015b;30:360–365.

Tatar I., Kurt A, Yavasoglu NG, Hekimoglu B. Carpal tunnel syndrome :

elastosonographic strain ratio and cross- sectional area evaluation for the diagnosis

and disease severity . Med Ultrason 2016;18:305–311.

Tse CTF, Keir PJ. External Compression and Partial Ischemia Decrease Human Finger

Flexor Tendon and Subsynovial Connective Tissue Relative Motion. J Orthop Res

2019;1–7.

Van Doesburg MHM, Yoshii Y, Henderson J, Villarraga HR, Moran SL, Amadio PC.

Speckle-tracking sonographic assessment of longitudinal motion of the flexor tendon

and subsynovial tissue in carpal tunnel syndrome. J Ultrasound Med 2012;31:1091–

1098.

Vanhees M, Morizaki Y, Thoreson AR, Larson D, Zhao C, An K-N, Amadio PC. The

effect of displacement on the mechanical properties of human cadaver subsynovial

connective tissue. J Orthop Res 2012;30:1732–1737.

Wang Y, Qiang B, Zhang X, Greenleaf JF, An K-N, Amadio PC, Zhao C. A non-invasive

technique for estimating carpal tunnel pressure by measuring shear wave speed in

tendon: A feasibility study. J Biomech 2012;45:2927–2930.

Wilson KE, Tat J, Keir PJ. Effects of Wrist Posture and Fingertip Force on Median Nerve

Blood Flow Velocity. BioMed Res Int 2017;2017:8 pages.

Xin H, Hu H, Liu B, Liu X, Li X, Li J. Ultrasound elastographic evaluation of the median

nerve in hemodialysis with carpal tunnel syndrome. J Med Ultrason 2017;44:123–

131.

Yoshii Y, Tung WL, Ishii T. Strain and Morphological Changes of Median Nerve After

    Carpal Tunnel Release. J Ultrasound Med 2017a;36:1153–1159.

Yoshii Y, Tung WL, Ishii T. Measurement of median nerve strain and applied pressure

    for the diagnosis of carpal tunnel syndrome. Ultrasound Med Biol 2017b;43:1205–

    1209.

Chapter 5: DISCUSSION

5.1 Thesis Contributions

The etiology of CTS is complex, developing as a result of numerous mechanical, anatomical, structural, vascular and individual factors. As such, in this thesis I aimed to take a multifaceted approach to investigating the potential mechanism(s) behind the development and progression of CTS. Using a number of techniques, and both patient and healthy populations, this thesis demonstrates the interconnectedness between local blood flow, nerve function, and tendon-connective tissue kinematics which has not previously been demonstrated simultaneously. This thesis contributes significantly to our current understanding of CTS given the multitude of outcome measures, techniques, populations and unique study designs that were employed. Significant contributions were made through investigating CTS patients and conducting a follow-up investigation with the same sample. The greatest strength of this thesis was the study design of chapter four which allowed for the non-invasive quantification of the temporal effects of occlusion. Previously, the effects of ischemia on nerve function had been investigated in animal models or by using invasive techniques such as catheters. Through the combination of NCS and ultrasound, I was able to quantify the temporal effects of ischemia on the function and morphology of the nerve and the important surrounding tissues including the tendons and SSCT. While many of the aspects within this thesis have been previously investigated individually, this thesis provides a comprehensive view of how these factors are interconnected and dependent on one another. The results from this thesis provides significant evidence for the vascular influence of CTS.

5.2 The Relationship Between Median Nerve Blood Flow, Function, and Tendon-SSCT

Mechanics

Throughout the three investigations a clear relationship between median nerve

intraneural blood flow, tendon-SSCT kinematics, and nerve function began to emerge.

Each study in this thesis provides unique information which supports the vascular

influence on CTS development and progression. Several authors have emphasized that

vascular factors play a significant role in the development and progression of CTS (Diao

et al., 2005; Gelberman et al., 1983; Lundborg et al., 1982, 1983; Myers et al., 1986;

Powell et al., 1986; Rydevik et al., 1981; Szabo et al., 1983). More recent studies using

spectral Doppler ultrasound have also found associations between intraneural blood flow

velocity and symptomatic (Joy et al., 2011; Tat et al., 2015; Wilson et al., 2017) and NCS

confirmed CTS patients (Evans et al., 2012). My results from Chapter 2 demonstrate an

inverse relationship between intraneural blood flow velocity and CTS severity when

blood flow velocity is measured in either wrist flexion or extension. Intraneural blood

flow velocity is highest in mild patients and decreases with increasing severity. Evans et

al. 2012 also reported an inverse relationship been median nerve blood flow velocity and

CTS severity (Figure 5.1). Evans et al. (2012) found that intraneural blood flow velocity

was highest in individuals with the classical symptoms of CTS (pain, numbness, tingling)

but not confirmed diagnosis through electrodiagnostic testing. Results from Wilson et al.

(2017) support this relationship as they found CTS symptomatic individuals who were not

clinically diagnosed with CTS to have higher intraneural blood flow velocities than

healthy controls.
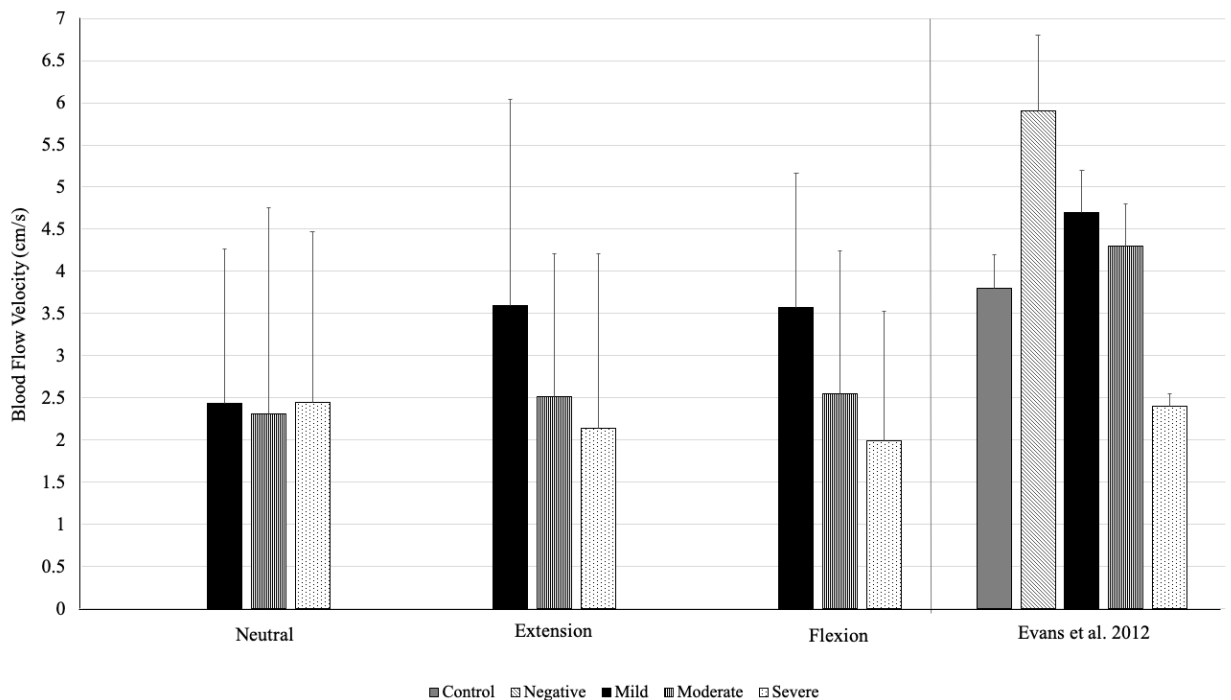
Figure 5. 1. Comparison of intraneural blood flow velocity (cm/s) results from Chapter 2 with results from Evans et al. (2012). Intraneural blood flow velocity was collected at the carpal tunnel inlet in both studies. Mean peak intraneural blood flow velocity is shown for each severity group, with control and negative participants from Evans et al. (2012). Overall, both studies demonstrate a negative relationship between intraneural blood flow velocity and CTS severity. Evans et al. (2012) did not define wrist posture in which intraneural blood flow velocity was collected.

In Chapter 3, we further observed a relationship between nerve blood flow and

function as we saw a concurrent increase in median nerve intraneural blood flow and an

improvement in nerve conduction outcomes over 6 months in this patient population. In

these patients, intraneural blood flow velocity increased by 11-39% across all three wrist

postures, while nerve motor latency improved (latency decreased) by 11% and amplitude

improved (increased) by 5%. Motor latency represents the fast conducting motor fibres,

while motor amplitude represents the number of muscle fibers that depolarize.

Improvement in both of these measures indicates less motor fibre blockage and a greater

number of axons that are activated (Gooch et al., 2007; Preston et al., 2005). Results

from Chapter 3 demonstrate the effects of local ischemia on nerve function, which were

only previously observed in animal models (Diao et al., 2005) or intervention studies of

median nerve compression via tourniquet application (Lundborg et al., 1982).

Additionally, in Chapter 3 we also observed a significant relationship between motor

latency and FDS-SSCT mechanics where individuals with higher motor latency (greater

nerve dysfunction) had higher peak relative FDS-SSCT displacement and higher SSI.

These results are in line with findings from Schrier et al. (2020) who found that SSCT

motion decreased as CTS severity increased, indicating greater potential for injury

through shear strain in these patients.

In Chapter 4 we directly tested the effect of blood flow occlusion on these

outcomes to further probe if vascular factors could be responsible for these results

observed in patients. Through the multidisciplinary study design, we were able to

investigate over ten outcome variables simultaneously, providing a unique insight into the

temporal effects of local ischemia not previously investigated in this fashion. In this final

study we found that partial ischemia through brachial occlusion immediately decreased

intraneural blood flow velocity, which was accompanied by both a decrease in nerve function and an increase in FDS-SSCT peak relative displacement and SSI. The results observed through Chapter 4 confirmed that our findings from the previous two studies were due partially to the effects of local ischemia. It is clear through this study that local ischemia directly affects median nerve blood flow velocity, and results in a cascade of events that includes nerve dysfunction and increased shear strain of the SSCT. Given that blood vessels going to the median nerve pass through the SSCT, it is evident from these results that the SSCT is also affected by perfusion of these small arterioles. The results from these three studies presented in this thesis strongly support the vascular hypothesis of CTS development, and indicate that ischemia is a strong driver of the structural, functional, and mechanical changes that occur with the condition.

We also observed the effects of wrist posture on intraneural blood flow through Chapters 2 and 3. In Chapter 2 we found that intraneural blood flow decreased with increasing severity when it was measured in either wrist flexion or extension. When we followed up with these patients 6 months later in Chapter 3, we also observed that intraneural blood flow, when measured in wrist flexion, was a significant predictor of sensory conduction velocity in patients. We observed that patients with higher intraneural blood flow during wrist flexion at baseline visit had higher sensory conduction velocity (less dysfunction) at 6-months follow-up. These results highlight the effect of a well-established risk factor, wrist posture, on nerve function and vascularity. Non-neutral wrist postures are known to place significant pressure on the median nerve within the

carpal tunnel. Wrist flexion in particular has been shown to increase contact pressure on

the median nerve (Keir et al., 1999, 1997) as the finger flexor tendons move in a volar

direction against the TCL. In a pathological state, the median nerve has reduced mobility

within the carpal tunnel (Filius et al., 2015; Wang et al., 2014), thereby increasing its

likelihood of being compressed against the TCL and the finger flexor tendons. Results

from Chapter 2 support the hypothesis that wrist flexion causes median nerve

compression and ischemia within the nerve, reflected in the observed decrease in

intraneural blood flow velocity. As it was observed in Chapter 3 that individuals with

greater intraneural blood flow velocity in wrist flexion maintained higher sensory

conduction velocity, the individual response to wrist flexion can be used as a "stress test."

Perhaps it is an indicator that individuals who maintain median nerve perfusion during

wrist flexion will have better NCS outcomes, and perhaps have greater chances of

recovering some nerve function and thereby improving CTS symptoms.

5.3 The Utility of Ultrasound in CTS Diagnosis

       Although NCS is currently the "gold standard" for assessing nerve function and

diagnosing CTS, there are several limitations to the technique, especially for early

detection of CTS. Nerve conduction studies are said to capture more severe changes to

nerve function, and a positive diagnosis of CTS occurs only once significant dysfunction

has occurred (Evans et al., 2012). There is also no universally accepted standard for

conducting NCS, or criteria for diagnosing CTS (Dillingham et al., 2016). Additionally,

NCS suffer from considerable false negative and false positive rates (El Miedany et al.,

2004; Redmond et al., 1988) due to this lack of testing standard and high dependency on

examiner skill and experience.

Several investigations have demonstrated that ultrasound can accurately diagnose

CTS (Azami et al., 2014; Bang et al., 2019; Cartwright et al., 2013; El Miedany et al.,

2004, 2015; Fowler et al., 2014; Gonzalez-Suarez et al., 2019; Moschovos et al., 2019;

Tai et al., 2012; Torres-Costoso et al., 2018) and has good prognostic value (El Miedany

et al., 2015). Many investigations have reported that median nerve CSA can accurately

diagnose CTS severity (Azami et al., 2014; Bang et al., 2019; Cartwright et al., 2013; El

Miedany et al., 2004; Moschovos et al., 2019), particularly when measured at the carpal

tunnel inlet (level of the pisiform) (Torres-Costoso et al., 2018). Measurements of

median nerve CSA from ultrasound images demonstrate good to excellent intra- and

inter-rater reliability (Junck et al., 2015), making it a feasible method for CTS diagnosis.

The combination of ultrasound parameters can increase the diagnostic accuracy, such as

combining median nerve blood flow with median nerve CSA (Ghasemi-Esfe et al., 2011;

Gonzalez-Suarez et al., 2019). A combination of median nerve CSA and intraneural

blood flow has been shown to have good prognostic value at 6 months post-initial

visit/treatment in patients with CTS (El Miedany et al., 2015). Ultrasound assessment of

FDS-SSCT motion have shown greater shear strain in CTS symptomatic (Tat et al.,

2015b) and clinically diagnosed patients (Schrier et al., 2020; van Doesburg et al., 2012b)

compared to controls, although limited correlation between SSCT motion and CTS

severity has been reported (Schrier et al., 2020). Additional ultrasound outcomes like elastography have also been reported to differentiate severity (Lin et al., 2019) since median nerve stiffness is consistently shown to increase with increasing severity. Results from Chapters 2 and 3 of this thesis support the prognostic value of ultrasound and the use of ultrasound to differentiate between CTS severity. In Chapter 2 we found that median nerve CSA measured at the carpal tunnel inlet increased with increasing severity, consistent with the literature. In Chapter 3 we found that intraneural blood flow velocity and FDS-SSCT relative displacement and SSI were predictive of NCS outcomes at 6-month follow-up. Our results, in combination with the literature, strongly suggest that a battery of ultrasound examinations can be used to diagnose CTS and distinguish among clinical severities. Ultrasound investigation has the potential to detect morphological and functional changes to carpal tunnel tissues, like the median nerve and SSCT, which likely occur before significant nerve dysfunction can be detected through NCS.

5.4 Neural Networking Approach to Address Data Analysis Challenges

The multidisciplinary studies that were developed in this thesis provide a unique insight into the relationships among vascular, mechanical and functional outcomes in the study of CTS. These studies generated a large amount of data given the many outcome measures that I was interested in studying jointly. This is particularly true for the final study, Chapter 4, where I investigated a total of ten outcome variables; four through NCS and six through ultrasound. While it was possible to analyze data from many of these

outcome variables through specialized software which automated much of the process,

analysis of the tendon-SSCT motion was particularly tedious and time consuming. For

instance, a 12-second colour Doppler ultrasound video of FDS-SSCT motion can take up

to 90 minutes to analyze. Due to the volume of data collected in Chapter 4, an estimated

400 hours of analysis is required to complete this analysis. As such, I was only able to

include a subset of this data in Chapter 4 of this thesis (analysis of all 40 subjects is

intended for publication of this manuscript). Briefly, analysis of these colour Doppler

videos is typically done in our laboratory using a combination of GE proprietary software

(EchoPac) and a custom program created in Matlab/Python (Matlab was used for analysis

in Chapter 2 and 3, Python was used for analysis in Chapter 4). The analysis begins in

EchoPac by using the *Q-analysis* function to digitize points along the FDS tendon and the

adjacent SSCT (Figure 2.4). Three markers are placed collinearly over each tissue (FDS

and SSCT). The video is then played through frame-by-frame and each marker is moved

between frames to ensure that the marker always remains on the same point on the tissue

of interest. EchoPac calculates the velocity of the tissue behind each marker, which is

why it is important that the marker is always on the tissue of interest. Once the trial has

been digitized for the entirety of the video, the velocity of each marker is exported from

EchoPac and imported into Matlab/Python for further analysis. In Matlab/Python, the

traces are filtered and integrated to obtain tissue displacements. While the analysis

through Matlab/Python has been optimized, the main limiting step continues to be the

digitization through EchoPac. The main issue stems from the movement of the FDS

tendon and adjacent SSCT as they move through repetitive finger flexion-extension

motion. In a number of subjects, FDS-SSCT motion does not occur in one plane; it

occurs in three dimensions. In particular, the FDS and SSCT exhibit significant palmar-

dorsal motion during finger flexion-extension, but radial-ulnar motion would be out-of-

plane. Due to this complex motion, digitization becomes a complex and time-consuming

task as digitization must be completed on a frame-by-frame basis in order to capture

motion in both planes.

To address these challenges in tendon-SSCT motion analysis, I attempted to

develop a tendon-SSCT tracking program using a deep neural network. An open source

deep convolutional neural network (CNN) package called *DeepLabCut* (DLC)

(mousemotorlab.org/deeplabcut) was used to provide automated position estimations of

the FDS tendon and adjacent SSCT. This deep CNN was originally created for pose

estimation of mice and *Drosophila* from videography, with accuracy comparable to that

achieved with manual human video digitization (Mathis et al., 2018; Nath et al., 2019).

The Applied Biomechanics Laboratory at The University of North Carolina at Chapel Hill

successfully used DLC to track muscle-tendon junction displacements from ultrasound

videos during functional activities. These results in ultrasound videos were promising

and I decided to explore if DLC could be used to track FDS and SSCT displacements

from our ultrasound videos.

A subset of four sonographic videos from the Chapter 2 study data was selected

for neural network training. The videos that were selected represented the "best" videos

in the sense that the FDS and SSCT were clearly visible for the whole duration of the

video (average length = 12 seconds) and exhibited motion in primarily two planes. These

videos were also selected as they had already been analyzed in EchoPac (for Chapter 2),

thereby providing a chance to compare the CNN output to our current "gold standard"

(i.e. manual EchoPac digitization). To train the neural network, I manually digitized both

the FDS and SSCT in each video following guidelines previously established in our

laboratory by placing three equally spaced markers colinearly on each tissue. Digitization

and training parameters were followed from DLC documentation recommendations. In

the end, 500 video frames were digitized for the initial training. Once trained, the CNN

was used to automatically digitize and provide position estimations for 12 additional

videos (novel trials). Position estimations from all the digitized videos were then

exported for further analysis in Matlab. In Matlab, these position estimations were low

pass filtered (3 Hz) and then differentiated to calculate tissue displacements and

velocities, respectively. These values were then compared to our tissue displacements

and velocities obtained for the same videos through EchoPac digitization and analysis.

Our EchoPac digitization contained two methods, a "static" and "dynamic" method. Our

"static" EchoPac method constituted our lab's previous method of tissue analysis through

EchoPac which just placed the 6 colinear markers (3 for FDS and 3 for SSCT) in the first

frame of the video and were not moved throughout the video to account for the palmar-

dorsal motion. Our "dynamic" EchoPac digitization method utilized the *Q-analysis*

function within EchoPac to allow "tracking" of the tissues through palmar-dorsal motion

by frame-to-frame placement of the markers (this method was used in Chapter 2-4). Root mean squared error (RMSE) and Pearson product-moment correlation coefficients (r) were calculated to compare FDS and SSCT velocities between DLC digitized videos and EchoPac digitized videos.

Overall, our results showed considerable variability in RMSE and r across trials (Table 5.1). Although both DLC and EchoPac methods aligned temporally and in magnitude for training trials (Figure 5.2a), results for novel trials were not as well aligned (Figure 5.2b). For the four training trials, good correlations were achieved between DLC and "dynamic" EchoPac velocity results for both the SSCT and FDS tissues (means: r_{SSCT} = 0.69, r_{FDS}= 0.73) with low RMSE (means: $RMSE_{SSCT}$ = 1.1 cm/s, $RMSE_{FDS}$ = 1.2 cm/s). However, r and RMSE varied greatly for novel trials (Table 5.1).

Table 5. 1. Pearson product-moment correlation coefficients (r) and Root Mean Square Error (RMSE)(cm/s) results between DeepLabCut (DLC) and "dynamic" EchoPac tissue analysis of the flexor digitorum superficialis (FDS) and subsynovial connective tissue (SSCT) velocity. Results are presented for both trained (highlighted) and novel trials.

	R		RMSE (cm/s)	
TRIAL	**SSCT**	**FDS**	**SSCT**	**FDS**
34-2	-0.45038	-0.6406	2.52079	3.71439
34-1	-0.33885	-0.40457	2.26656	2.93842
30-2	0.283608	0.368072	1.88625	2.0952
30-1	-0.07267	0.446716	2.49463	2.01893
29-2	-0.16675	-0.31457	6.01855	3.06355
26-2	0.110913	-0.00486	1.47292	1.65453
25-1	-0.41503	0.01352	2.32134	1.94002
24-2	-0.15244	-0.09263	3.26563	2.71042
17-1	0.315894	0.291651	2.54308	2.77454
15-2	0.699504	0.60128	0.971652	1.1526
15-1	-0.45864	-0.51602	2.34655	2.27747
13-2	0.830255	0.844426	0.889072	1.15667
13-1	0.860079	0.863458	0.733342	1.08721
10-2	-0.09236	0.042273	1.47882	1.2544
10-1	0.004665	0.0179	1.05542	1.04095
9-2	0.390765	0.612407	1.8684	1.60315
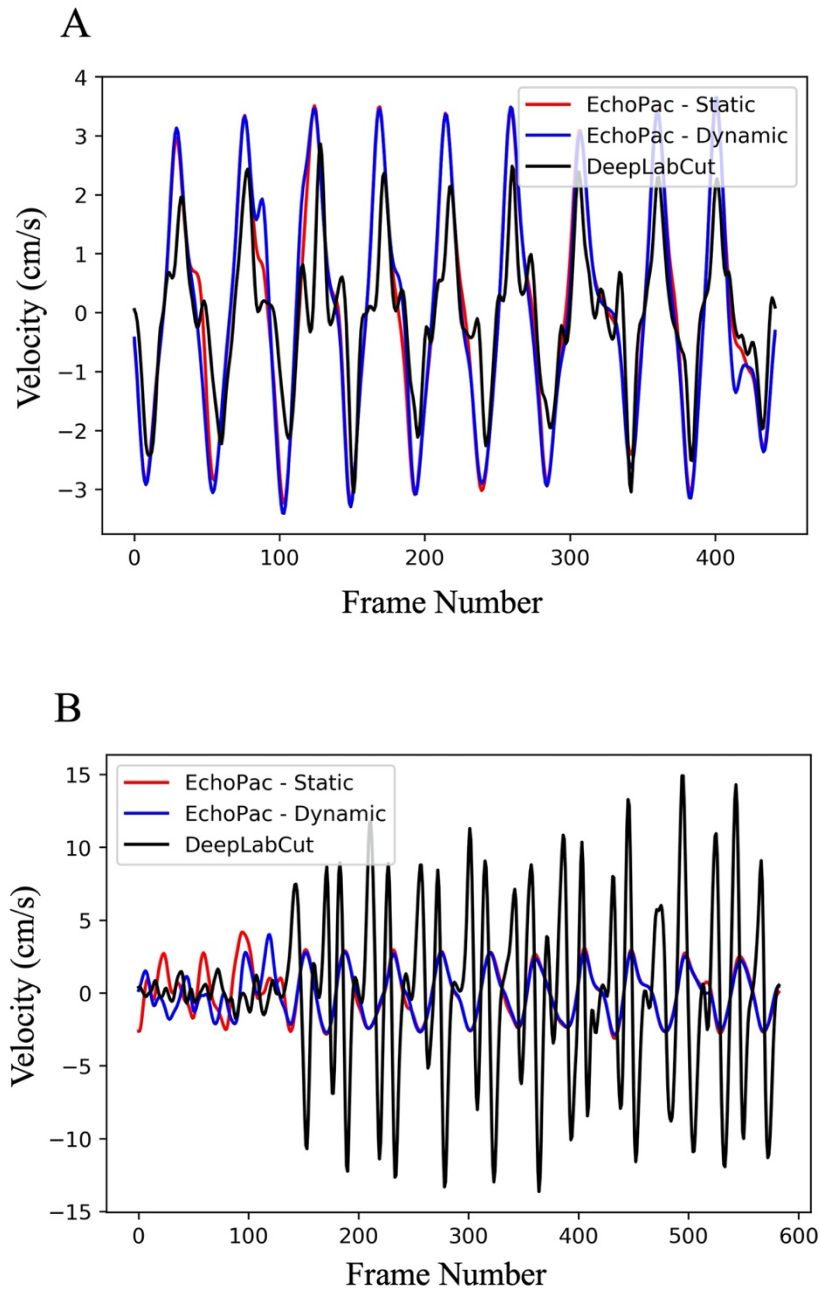
Figure 5. 2. Comparisons of flexor digitorum superficialis (FDS) tissue velocity (cm/s) obtained from each digitization method; "static" EchoPac method (red), "dynamic" EchoPac method (blue) and DeepLabCut (DLC)(black) for both a (A) trained trial and (B) a novel trial.

The results from the initial analysis were promising at first for some of the training and novel trials, and we proceeded by including more training videos into the CNN. We believed that by adding more training videos we would be able to improve the results from DLC. However, results did not significantly improve after adding two more videos (~500 frames) to the training set. RMSE and r values for trained trials remained good to excellent, but results for novel trials continued to be highly variable and showed poor correlation with EchoPac results. Overall, the average correlation coefficients and RMSE for both SSCT and FDS tissue velocities were poor ($r_{SSCT} = 0.2$, $r_{FDS} = 0.2$; $RMSE_{SSCT} = 3.3$ cm/s, $RMSE_{FDS} = 4.1$ cm/s). From the RMSE and r results, along with visual inspection of the output graphs, we observed that DLC results from numerous trials were phase shifted from EchoPac outputs, and that DLC either over- or underestimated tendon velocities for numerous trials (Figure 5.2b). It was clear from these results that continued training of our CNN would not improve tissue position estimations, and the method would not be valid and reliable for automated analysis for tissue velocities and displacements. As such, I decided to continue using EchoPac *Q-analysis* to analyze all tissue motion ultrasound videos in this thesis.

Upon further reflection of these results, I believe there are two main reasons for the poor results achieved through DLC: out-of-plane motion and low resolution. As mentioned previously, the FDS tendon and SSCT experience three-dimensional motion which cannot be captured with a two-dimensional imaging modality. This complex

motion is also difficult to quantify with 2D analysis methods. Indeed, even by analyzing

the videos through EchoPac there are still considerable challenges given this type of

motion. When manual digitization is done through EchoPac, the trained digitizer must

estimate the location of the marker in the next frame when the FDS and SSCT move out

of plane and the tissues are no longer clearly visible. It can be appreciated that these

instances are much more difficult for a CNN to learn and to apply the algorithm correctly.

These instances therefore produce higher error in the digitized videos and can over- or

underestimate tissue positions. The second challenge is low resolution of the ultrasound

videos. A sonographic system (Vivid Q BT10, GE Healthcare, Milwaukee, WI) with a 12

MHz linear array transducer was used for collection of all ultrasound videos included in

this analysis. While this high frequency transducer allowed for good resolution to

distinguish the FDS tendon and the SSCT, it did not provide high enough resolution to

highlight the distinguishing features between pixels of each tissue of interest. As a result,

pixels on the image appeared homogenous, especially between the FDS and adjacent

SSCT, and there was little unique pixel pattern to distinguish the two tissues from each

other. Previous efforts have also been made in our lab to utilize commercial speckle

tracking algorithms to track FDS and SSCT motion. These efforts were also not

successful due to the resolution of the transducer and lack of unique pixilation patterns on

the tissues. The homogeneity of pixels likely also made it difficult for the CNN algorithm

to correctly identify and track the two tissues of interest throughout the movement since

extraction of meaningful differentiating features is the basis for deep learning algorithms

(Zhou et al., 2017). I believe that future attempts at using this neural network will be successful if the ultrasound resolution is improved where distinguishing features between the tissues can be emphasized and the pixilation pattern is less homogeneous. This can be achieved by using higher frequency transducers which will yield better resolution at the shallow depth (~1 cm) needed for imaging these tissues.

5.5 Future Research Directions

This thesis provides a unique framework for future investigations on the mechanisms behind CTS. Chapter 4 provides a viable occlusion protocol that can be used in future investigations to study the effects of ischemia with minimal discomfort to participants. This protocol can be adapted to allow for collection of blood flow parameters with modalities such as near-infrared spectroscopy.   Continuous wave near infrared spectroscopy would provide deeper insight into median nerve blood flow and nerve oxygenation. Results from this thesis clearly point to the influence of blood flow on CTS development, therefore future studies using this protocol will further clarify the role of adequate blood flow on carpal tunnel tissue mechanics, structure and function.

Although injury and fibrosis of the SSCT have been demonstrated in histological studies in cadaver models, they have yet to be confirmed in vivo. The numerous ultrasound studies discussed in this thesis provide evidence for the potential of increased shear injury between the finger flexor tendons and the SSCT with exposure to known biomechanical risk factors. However, shear injury directly as a result from exposure to

these risk factors has not been observed in vivo. Future investigations should aim to

observe and quantify changes in the structure of the SSCT to confirm that SSCT injury

and fibrosis occurs as a result of increased shear strain injury between the tendon and the

SSCT. Diffusion tensor imaging is a magnetic resonance imaging (MRI) sequence that

can provide information on the structure of biological tissues. Improvements in the

resolution of this technique will allow for future detailed investigation into the structure

of the SSCT and will allow for in-vivo observation of SSCT injury.

5.6 Conclusions

The etiology of CTS is multidimensional and is likely due to the combination of

several factors occurring at once. The findings presented in this thesis support the

influence of vascular factors in the development and progression of CTS, specifically the

influence of local ischemia. It was shown through the three thesis studies that local blood

flow has significant effects on vascular dynamics, kinematics and function of the tissues

within the carpal tunnel. This relationship was demonstrated in both CTS confirmed

patients, and in healthy participants through intervention with an occlusion protocol.

These results indicate that individuals with compromised systemic blood flow, or those

working in postures that constrict circulation, may be at higher risk of developing CTS.

This is the case in special populations such as diabetic individuals or in pregnancy where

circulatory disturbances are believed to be responsible for the onset of CTS. Adopting a

wholistic approach to the investigation of CTS will aid in elucidating the mechanisms and

drivers of the condition and provide a more comprehensive understanding of CTS.

References

Note: The references listed in this section are for the Introduction (Chapter 1) and Discussion (Chapter 5) chapters. The references for each thesis study are listed in their respective chapters (Chapters 2- 4).

Allan, C. H. (2005). Flexor tendons: Anatomy and surgical approaches. *Hand Clinics*, *21*(2), 151–157.

Arslan, H., Yavuz, A., İlgen, F., Aycan, A., Ozgokce, M., & Akdeniz, H. (2018). The efficiency of acoustic radiation force impulse (ARFI) elastography in the diagnosis and staging of carpal tunnel syndrome. *Journal of Medical Ultrasonics*, 1–7.

Azami, A., Maleki, N., Anari, H., & Iranparvar, M. (2014). The diagnostic value of ultrasound compared with nerve conduction velocity in carpal tunnel syndrome. *International Journal of Rheumatic Diseases*, *17*, 612–620.

Babski-Reeves, K., & Crumpton-Young, L. (2003). Interaction effects of wrist and forearm posture on the prediction of carpal tunnel syndrome cases within a fish-processing facility. *Human and Ecological Risk Assessment*, *9*(4), 1011–1022.

Bang, M., Kim, J. M., & Kim, H. S. (2019). The usefulness of ultrasonography to diagnose the early stage of carpal tunnel syndrome in proximal to the carpal tunnel inlet: A prospective study. *Medicine*, *98*(26), e16039.

Barcenilla, A., March, L. M., Chen, J. S., & Sambrook, P. N. (2012). Carpal tunnel syndrome and its relationship to occupation: A meta-analysis. *Rheumatology*, *51*(2), 250–261.

Bates, D., Maechler, M., Bolker, B., Walker, S., Christensen, R. H. ., Singmann, H., Dai,

B., Scheipl, F., Grothendieck, G., Green, P., & Fox, J. (2012). Package "lme4".

CRAN. *R Foundation of Statistical Computing, Vienna, Austria*.

Bauman, T. D., Gelberman, R. H., Mubarak, S. J., & Garfin, S. R. (1981). The acute

carpal tunnel syndrome. *Clin Orthop Relat Res*, *156*(156), 151–156.

Bernard, B., Putz-Anderson, V., Burt, S. E., Cole, L. L., Fairfield-Estill, C., Fine, L. J.,

Grant, K. A., Gjessing, C., Jenkins, L., Hurrell, J. J. J., Nelson, N., Pfirman, D.,

Roberts, R., Stetson, D., Haring-Sweeney, M., & Tanaka, S. (1997). *Musculoskeletal*

disorders and workplace factors; a critical review of epidemiologic evidence for

work-related musculoskeletal disorders of the neck, upper extremity, and low back.

Bland, J. D. (2000). A neurophysiological grading scale for carpal tunnel syndrome.

Muscle & Nerve, *23*(8), 1280–1283.

Borire, A. A., Arnold, R., Pussell, B. A., Kwai, N. C., Visser, L. H., Simon, N. G.,

Kiernan, M. C., & Krishnan, A. V. (2018). Effects of hemodialysis on intraneural

blood flow in end-stage kidney disease. *Muscle and Nerve*, *57*(2), 287–293.

Borire, A. A., Hughes, A. R., Lueck, C. J., Colebatch, J. G., & Krishnan, A. V. (2016).

Sonographic differences in carpal tunnel syndrome with normal and abnormal nerve

conduction studies. *Journal of Clinical Neuroscience*, *34*, 77–80.

Borire, A. A., Issar, T., Kwai, N. C., Visser, L. H., Simon, N. G., Poynten, A. M.,

Kiernan, M. C., & Krishnan, A. V. (2018). Correlation between markers of

peripheral nerve function and structure in type 1 diabetes. *Diabetes/Metabolism*

Research and Reviews, *34*(7), 1–8.

Borire, A. A., Visser, L. H., Padua, L., Colebatch, J. G., Huynh, W., Simon, N. G.,

    Kiernan, M. C., & Krishnan, A. V. (2017). Utility of maximum perfusion intensity

    as an ultrasonographic marker of intraneural blood flow. *Muscle & Nerve*, *55*(1), 77–

    83.

Bortolotto, C., Turpini, E., Felisaz, P., Fresilli, D., Fiorina, I., Raciti, M. V., Belloni, E.,

    Bottinelli, O., Cantisani, V., & Calliada, F. (2017). Median nerve evaluation by

    shear wave elastosonography : impact of " bone - proximity " hardening artifacts and

    inter - observer agreement. *J Ultrasound*, *20*(4), 293–299.

Bower, J. A., Stanisz, G. J., & Keir, P. J. (2006). An MRI evaluation of carpal tunnel

    dimensions in healthy wrists: Implications for carpal tunnel syndrome. *Clinical

    Biomechanics*, *21*(8), 816–825.

Braun, R. M., & Jackson, W. J. (1994). Electrical studies as a prognostic factor in the

    surgical treatment of carpal tunnel syndrome. *The Journal of Hand Surgery*, *19*(A),

    893–900.

Cartwright, M. S., Walker, F. O., Blocker, J. N., Schulz, M. R., Arcury, T. A., Grzywacz,

    J. G., Mora, D., Chen, H., Marín, A. J., & Quandt, S. A. (2013). Ultrasound for

    carpal tunnel syndrome screening in manual laborers. *Muscle & Nerve*, *48*(1), 127–

    131.

Chen, S., Andary, M., Buschbacher, R., Del Toro, D., Smith, B., So, Y., Zimmermann,

    K., & Dillingham, T. R. (2016). Electrodiagnostic reference values for upper and

    lower limb nerve conduction studies in adult populations. *Muscle & Nerve*, (54),

371–377.

Coppieters, M. W., Schmid, A. B., Kubler, P. A., & Hodges, P. W. (2012). Description, reliability and validity of a novel method to measure carpal tunnel pressure in patients with carpal tunnel syndrome. *Man Ther*, *17*(6), 589–592.

Cramp, F. L., McCullough, G. R., Lowe, A. S., & Walsh, D. M. (2002). Transcutaneous electric nerve stimulation: The effect of intensity on local and distal cutaneous blood flow and skin temperature in healthy subjects. *Archives of Physical Medicine and Rehabilitation*, *83*(1), 5–9.

D'Arcy, C. A., & McGee, S. (2010). Does This Patient Have Carpal Tunnel Syndrome? *JAMA*, *283*(23), 3110–3117.

Dale, A. M., Harris-Adamson, C., Rempel, D. M., Gerr, F., Hegmann, K., Silverstein, B. A., Burt, S., Garg, A., Merlino, L., Thiese, M. S., Eisen, E. A., & Evanoff, B. (2013). Prevalence and incidence of carpal tunnel syndrome in US working populations: pooled analysis of six prospective studies. *Scand J Work Environ Health*, *39*(5), 495–505.

Dejaco, C., Stradner, M., Zauner, D., Seel, W., Simmet, N. E., Klammer, A., Heitzer, P., Brickmann, K., Gretler, J., Furst-Moazedi, F. C., Thonhofer, R., Husic, R., Hermann, J., Graninger, W. B., & Quasthoff, S. (2013). Ultrasound for diagnosis of carpal tunnel syndrome: comparison of different methods to determine median nerve volume and value of power Doppler sonography. *Annals of the Rheumatic Diseases*, *72*(12), 1934–1939.

Diao, E., Shao, F., Liebenberg, E., Rempel, D. M., & Lotz, J. C. (2005). Carpal tunnel

pressure alters median nerve function in a dose-dependent manner: A rabbit model

for carpal tunnel syndrome. *J Orthop Res*, *23*(1), 218–223.

Dillingham, T. R., Chen, S., Andary, M., Buschbacher, R., Del Toro, D., Smith, B.,

Zimmermann, K., So, Y., & Yuen, S. O. (2016). Establishing high-quality reference

values for nerve conduction studies: A report from the normative data task force of

the American Association Of Neuromuscular & Electrodiagnostic Medicine. *Muscle

& Nerve*, *54*(3), 366–370.

Ehmke, S. G. (2015). *The Effect of Force, Posture, and Repetitive Wrist Motion on

Intraneural Blood Flow in the Median Nerve*. McMaster University.

El Miedany, Y. M., Aty, S. A., & Ashour, S. (2004). Ultrasonography versus nerve

conduction study in patients with carpal tunnel syndrome: Substantive or

complementary tests? *Rheumatology*, *43*(7), 887–895.

El Miedany, Y. M., El Gaafary, M., Youssef, S., Ahmed, I., & Nasr, A. (2015).

Ultrasound assessment of the median nerve: a biomarker that can help in setting a

treat to target approach tailored for carpal tunnel syndrome patients. *SpringerPlus*,

4(1), 1–10.

Ettema, A. M., Amadio, P. C., Zhao, C., Wold, L. E., & An, K. N. (2004). A histological

and immunohistochemical study of the subsynovial connective tissue in idiopathic

carpal tunnel syndrome. *The Journal of Bone and Joint Surgery*, *86*(7), 1458–1466.

Ettema, A. M., Amadio, P. C., Zhao, C., Wold, L. E., O'Byrne, M. M., Moran, S. L., &

An, K.-N. (2006). Changes in the functional structure of the tenosynovium in

idiopathic carpal tunnel syndrome: a scanning electron microscope study. *Plastic

and Reconstructive Surgery*, *118*(6), 1413–1422.

Ettema, A. M., Belohlavek, M., Zhao, C., Oh, S.-H., Amadio, P. C., & An, K.-N. (2006).

High-Resolution Ultrasound Analysis of Subsynovial Connective Tissue in Human

Cadaver Carpal Tunnel. *Journal of Orthopaedic Research*, *24*(10), 2011–2020.

Evans, K. D., Roll, S. C., Volz, K. R., & Freimer, M. (2012). Relationship between

Intraneural Vascular Flow measured with sonography and Carpal Tunnel Syndrome

Diagnosis based on Electrodiagnostic Testing. *J Ultrasound Med*, *31*, 729–736.

Evans, K. D., Volz, K. R., Hutmire, C., & Roll, S. C. (2012). Morhphologic

Characterization of Intraneural Flow Associated With Median Nerve Pathology.

Journal of Diagnostic Medical Sonography, *28*(1), 11–19.

Faller, D. V. (1999). Endothelial cell responses to hypoxic stress. *Clin Exp Pharmacol

Physiol.*, *26*(1), 74–84.

Farias Zuniga, A., Ghavanini, A. A., Israelian, G., & Keir, P. J. (2020). Blood flow

velocity but not tendon mechanics relates to nerve function in carpal tunnel

syndrome patients. *Journal of the Neurological Sciences*, *411*(116694).

Ferguson, S. A., Fathallah, F. A., & Granata, K. P. (1993). Coactivity effects upon carpal

tunnel contact forces. *Proceedings of the Human Factors and Ergonomics Society

Annual Meeting*, 705–709.

Ferry, S., Pritchard, T., Keenan, J., Croft, P., & Silman, A. J. (1998). Estimating the

prevalence of delayed median nerve conduction in the general population. *Br J Rheumatol*, *37*(6), 630–635.

Festen-Schrier, V. J. M. M., & Amadio, P. C. (2018). The biomechanics of subsynovial connective tissue in health and its role in carpal tunnel syndrome. *J Electromyogr Kinesiol*, *38*(September 2017), 232–239.

Filius, A., Scheltens, M., Bosch, H. G., Van Doorn, P. A., Stam, H. J., Hovius, S. E. R., Amadio, P. C., & Selles, R. W. (2015). Multidimensional ultrasound imaging of the wrist: Changes of shape and displacement of the median nerve and tendons in carpal tunnel syndrome. *J Orthop Res*, *33*(9), 1332–1340.

Filius, A., Thoreson, A. R., Wang, Y., Passe, S. M., Zhao, C., An, K.-N., & Amadio, P. C. (2015). The effect of tendon excursion velocity on longitudinal median nerve displacement: Differences between carpal tunnel syndrome patients and controls. *Journal of Orthopaedic Research*, *33*(4), 483–487.

Filius, A., Thoreson, A. R., Yang, T. H., Vanhees, M., An, K. N., Zhao, C., & Amadio, P. C. (2014). The effect of low- and high-velocity tendon excursion on the mechanical properties of human cadaver subsynovial connective tissue. *J Orthop Res*, *32*(1), 123–128.

Fowler, J. ., Munsch, M., Tosti, R., Hagberg, W. C., & Imbriglia, J. E. (2014). Comparison of ultrasound and electrodiagnostic testing for diagnosis of carpal tunnel syndrome: study using a validated clinical tool as the reference standard. *The Journal of Bone and Joint Surgery. American Volume*, *96*(17), e148.

Freeland, A. E., Tucci, M. A., Barbieri, R. A., Angel, M. F., & Nick, T. G. (2002).

Biochemical Evaluation of Serum and Flexor Tenosynovium in Carpal Tunnel

Syndrome. *Microsurgery*, *22*, 378–385.

Fujimoto, K., Kanchiku, T., Kido, K., Imajo, Y., Funaba, M., & Taguchi, T. (2015).

Diagnosis of Severe Carpal Tunnel Syndrome Using Nerve Conduction Study and

Ultrasonography. *Ultrasound in Medicine and Biology*, *41*(10), 2575–2580.

Gabra, J. N., Gordon, J. L., Marquardt, T. L., & Li, Z.-M. (2016). In vivo tissue

interaction between the transverse carpal ligament and finger flexor tendons.

Medical Engineering & Physics, *0*, 1–8.

Gelberman, R. H., Hergenroeder, P., Hargens, A. R., Lundborg, G. N., & Akeson, W. H.

(1981). The carpal tunnel syndrome: A study of carpal canal pressures. *The Journal

of Bone and Joint Surgery*, *63A*(3), 380–383.

Gelberman, R. H., Szabo, R. M., Williamson, R. V., Hargens, A. R., Yaru, N. C., &

Minteer-Convery, M. A. (1983). Tissue pressure threshold for peripheral nerve

viability. *Clinical Orthopaedics and Related Research*, *No. 178*(178), 285–291.

Gennisson, J. L., Deffieux, T., Fink, M., & Tanter, M. (2013). Ultrasound elastography:

Principles and techniques. *Diagnostic and Interventional Imaging*, *94*(5), 487–495.

Ghajarzadeh, M., Dadgostar, M., Sarraf, P., Emami-Razavi, S., Miri, S., & Malek, M.

(2015). Application of ultrasound elastography for determining carpal tunnel

syndrome severity. *Japanese Journal of Radiology*, *33*, 273–278.

Ghasemi-Esfe, A. R., Khalilzadeh, O., Mazloumi, M., Vaziri-Bozorg, S. M., Niri, S. G.,

Kahnouji, H., & Rahmani, M. (2011). Combination of high-resolution and color

Doppler ultrasound in diagnosis of carpal tunnel syndrome. *Acta Radiol*, *52*(2), 191–

197.

Gonzalez-Suarez, C. B., Fidel, B. C., Cabrera, J. T. C., Dela Cruz, F. C., Gesmundo, M.

V. T., Regala, C. F. G., Saratan, R., Suarez, C. G., & Grimmer, K. (2019).

Diagnostic Accuracy of Ultrasound Parameters in Carpal Tunnel Syndrome:

Additional Criteria for Diagnosis. *Journal of Ultrasound in Medicine*.

Gooch, C. L., & Weimer, L. H. (2007). The Electrodiagnosis of Neuropathy: Basic

Principles and Common Pitfalls. *Neurologic Clinics*, *25*(1), 1–28.

Guimberteau, J. C., Delage, J. P., McGrouther, D. A., & Wong, J. K. F. (2010). The

microvacuolar system: how connective tissue sliding works. *The Journal of Hand

Surgery, European Volume*, *35*(8), 614–622.

Gupta, R., Rowshan, K., Chao, T., Mozaffar, T., & Steward, O. (2004). Chronic nerve

compression induces local demyelination and remyelination in a rat model of carpal

tunnel syndrome. *Experimental Neurology*, *187*(2), 500–508.

Haines, A., Levis, C., Goldsmith, C. H., Kaur, M., Duku, E., Wells, R., Walter, S. D.,

Rook, C., Stock, S., Liss, G., Murphy, J., & Thoma, A. (2017). Dupuytren's

contracture and handwork: A case-control study. *American Journal of Industrial

Medicine*, *60*(8), 724–733.

Harris-Adamson, C., Eisen, E. A., Neophytou, A., Kapellusch, J., Garg, A., Hegmann, K.

T., Thiese, M. S., Dale, A. M., Evanoff, B., Bao, S., Silverstein, B. A., Gerr, F., Burt,

S., & Rempel, D. M. (2016). Biomechanical and psychosocial exposures are independent risk factors for carpal tunnel syndrome: assessment of confounding using causal diagrams. *Occup Environ Med*, *73*(11), 727–734.

Heckel, A., Weiler, M., Xia, A., Ruetters, M., Pham, M., Bendszus, M., Heiland, S., & Baeumer, P. (2015). Peripheral Nerve Diffusion Tensor Imaging: Assessment of Axon and Myelin Sheath Integrity. *Plos One*, *10*(6), e0130833.

Hochman, M. G., & Zilberfarb, J. L. (2004). Nerves in a pinch: Imaging of nerve compression syndromes. *Radiologic Clinics of North America*, *42*(1), 221–245.

Jablecki, C. K., Andary, M. T., So, Y. T., Wilkins, D. E., & Williams, F. H. (1993). Literature review of the usefulness of nerve conduction studies and electromyography for the evaluation of patients with carpal tunnel syndrome. *Muscle & Nerve*, *16*, 1392–1414.

Jayaraman, S., & Naidich, T. P. (2004). The carpal tunnel: Ultrasound display of normal imaging anatomy and pathology. *Neuroimaging Clinics of North America*, *14*(1), 103–113.

Jinrok, O., Zhao, C., Amadio, P. C., An, K.-N., Zobitz, M. E., & Wold, L. E. (2004). Vascular pathologic changes in the flexor tenosynovium (subsynovial connective tissue) in idiopathic carpal tunnel syndrome. *Journal of Orthopaedic Research*, *22*(6), 1310–1315.

Joy, V., Therimadasamy, A. K., Chan, Y. C., & Wilder-Smith, E. P. (2011). Combined Doppler and B-mode sonography in carpal tunnel syndrome. *Journal of the*

Neurological Sciences, *308*, 16–20.

Junck, A. D., Escobedo, E. ., Lipa, B. M., Cronan, M., Anthonisen, C., Poltavskiy, E., Bang, H., & Han, J. J. (2015). Reliability Assessment of Various Sonographic Techniques for Evaluating Carpal Tunnel Syndrome. *J Ultrasound Med*, *34*(11), 2077–2088.

Kantarci, F., Ustabasioglu, F. E., Delil, S., Olgun, D. C., Korkmazer, B., Dikici, A. S., Tutar, O., Nalbantoglu, M., Uzun, N., & Mihmanli, I. (2014). Median nerve stiffness measurement by shear wave elastography: A potential sonographic method in the diagnosis of carpal tunnel syndrome. *European Radiology*, *24*(2), 434–440.

Karadaĝ, Y. S., Karadaĝ, Ö., Çiçekli, E., Öztürk, Ş., Kiraz, S., Özbakir, Ş., Filippucci, E., & Grassi, W. (2010). Severity of Carpal tunnel syndrome assessed with high frequency ultrasonography. *Rheumatology International*, *30*(6), 761–765.

Katz, J. N., & Stirrat, C. R. (1990). A self-administered hand diagram for the diagnosis of carpal tunnel syndrome. *Journal of Hand Surgery*, *15*(2), 360–363.

Keir, P. J., Bach, J. M., & Rempel, D. M. (1998). Fingertip loading and carpal tunnel pressure: Differences between a pinching and a pressing task. *J Orthop Res*, *16*(1), 112–115.

Keir, P. J., Farias Zuniga, A., Mulla, D. M., & Somasundram, K. G. (2019). Relationships and Mechanisms Between Occupational Risk Factors and Distal Upper Extremity Disorders. *Human Factors*, 001872081986068.

Keir, P. J., & Wells, R. P. (1999). Changes in geometry of the finger flexor tendons in the

carpal tunnel with wrist posture and tendon load: An MRI study on normal wrists. *Clinical Biomechanics*, *14*(9), 635–645.

Keir, P. J., Wells, R. P., Ranney, D. D. A., & Lavery, W. (1997). The effects of tendon load and posture on carpal tunnel pressure. *Journal of Hand Surgery*, *22*(4), 628–634.

Kilmer, D. D., & Davis, B. A. (2002). Electrodiagnosis in carpal tunnel syndrome. *Hand Clinics*, *18*(2), 243–255.

Kociolek, A. M., & Keir, P. J. (2015). Development of a kinematic model to predict finger flexor tendon and subsynovial connective tissue displacement in the carpal tunnel. *Ergonomics*, *58*(July), 1–12.

Kociolek, A. M., & Keir, P. J. (2016). Relative motion between the flexor digitorum superficialis tendon and paratenon in zone V increases with wrist flexion angle. *J Orthop Res*, *34*(7), 1248–1255.

Kozak, A., Schedlbauer, G., Wirth, T., Euler, U., Westermann, C., & Nienhaus, A. (2015). Association between work-related biomechanical risk factors and the occurrence of carpal tunnel syndrome: an overview of systematic reviews and a meta-analysis of current research. *BMC Musculoskeletal Disorders*, *16*(231), 1–19.

Kubo, K., Zhou, B., Cheng, Y.-S., Yang, T.-H., Qiang, B., An, K.-N., Moran, S. L., Amadio, P. C., Zhang, X., & Zhao, C. (2017). Ultrasound elastography for carpal tunnel pressure measurement: A cadaveric validation study. *J Orthop Res*, 1–7.

Kutlar, N., Bayrak, A. ., Bayrak, İ. ., Canbaz, S., & Türker, H. (2017). Diagnosing carpal

tunnel syndrome with Doppler ultrasonography: a comparison of ultrasonographic measurements and electrophysiological severity. *Neurological Research*, *39*(2), 126–132.

Kuznetsova, A., Brockhoff, P. B., & Christensen, R. H. . (2017). lmerTest Package: Tests in Linear Mixed Effects Models. *Journal of Statistical Software*, *82*(13), 1–26.

Latko, W. A., Armstrong, T. J., Franzblau, A., Ulin, S. S., Werner, R. A., & Albers, J. W. (1999). A cross-sectional study of the relationship between repetitive work and upper extremity musculoskeletal disorders. *American Journal of Industrial Medicine*, *36*, 248–259.

Lee, C., Kim, T., Yoon, E., & Dhong, E. (2005). Correlation of high-resolution ultrasonographic findings with the clinical symptoms and electrodiagnostic data in carpal tunnel syndrome. *Annals of Plastic Surgery*, *54*(1), 20–23.

Lee, S., Kwak, J., Lee, S., Cho, H., Oh, E., & Park, J. W. (2019). Quantitative stiffness of the median nerve, flexor tendons, and flexor retinaculum in the carpal tunnel measured with acoustic radiation force impulse elastography in various wrist and finger positions. *Medicine*, *36*(January).

Leis, A. A., & Trapani, V. C. (2000). *Atlas of Electromyography*. Oxford: Oxford University Press.

Levine, D. W., Simmons, B. P., Koris, M. J., Daltroy, L. H., Hohl, G. ., Fossel, A. H., & Katz, J. N. (1993). A self-administered questionnaire for the assessment of severity of symptoms and functional status in carpal tunnel syndrome. *Classic Papers in*

Orthopaedics, *75*(11), 1585–1592.

Liao, Y., Lee, W., Lee, M., Chen, W., Chiou, H.-J., Kuo, T.-T., & Yeh, C.-K. (2015). Carpal Tunnel Syndrome : US Strain Imaging for Diagnosis. *Radiology*, *275*(1), 205–214.

Lin, C.-P., Chen, I.-J., Chang, K.-V., Wu, W.-T., & Özçakar, L. (2019). Utility of Ultrasound Elastography in Evaluation of Carpal Tunnel Syndrome: A Systematic Review and Meta-analysis. *Ultrasound in Medicine & Biology*, *00*(00), 1–11.

Lindström, K., Elo, A.-L., Skogstad, A., Dallner, M., Gamberale, F., Hottinen, V., Knardahl, S., & Ørhede, E. (2000). *User's Guide for the QPSNordic: General Nordic Questionnaire for psychological and social factors at work*. Nordic Council of Ministers.

Luchetti, R., Schoenhuber, R., Alfarano, M., Deluca, S., De Cicco, G., & Landi, A. (1990). Carpal tunnel syndrome: Correlations between pressure measurement and intraoperative electrophysiological nerve study. *Muscle & Nerve*, *13*(12), 1164–1168.

Luchetti, R., Schoenhuber, R., & Nathan, P. A. (1998). Correlation of segmental carpal tunnel pressures with changes in hand and wrist positions in patients with carpal tunnel syndrome and controls. *Journal of Hand Surgery*, *23 B*(5), 598–602.

Luckhaupt, S., & Dahlhamer, J. (2013). Prevalence and work-relatedness of carpal tunnel syndrome in the working population, United States, 2010 national health interview survey. *American Journal of Industrial Medicine*, *56*(6), 615–624.

Lundborg, G. N. (1975). Structure and Function of the Intraneural Microvessels as Related to Trauma, Edema Formation, and Nerve Function. *Journal of Bone and Joint Surgery*, *57-A*(7), 938–948.

Lundborg, G. N., Gelberman, R. H., Minteer-Convery, M., Lee, Y. F., & Hargens, A. R. (1982). Median nerve compression in the carpal tunnel—Functional response to experimentally induced controlled pressure. *Journal of Hand Surgery*, *7*(3), 252–259.

Lundborg, G. N., Myers, R., & Powell, H. (1983). Nerve compression injury and increased endoneurial fluid pressure : a " miniature compartment syndrome ". *Journal of Neurology, Neurosurgery and Psychiatry*, *46*, 1119–1124.

Mackinnon, S. E. (2002). Pathophysiology of nerve compression. *Hand Clinics*, *18*(2), 231–241.

Mallouhi, A., Pültzl, P., Trieb, T., Piza, H., & Bodner, G. (2006). Predictors of carpal tunnel syndrome: Accuracy of gray-scale and color doppler sonography. *American Journal of Roentgenology*, *186*(5), 1240–1245.

Marquardt, T. L., Gabra, J. N., & Li, Z. M. (2015). Morphological and positional changes of the carpal arch and median nerve during wrist compression. *Clinical Biomechanics*, *30*(3), 248–253.

Martin, M. J., & Cartwright, M. S. (2017). A Pilot Study of Strain Elastography in the Diagnosis of Carpal Tunnel Syndrome. *Journal of Clinical Neurophysiology*, *34*(2), 114–118.

Mathis, A., Mamidanna, P., Cury, K. M., Abe, T., Murthy, V. N., Mathis, M. W., & Bethge, M. (2018). DeepLabCut: markerless pose estimation of user-defined body parts with deep learning. *Nature Neuroscience*, *21*(9), 1281–1289.

Miyamoto, H., Halpern, E. J., Kastlunger, M., Gabl, M., Arora, R., Bellmann-Weiler, R., Feuchtner, G. M., Jaschke, W. R., & Klauser, A. S. (2014). Carpal Tunnel Syndrome : Diagnosis by Means of Median Nerve Elasticity — Improved Diagnostic Accuracy of US with Sonoelastography. *Radiology*, *270*(2), 481–486.

Moran, L., Perez, M., Esteban, A., Bellon, J., Arranz, B., & Del Cerro, M. (2009). Sonographic measurement of cross-sectional area of the median nerve in the diagnosis of carpal tunnel syndrome: Correlation with nerve conduction studies. *Journal of Clinical Ultrasound*, *37*(3), 125–131.

Moschovos, C., Tsivgoulis, G., Kyrozis, A., Ghika, A., Karachalia, P., Voumvourakis, K., & Chroni, E. (2019). The diagnostic accuracy of high-resolution ultrasound in screening for carpal tunnel syndrome and grading its severity is moderated by age. *Clinical Neurophysiology*, *130*(3), 321–330.

Motomiya, M., Funakoshi, T., Ishizaka, K., Nishida, M., Matsui, Y., & Iwasaki, N. (2018). Blood Flow Changes in Subsynovial Connective Tissue on Contrast-Enhanced Ultrasonography in Patients With Carpal Tunnel Syndrome Before and After Surgical Decompression. *J Ultrasound Med*, *37*(7), 1597–1604.

Myer, C., & Fowler, J. R. (2016). Flexor Tendon Repair. Healing, Biomechanics, and Suture Configurations. *Orthopedic Clinics of North America*, *47*(1), 219–226.

Myers, R. R., Murakami, H., & Powell, H. C. (1986). Reduced nerve blood flow in

edematous neuropathies: A biomechanical mechanism. *Microvascular Research*,

32(2), 145–151.

Nakamichi, K.-I., & Tachibana, S. (2000). Enlarged median nerve in idiopathic carpal

tunnel syndrome. *Muscle & Nerve*, *23*(11), 1713–1718.

Nakamichi, K.-I., & Tachibana, S. (2002). Cross-Sectional Area in Idiopathic Carpal

Tunnel Syndrome : Diagnostic Accuracy. *Muscle & Nerve*, *26*, 798–803.

Nath, T., Mathis, A., Chen, A. C., Patel, A., Bethge, M., & Mathis, M. W. (2019). Using

DeepLabCut for 3D markerless pose estimation across species and behaviors. *Nature

Protocols*, *14*, 2152–2176.

Nathan, P. A., Istvan, J. A., & Meadows, K. D. (2005). A longitudinal study of predictors

of research-defined carpal tunnel syndrome in industrial workers.: Findings at 17

years. *The Journal of Hand Surgery*, *30B*(6), 593–598.

Ng, E. S., Ng, K. W., & Wilder-Smith, E. P. (2013). Provocation tests in doppler

ultrasonography for carpal tunnel syndrome. *Muscle and Nerve*, *47*(1), 116–117.

Nordander, C., Ohlsson, K., Åkesson, I., Arvidsson, I., Balogh, I., Hansson, G. A.,

Strömberg, U., Rittner, R., & Skerfving, S. (2013). Exposure-response relationships

in work-related musculoskeletal disorders in elbows and hands - A synthesis of

group-level data on exposure and response obtained using uniform methods of data

collection. *Applied Ergonomics*, *44*(2), 241–253.

Ochiai, N., Matsui, T., Miyaji, N., Merklin, R. J., & Hunter, J. M. (1979). Vascular

anatomy of flexor tendons. I. Vincular system and blood supply of the profundus tendon in the digital sheath. *Journal of Hand Surgery*, *4*(4), 321–330.

Ogur, T., Yakut, Z., Teber, M., Alp, F., Turan, A., Tural, A., & Gelisen, O. (2015). Ultrasound elastographic evaluation of the median nerve in pregnant women with carpal tunnel syndrome. *European Review for Medical and Pharmacological Sciences*, *18*, 23–30.

Orman, G., Ozben, S., Huseyinoglu, N., Duymus, M., & Orman, K. G. (2013). Ultrasound Elastographic Evaluation in the Diagnosis of Carpal Tunnel Syndrome: Initial Findings. *Ultrasound in Medicine and Biology*, *39*(7), 1184–1189.

Osamura, N., Zhao, C., Zobitz, M. E., An, K.-N., & Amadio, P. C. (2007a). Evaluation of the material properties of the subsynovial connective tissue in carpal tunnel syndrome. *Clinical Biomechanics*, *22*(9), 999–1003.

Osamura, N., Zhao, C., Zobitz, M. E., An, K.-N., & Amadio, P. C. (2007b). Permeability of the subsynovial connective tissue in the human carpal tunnel: A cadaver study. *Clinical Biomechanics*, *22*(5), 524–528.

Padua, L., Padua, R., Aprile, I., Pasqualetti, P., & Tonali, P. (2001). Multiperspective follow-up of untreated carpal tunnel syndrome: A multicenter study. *Neurology*, *56*(11), 1459–1466.

Padua, L., Pazzaglia, C., Caliandro, P., Granata, G., Foschini, M., Briani, C., & Martinoli, C. (2008). Carpal tunnel syndrome: Ultrasound, neurophysiology, clinical and patient-oriented assessment. *Clinical Neurophysiology*, *119*(9), 2064–2069.

Pastare, D., Therimadasamy, A. K., Lee, E., & Wilder-Smith, E. P. (2009). Sonography

versus nerve conduction studies in patients referred with a clinical diagnosis of

carpal tunnel syndrome. *Journal of Clinical Ultrasound*, *37*, 389–393.

Perumal, V., & Stringer, M. D. (2014). The intrinsic arterial vascularity and morphology

of the median nerve within the carpal tunnel: A microscopic study. *Anatomical

Science International*, *89*(1), 28–33.

Pinilla, I., Martin-Hervas, C., Sordo, G., & Santiago, S. (2008). The usefulness of

ultrasonography in the diagnosis of carpal tunnel syndrome. *The Journal of Hand

Surgery, European Volume*, *33E*(4), 435–439.

Powell, H. C., & Myers, R. R. (1986). Pathology of experimental nerve compression.

Laboratory Investigation; a Journal of Technical Methods and Pathology, *55*(1),

91—100.

Presazzi, A., Bortolotto, C., Zacchino, M., Madonia, L., & Draghi, F. (2011). Carpal

tunnel: Normal anatomy, anatomical variants and ultrasound technique. *J

Ultrasound*, *14*(1), 40–46.

Preston, D. C., & Shapiro, B. (2005). *Electromyography and Neuromuscular Disorders:

Clinical Electrophysiologic Correlations*. Elsevier.

Pulikkottil, B. J., Schub, M., Kadow, T. R., Wang, W., & Fowler, J. R. (2016).

Correlating Median Nerve Cross-sectional Area With Nerve Conduction Studies.

Journal of Hand Surgery, *41*(10), 958–962.

Redmond, M. D., & Rivner, M. . (1988). False positive electrodiagnostic tests in carpal

tunnel syndrome. *Muscle & Nerve*, *11*, 511–517.

Rempel, D. M., Dahlin, L., & Lundborg, G. N. (1999). Pathophysiology of nerve
compression syndromes: response of peripheral nerves to loading. *The Journal of
Bone and Joint Surgery. American Volume*, *81*(11), 1600–1610.

Rempel, D. M., Gerr, F., Harris-Adamson, C., Hegmann, K. T., Thiese, M. S.,
Kapellusch, J., Garg, A., Burt, S., Bao, S., Silverstein, B. A., Merlino, L., Dale, A.
M., & Evanoff, B. (2015). Personal and workplace factors and median nerve
function in a pooled study of 2396 US workers. *J Occup Environ Med*, *57*(1).

Rempel, D. M., Keir, P. J., Smutz, W. P., & Hargens, A. (1997). Effects of static fingertip
loading on carpal tunnel pressure. *J Orthop Res*, *15*(3), 422–426.

Rempel, D. M., Manojlovic, R., Levinsohn, D. G., Bloom, T., & Gordon, L. (1994). The
effect of wearing a flexible wrist splint on carpal tunnel pressure during repetitive
hand activity. *Journal of Hand Surgery*, *19*(1), 106–110.

Rojviroj, S., Sirichativapee, W., Kowsuwon, W., Wongwiwattananon, J., Tamnanthong,
N., & Jeeravipoolvarn, P. (1990). Pressures in the Carpal: A comparison between
patients with carpal tunnel syndrome and normal subjects. *The Journal of Bone and
Joint Surgery*, *72B*(3), 516–518.

Roquelaure, Y., Chazelle, E., Gautier, L., Plaine, J., Descatha, A., Evanoff, B., Bodin, J.,
Fouquet, N., & Buisson, C. (2017). Time trends in incidence and prevalence of
carpal tunnel syndrome over eight years according to multiple data sources: Pays de
la Loire study. *Scandinavian Journal of Work, Environment and Health*, *43*(1), 75–

85.

Roquelaure, Y., Garlantézec, R., Evanoff, B. A., Descatha, A., Fassier, J.-B., & Bodin, J.

(2020). Personal, biomechanical, psychosocial, and organizational risk factors for

carpal tunnel syndrome: a structural equation modeling approach. *Pain*, *161*(4), 749–

757.

Rydevik, B., Lundborg, G., & Bagge, U. (1981). Effects of graded compression on

intraneural blood flow: An in vivo study on rabbit tibial nerve. *Journal of Hand

Surgery*, *6*(1), 3–12.

Sarafraz, H., Hadian, M. R., Yazdi, N. A., Olyaei, G., & Bagheri, H. (2018). Test-retest

reliability of nerve and muscle morphometric characteristics utilizing ultrasound

imaging in individuals with unilateral sciatica and controls. *Chiropractic & Manual

Therapies*, *26*(47), 1–10.

Schrier, V. J. M. M., Evers, S., Geske, J. R., Kremers, W. K., Villarraga, H. R., Selles, R.

W., Hovius, S. E. R., Gelfman, R., & Amadio, P. C. (2020). Relative Motion of the

Connective Tissue in Carpal Tunnel Syndrome: The Relation with Disease Severity

and Clinical Outcome. *Ultrasound in Medicine & Biology*, *00*(00), 1–9.

Seradge, H., Jia, Y., & Owens, W. (1995). In Vivo measurement of Carpal Tunnel

Pressure in the functioning Hand. *J Hand Surg*, *20A*, 855–859.

Shen, Z. L., Geoffrey Vince, D., & Li, Z.-M. (2013). In Vivo Study of Transverse Carpal

Ligament Stiffness Using Acoustic Radiation Force Impulse (ARFI) Imaging. *PLoS

ONE*, *8*(7), 1–11.

Shiina, T., Nightingale, K. R., Palmeri, M. L., Hall, T. J., Bamber, J. C., Barr, R. G., Castera, L., Choi, B. I., Chou, Y. H., Cosgrove, D., Dietrich, C. F., Ding, H., Amy, D., Farrokh, A., Ferraioli, G., Filice, C., Friedrich-Rust, M., Nakashima, K., Schafer, F., Sporea, I., Suzuki, S., Wilson, S., Udo, M. A. K. (2015). WFUMB guidelines and recommendations for clinical use of ultrasound elastography: Part 1: Basic principles and terminology. *Ultrasound in Medicine and Biology*, *41*(5), 1126–1147.

Stapleton, M. J. (2006). Occupation and carpal tunnel syndrome. *ANZ Journal of Surgery*, *76*(6), 494–496.

Sugimoto, H., Miyaji, N., & Ohsawa, T. (1994). Carpal Tunnel Syndrome: Evaluation of Median Nerve Circulation with Dynamic Contrast-enhanced MR Imaging. *Radiology*, *190*(2), 459–466.

Sunderland, S. (1976). The nerve lesion in the carpal tunnel syndrome. *Journal of Neurology, Neurosurgery and Psychiatry*, *39*(7), 615–626.

Szabo, R. M., & Chidgey, L. K. (1989). Stress carpal tunnel pressures in patients with carpal tunnel syndrome and normal patients. *The Journal of Hand Surgery*, *14*(4), 624–627.

Szabo, R. M., Gelberman, R. H., Williamson, R. V., & Hargens, A. R. (1983). Effects of increased systemic blood pressure on the tissue fluid pressure threshold of peripheral nerve. *J Orthop Res*, *1*(2), 172–178.

Tai, T.-W., Wu, C.-Y., Su, F.-C., Chern, T.-C., & Jou, I.-M. (2012). Ultrasonography for Diagnosing Carpal Tunnel Syndrome: A Meta-Analysis of Diagnostic Test

Accuracy. *Ultrasound in Medicine and Biology*, *38*(7), 1121–1128.

Tang, D. T., Barbour, J. R., Davidge, K. M., Yee, A., & Mackinnon, S. E. (2015). Nerve entrapment: Update. *Plastic and Reconstructive Surgery*, *135*(1), 199e-215e.

Tat, J., Holmes, M. W. R., & Keir, P. J. (2014). Cycle to cycle variability in a repetitive upper extremity task. *Ergonomics*, *57*(9), 1405–1415.

Tat, J., Kociolek, A. M., & Keir, P. J. (2013). Repetitive differential finger motion increases shear strain between the flexor tendon and subsynovial connective tissue. *J Orthop Res*, *31*(10), 1533–1539.

Tat, J., Kociolek, A. M., & Keir, P. J. (2015a). Validation of Color Doppler Sonography for Evaluating Relative Displacement Between the Flexor Tendon and Subsynovial Connective Tissue. *J Ultrasound Med*, *34*(4), 679–687.

Tat, J., Kociolek, A. M., & Keir, P. J. (2016). Relative displacement of the tendon and subsynovial connective tissue using ultrasound captures different phenomena than mechanical tendon shear. *Journal of Biomechanics*, *49*(15), 3682–3687.

Tat, J., Wilson, K. E., & Keir, P. J. (2015b). Pathological changes in the subsynovial connective tissue increase with self-reported carpal tunnel syndrome symptoms. *Clinical Biomechanics*, *30*(4), 360–365.

Tatar, I. ., Kurt, A., Yavasoglu, N. G., & Hekimoglu, B. (2016). Carpal tunnel syndrome : elastosonographic strain ratio and cross- sectional area evaluation for the diagnosis and disease severity . *Med Ultrason*, *18*(3), 305–311.

Therimadasamy, A. K., Li, E., & Wilder-Smith, E. P. (2007). Can studies of the second

lumbrical interossei and its premotor potential reduce the number of tests for carpal tunnel syndrome? *Muscle and Nerve*, *36*(4), 491–496.

Thomsen, J. F., Hansson, G. Å., Mikkelsen, S., & Lauritzen, M. (2002). Carpal tunnel syndrome in repetitive work: A follow-up study. *American Journal of Industrial Medicine*, *42*(4), 344–353.

Topp, K. S., & Boyd, B. S. (2006). Structure and biomechanics of peripheral nerves: nerve responses to physical stresses and implications for physical therapist practice. *Physical Therapy*, *86*(1), 92–109.

Torres-Costoso, A., Martínez-Vizcaíno, V., Álvarez-Bueno, C., Ferri-Morales, A., & Cavero-Redondo, I. (2018). Accuracy of Ultrasonography for the Diagnosis of Carpal Tunnel Syndrome: A Systematic Review and Meta-Analysis. *Archives of Physical Medicine and Rehabilitation*, *99*(4), 758-765.e10.

Tse, C. T. F., & Keir, P. J. (2019). External Compression and Partial Ischemia Decrease Human Finger Flexor Tendon and Subsynovial Connective Tissue Relative Motion. *Journal of Orthopaedic Research*, 1–7.

van Beek, N., Gijsbertse, K., Selles, R., de Korte, C. L., Veeger, D. (H. E. J. ., Stegeman, D. F., & Maas, H. (2018). Tendon displacements during voluntary and involuntary finger movements. *Journal of Biomechanics*, *67*, 62–68.

van Doesburg, M. H. M., Henderson, J., Mink van der Molen, A. B., An, K.-N., & Amadio, P. C. (2012a). Transverse plane tendon and median nerve motion in the carpal tunnel: Ultrasound comparison of carpal tunnel syndrome patients and healthy

volunteers. *PLoS ONE*, *7*(5), 1–5.

van Doesburg, M. H. M., Yoshii, Y., Henderson, J., Villarraga, H. R., Moran, S. L., & Amadio, P. C. (2012b). Speckle-tracking sonographic assessment of longitudinal motion of the flexor tendon and subsynovial tissue in carpal tunnel syndrome. *J Ultrasound Med*, *31*(7), 1091–1098.

Vanhees, M., Morizaki, Y., Thoreson, A. R., Larson, D., Zhao, C., An, K.-N., & Amadio, P. C. (2012). The effect of displacement on the mechanical properties of human cadaver subsynovial connective tissue. *J Orthop Res*, *30*(11), 1732–1737.

Wang, Y., Filius, A., Zhao, C., Passe, S. M., Thoreson, A. R., An, K.-N., & Amadio, P. C. (2014). Altered median nerve deformation and transverse displacement during wrist movement in patients with carpal tunnel syndrome. *Academic Radiology*, *21*(4), 472–480.

Wang, Y., Qiang, B., Zhang, X., Greenleaf, J. F., An, K.-N., Amadio, P. C., & Zhao, C. (2012). A non-invasive technique for estimating carpal tunnel pressure by measuring shear wave speed in tendon: A feasibility study. *Journal of Biomechanics*, *45*(16), 2927–2930.

Werner, C.-O., Elmqvist, D., & Ohlin, P. (1983). Pressure and nerve lesion in the carpal tunnel. *Acta Orthopaedica Scandinavica*, *54*, 312–316.

Werner, R. A., Franzblau, A., Albers, J. W., & Armstrong, T. J. (1998). Median mononeuropathy among active workers: Are there differences between symptomatic and asymptomatic workers? *American Journal of Industrial Medicine*, *33*(4), 374–

378.

Werthel, J.-D. R., Zhao, C., An, K. N., & Amadio, P. C. (2014). Carpal Tunnel Syndrome

    Pathophysiology : Role of Subsynovial Connective Tissue. *J Wrist Surg*, *3*, 220–226.

Wiesler, E. R., Chloros, G. D., Cartwright, M. S., Smith, B. P., Rushing, J., & Walker, F.

    O. (2006). The use of diagnostic ultrasound in carpal tunnel syndrome. *J Hand Surg*,

    31A(1), 726–732.

Wilson, K. E., Tat, J., & Keir, P. J. (2017). Effects of Wrist Posture and Fingertip Force

    on Median Nerve Blood Flow Velocity. *BioMed Research International-Biophysics*,

    2017, 8 pages.

Xin, H., Hu, H., Liu, B., Liu, X., Li, X., & Li, J. (2017). Ultrasound elastographic

    evaluation of the median nerve in hemodialysis with carpal tunnel syndrome.

    Journal of Medical Ultrasonics, *44*(1), 123–131.

Yoshii, Y., Tung, W. L., & Ishii, T. (2017a). Measurement of median nerve strain and

    applied pressure for the diagnosis of carpal tunnel syndrome. *Ultrasound in*

    Medicine & Biology, *43*(6), 1205–1209.

Yoshii, Y., Tung, W. L., & Ishii, T. (2017b). Strain and Morphological Changes of

    Median Nerve After Carpal Tunnel Release. *J Ultrasound Med*, *36*, 1153–1159.

Yoshii, Y., Zhao, C., Henderson, J., Zhao, K. D., An, K.-N., & Amadio, P. C. (2011).

    Velocity-dependent changes in the relative motion of the subsynovial connective

    tissue in the human carpal tunnel. *J Orthop Res*, *29*, 62–66.

Yoshii, Y., Zhao, C., Zhao, K. D., Zobitz, M. E., An, K.-N., & Amadio, P. C. (2008). The

effect of wrist position on the relative motion of tendon, nerve, and subsynovial

connective tissue within the carpal tunnel in a human cadaver model. *J Orthop Res*,

26(8), 1153–1158.

Zhang, C., Li, M., Jiang, J., Zhou, Q., Xiang, L., Huang, Y., Ban, W., & Peng, W. (2017).

Diagnostic Value of Virtual Touch Tissue Imaging Quantification for Evaluating

Median Nerve Stiffness in Carpal Tunnel. *J Ultrasound Med*, *36*, 1783–1791.

Zhao, C., Ettema, A. M., Berglund, L. J., An, K.-N., & Amadio, P. C. (2011). Gliding

resistance of flexor tendon associated with carpal tunnel pressure: A biomechanical

cadaver study. *J Orthop Res*, *29*(1), 58–61.

Zhou, S. K., Greenspan, H., & Shen, D. (2017). Deep Learning for Medical Image

Analysis. *Annu Rev Biomed Eng*, *19*, 221–248.

Ziswiler, H.-R., Reichenbach, S., Vögelin, E., Bachmann, L. M., Villiger, P. M., & Jüni,

P. (2005). Diagnostic value of sonography in patients with suspected carpal tunnel

syndrome: A prospective study. *Arthritis & Rheumatism*, *52*(1), 304–311.

APPENDICES

Appendix A: Ethics Approval for Chapter 2 & 3

HiREB
Hamilton Integrated Research Ethics Board

Hamilton Integrated Research Ethics Board
AMENDMENT REQUEST

REB Project #: 12-686

Principal Investigator: Dr. Peter Keir

Project Title: Changes in Intraneural Blood Flow in the Median Nerve Following Postures Associated with Risk of Carpal Tunnel Syndrome

Document(s) Amended with version # and date:

> ➢ Protocol - Version: 4.0 Dated: 05 July, 2017
> ➢ Consent Form - Version: 4.0 Dated: 05 July, 2017

[X] **Amendment approved as submitted**

[ ] **Amendment approved conditional on changes noted in "Conditions" section below**
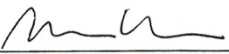
[ ] **New enrolment suspended**

[ ] **Study suspended pending further review**

Level of Review:
   [ ] Full Research Ethics Board
   [X] Research Ethics Board Executive

The Hamilton Integrated Research Ethics Board operates in compliance with and is constituted in accordance with the requirements of: The Tri-Council Policy Statement on Ethical Conduct of Research Involving Humans; The International Conference on Harmonization of Good Clinical Practices; Part C Division 5 of the Food and Drug Regulations of Health Canada, and the provisions of the Ontario Personal Health Information Protection Act 2004 and its applicable Regulations; For studies conducted at St. Joseph's Hospital, HIREB complies with the health ethics guide of the Catholic Alliance of Canada

_____   7/12/2017
Raelene Rathbone, MB BS, MD, PhD, Chair   Date
Mark Inman, MD, PhD, Chair

All Correspondence should be addressed to the HIREB Chair(s) and forwarded to:
HIREB Coordinator
293 Wellington St. N, Suite 102, Hamilton ON L8L 8E7
Tel. 905-521-2100 Ext. 42013 Fax: 905-577-8378

Appendix B: Ethics Approval for Chapter 4

Hamilton Integrated Research Ethics Board

Oct-25-2019

Project Number: 7702

Project Title: Changes in Median Nerve Intraneural Blood Flow and Conductivity, Carpal Tunnel Tissue Stiffness and Tendon Mechanics Over 30-Minutes of Sub-Diastolic Blood Flow Occlusion

Principal Investigator: Dr. Peter Keir

This will acknowledge receipt of your letters dated September 6, 2019, September 25, 2019, October 24, 2019, which enclosed revised copies of the Information/Consent Form, Advertisement, Ethics Certificate and the Application Form along with a response to the additional queries of the Board for the above-named study. These issues were raised by the Hamilton Integrated Research Ethics Board at their meeting held on August 20, 2019. Based on this additional information, we wish to advise your study had been given **final** approval from the full HiREB.

The following documents have been approved on both ethical and scientific grounds:

Document Name	Document Date	Document Version
Data Collection Sheet- July 17:19	Jul-17-2019	1
FariasZ_Letter of Information - Consent Form-Sept 6:19- cleanREVISED	Sep-06-2019	2
FariasZ-Advertisement-Sept 6:19-cleanREVISED	Sep-06-2019	2
FariasZ-ResearchProtocol-July17:19-clean	Jul-17-2019	1
Katz Hand Diagram	Jul-15-2019	1
Levine's Questionnaire	Jul-15-2019	1

The following documents have been acknowledged:

Document Name	Document Date	Document Version
Health-Record-review-certificate191983(Keir)	Sep-24-2019	3
tcps2_core_certificate	Aug-14-2018	1

Please Note: All consent forms and recruitment materials used in this study must be copies of the above referenced documents.

We are pleased to issue final approval for the above-named study for a period of 12 months from the date of the HiREB meeting on August 20, 2019. Continuation beyond that date will require further review and renewal of HiREB approval. Any changes or revisions to the original submission must be submitted on a HiREB amendment form for review and approval by the Hamilton Integrated Research Ethics Board.

PLEASE QUOTE THE ABOVE REFERENCED PROJECT NUMBER ON ALL FUTURE CORRESPONDENCE

Sincerely,

Dr. Mark Inman, MD, PhD
Chair, Hamilton Integrated Research Ethics Board

The Hamilton Integrated Research Ethics Board (HiREB) represents the institutions of Hamilton Health Sciences, St. Joseph's Healthcare Hamilton, Research St. Joseph's-Hamilton, and the Faculty of Health Sciences at McMaster University and operates in compliance with and is constituted in accordance with the requirements of: The Tri-Council Policy Statement on Ethical Conduct of Research Involving Humans; The International Conference on Harmonization of Good Clinical Practices; Part C Division 5 of the Food and Drug Regulations of Health Canada, and the provisions of the Ontario Personal Health Information Protection Act 2004 and its applicable Regulations; For studies conducted at St. Joseph's Healthcare Hamilton, HiREB complies with the Health Ethics Guide of the Catholic Alliance of Canada

Appendix C: Consent Form for Chapter 2 & 3

McMaster University

Inspiring Innovation and Discovery

DATE: July 5, 2017

LETTER OF INFORMATION / CONSENT

Changes in Intraneural Blood Flow in the Median Nerve Following Postures Associated with Risk of Carpal Tunnel Syndrome

Principal Investigator: **Student Investigator:**

Dr. Peter Keir   Amanda Farias Zuniga, MSc

Department of Kinesiology   Department of Kinesiology

McMaster University   McMaster University

Hamilton, Ontario, Canada   Hamilton, Ontario, Canada

(905) 525-9140 ext. 23543   **(905) 525-9140 ext. 20175**

E-mail: *pjkeir@mcmaster.ca*   E-mail: *fariasza@mcmaster.ca*

Purpose of the Study:

The purpose of this study is to test the effect of different wrist postures on intraneural blood flow of the median nerve and the effect of repetitive finger motion on tendon-connective tissue motion in symptomatic individuals. A secondary purpose is to quantify the sensitivity of ultrasonography in differentiating mechanics in relation to posture, symptom severity and work history.

You are invited to participate in this study about musculoskeletal disorders of the wrist and hand. Carpal tunnel syndrome is a common musculoskeletal disorder of the wrist and hand that is caused by compression of the median nerve at the wrist. Understanding how the nerve becomes damaged inside the carpal tunnel (or wrist) is important in determining the development of wrist and hand musculoskeletal disorders. The median nerve can be seen non-invasively using ultrasound.

Procedures involved in the Research:

You will be asked to complete a questionnaire about your handedness (i.e. left-handed or right-handed), general health, as well as musculoskeletal disorders of the wrist and hand. Following the questionnaire, you will complete a testing protocol no longer than 0.5 hours. You will be seated comfortably while the ultrasound technician applies ultrasound gel on the wrist of your dominant hand. Next, your wrist will be placed in 3 different wrist postures while an ultrasound probe records images of the nerve in the carpal tunnel. Each posture will last no longer than 5 minutes (with rest in between each posture). After these postures, you will be asked to perform repetitive finger motions of your middle finger while grasping a hand grip. Ultrasound measurement of blood flow and finger tendon motion will be measured.

Potential Harms, Risks or Discomforts:

Ultrasound is a safe imaging tool used to visualize tissues within your body. The wrist postures and repetitive finger motions in this study might cause you minimal discomfort due to fatigue in some rare cases. However, we do not foresee any risks from your participation in this research. If you do feel any muscular discomfort or pain, please tell the technician. In the event that you do feel pain while performing any of the tasks, the study will be stopped immediately to ensure your safety.

Potential Benefits:
This research will not benefit you directly, except for knowing that you are helping further our understanding about the influence of wrist postures, aspects of pinching, and repetitive wrist motions on the vascular structures in the median nerve. Ultimately, we hope to prevent musculoskeletal disorders in the workplace.

Payment or Reimbursement:

You will receive $20 for your time for participating in this study. If you withdraw from this study at any time, you will still receive prorated compensation.

Confidentiality:

Your identity will be kept confidential. We will not use your name or any information that would allow you to be identified. The data obtained in this study will be used for research and teaching purposes only. Information directly pertaining to you will be stored in a locked cabinet or on a password protected computer.

Participation and Withdrawal:

Your participation in this study is voluntary. If you decide to participate, you can choose to stop at any time, even after signing the consent form, or partway through the study. If

you decide to stop participating in this study, there will be no consequences to you. Also, all of your data will be permanently deleted.

This study has been reviewed by the Hamilton Integrated Research Ethics Board (HIREB). If you have any concerns or questions about your rights as a participant or about the way this study is conducted, contact the Office of the Chair at the HIREB at (905) 521-2199 (x 44405 or x43838).

Information about the Study Results:

You may obtain information about the study results by contacting Amanda Farias Zuniga at (905) 525-9140 (x 20175) or Dr. Peter Keir at (905) 525-9140 (x 23543).

Questions about the Study:
If you have questions or need more information about the study itself, please contact me at:

| Amanda Farias Zuniga |
| fariasza@mcmaster.ca |

This study has been reviewed by the Hamilton Integrated Research Ethics Board (HiREB). The HiREB is responsible for ensuring that participants are informed of the risks associated with the research, and that participants are free to decide if participation is right for them. If you have any questions about your rights as a research participant, please call the Office of the Chair, HiREB, at 905.521.2100 x 42013.

CONSENT

- I have read the information presented in the information letter about a study being conducted by Amanda Farias Zuniga and Dr. Peter Keir of McMaster University.
- I have had the opportunity to ask questions about my involvement in this study and to receive additional details I requested.
- I understand that if I agree to participate in this study, I may withdraw from the study at any time or up until approximately December, 2017
- I have been given a copy of this form.
- I agree to participate in the study.

Signature: _____

Date: _____

Name of Participant (Printed) _____

1. ___Yes, I would like to receive a summary of the study's results.
Please send them to me at this email address _____

Or to this mailing address: _____

                                             _____

                                             _____

___ No, I do not want to receive a summary of the study's results.

2. I agree to be contacted about a follow-up interview, and understand that I can always decline the request.
___ Yes. Please contact me at: _____
___ No.

3. I would like to be contacted for future studies from the Occupational Biomechanics Laboratory at McMaster University.
____ Yes. Please contact me at: _____
____ No.

LETTER OF INFORMATION / CONSENT

**Changes in Median Nerve Intraneural Blood Flow and
Conductivity, Carpal Tunnel Tissue Stiffness and Tendon
Mechanics Over 30-Minutes of Sub-Diastolic Blood Flow
Occlusion**

Principal Investigator:	**Student Investigator:**
Dr. Peter Keir	Amanda Farias Zuniga, MSc
Department of Kinesiology	Department of Kinesiology
McMaster University	McMaster University
Hamilton, Ontario, Canada	Hamilton, Ontario, Canada
(905) 525-9140 ext. 23543	**(905) 525-9140 ext. 20175**
E-mail: pjkeir@mcmaster.ca	E-mail: fariasza@mcmaster.ca

Purpose of the Study:

The purpose of this study is to test the effect of different wrist postures and local blood
flow occlusion on intraneural blood flow of the median nerve, median nerve conduction,
median nerve and tendon stiffness, tendon-connective tissue motion and symptoms of
discomfort in healthy participants**.**

You are invited to participate in this study about musculoskeletal disorders of the wrist
and hand. Carpal tunnel syndrome is a common musculoskeletal disorder of the wrist and
hand that is caused by compression of the median nerve at the wrist. Understanding how
the nerve becomes damaged inside the carpal tunnel (or wrist) is important in determining
the development of wrist and hand musculoskeletal disorders. The median nerve can be
seen non-invasively using ultrasound.

Procedures involved in the Research:

You will be asked to complete a questionnaire about your general health, as well as
musculoskeletal disorders of the wrist and hand. Following the questionnaire, you will
complete a testing protocol no longer than 1.5 hours. You will be laying down
comfortably while the ultrasound technician applies ultrasound gel on the wrist of your
right hand. A blood pressure cuff will be placed on your upper arm and inflated for a
period of 30 minutes. You will also be asked to perform repetitive finger motions of your
middle finger while grasping a hand grip, and your wrist may be placed in different
postures as well. A nerve conduction study will also be performed which will test the

187

ability of your nerve to conduct electrical impulses. Ultrasound measurement of blood flow, nerve conduction, tissue stiffness and finger tendon motion will be measured.

Potential Harms, Risks or Discomforts:

Ultrasound is a safe imaging tool used to visualize tissues within your body. Nerve conduction testing is a safe and a commonly administered test, but will cause some discomfort. The wrist postures and repetitive finger motions in this study might cause you minimal discomfort due to fatigue in some rare cases. The period of blood flow occlusion (30 minutes) will also cause some discomfort and may induce slight sensations of tingling in your hand. However, we do not foresee any risks from your participation in this research. If you do feel any muscular discomfort or pain, please tell the technician. In the event that you do feel pain while performing any of the tasks, the study will be stopped immediately to ensure your safety.

Potential Benefits:

This research will not benefit you directly, except for knowing that you are helping further our understanding about the influence of wrist postures, aspects of pinching, and repetitive wrist motions on the vascular structures in the median nerve. Ultimately, we hope to prevent musculoskeletal disorders in the workplace.

Payment or Reimbursement:

You will receive $20 for your time for participating in this study. If you withdraw from this study at any time, you will still receive prorated compensation. This study is funded by an NSERC Discovery Grant (RGPIN-2016-06460).

Confidentiality:

Your identity will be kept confidential. We will not use your name or any information that would allow you to be identified. The data obtained in this study will be used for research and teaching purposes only. Information directly pertaining to you will be stored in a locked cabinet or on a password protected computer. For the purposes of ensuring the proper monitoring of the research study, it is possible that a member of the Hamilton Integrated Research Ethics Board and this institution and affiliated sites may consult your research data for quality assurance purposes. However, no records that identify you by name or initials will be allowed to leave the research office. By signing this consent form, you authorize such access.

Participation and Withdrawal:

Your participation in this study is voluntary. If you decide to participate, you can choose to stop at any time, even after signing the consent form, or partway through the study. If you decide to stop participating in this study, there will be no consequences to you. Also, all of your data will be permanently deleted. To withdraw from this study, please contact the student investigator Amanda Farias Zuniga through telephone at (905) 525-9140 (x 20175) or by email at fariasza@mcmaster.ca.

Information about the Study Results:

You may obtain information about the study results by contacting Amanda Farias Zuniga at (905) 525-9140 (x 20175) or Dr. Peter Keir at (905) 525-9140 (x 23543).

Questions about the Study:
If you have questions or need more information about the study itself, please contact me at:

Amanda Farias Zuniga
fariasza@mcmaster.ca

This study has been reviewed by the Hamilton Integrated Research Ethics Board (HiREB). The HiREB is responsible for ensuring that participants are informed of the risks associated with the research, and that participants are free to decide if participation is right for them. If you have any questions about your rights as a research participant, please call the Office of the Chair, HiREB, at 905.521.2100 x 42013.

CONSENT

- I have read the information presented in the information letter about a study being conducted by Amanda Farias Zuniga and Dr. Peter Keir of McMaster University.
- I have had the opportunity to ask questions about my involvement in this study and to receive additional details I requested.
- I understand that if I agree to participate in this study, I may withdraw from the study at any time or up until approximately December 2019
- You will be given a signed copy of this form.
- I agree to participate in the study.

Signature: _____ Date: _____

Name of Participant (Printed) _____

1. ___Yes, I would like to receive a summary of the study's results.
Please send them to me at this email address _____
Or to this mailing address: _____

_____

_____

___ No, I do not want to receive a summary of the study's results.

2. I agree to be contacted about a follow-up interview, and understand that I can always decline the request.
___ Yes. Please contact me at: _____
___ No.

3. I would like to be contacted for future studies from the Occupational Biomechanics Laboratory at McMaster University.
____ Yes. Please contact me at: _____
____ No.

Appendix E: Work practices questionnaire from Chapter 3

Work practices and hand use questionnaire

Please select the response that most closely matches your answer, or provide your answer in the space provided where needed.

Demographics

   1. Age:_____   2. Sex (circle one): Male Female

Current work practices

3. How many hours do you work per week?
     Full time (30 hours or more per week)
     Part time (less than 30 hours per week)
	4. How many years of total work experience do you have?
	     0-5 years
	     6-10 years
	     11-15 years
	     16-20 years
	     21-25 years
	     26-30 years
	     31-35 years
	     36-40 years
	     40+ years

5. What is the nature of your **current** work?
     Homemaker
     Retired
     Student
     Unemployed
     Agriculture, forestry, fishing or hunting
     Arts, entertainment, or recreation
     Broadcasting
     Education
     Construction
     Finance and Insurance
     Government and Public Administration
     Health Care and Social Assistance
     Hotel and Food Services
	Information- Services and Data Processing
	 Legal Services
	 Manufacturing- computer and electronics
	 Manufacturing- Other
	 Military
	 Mining
	 Publishing
	 Real Estate, Rental or Leasing
	 Religious
	 Retail
	 Scientific or Technical Services
	 Software
	 Telecommunications
	 Transportation and Warehousing
	 Utilities
	 Other:_____

6. Current job title: _____

7. How many years have you been at your **current** job? _____years

8. What are your main activities at your job, and what percentage of your day do they require/occur? (list up to 5 main activities). **Total percent of day must equal to 100%.**
    1) Activity_____
    Percent of day:_____
    2) Activity_____
    Percent of day:_____
    3) Activity_____
    Percent of day:_____
    4) Activity_____
    Percent of day:_____
    5) Activity_____
    Percent of day:_____

9. Is your work load irregular so that the work piles up? (circle the number that best corresponds to your response)
> 1- very seldom or never
> 2- seldom
> 3- sometimes
> 4- often
> 5- very often or always

10. Do you have to work overtime? (circle the number that best corresponds to your response)
> 1- very seldom or never
> 2- seldom
> 3- sometimes
> 4- often
> 5- very often or always

11. Is it necessary to work at a rapid pace? (circle the number that best corresponds to your response)
> 1- very seldom or never
> 2- seldom
> 3- sometimes
> 4- often
> 5- very often or always

12. Please indicate the **frequency** of repetitive handwork that your **current** job requires (circle the number that best corresponds to your response):
> 0- hands idle most of the time, no regular exertions
> 1
> 2- consistent slow, conspicuous pauses, or very slow motions
> 3
> 4- steady exertion/ motion, may have frequent pauses
> 5
> 6- steady exertion/motion, may have infrequent pauses
> 7
> 8- rapid steady exertion/motion, few, if any pauses
> 9
> 10- rapid steady exertion/motion, no pauses, difficulty keeping up

13. Please indicate the **intensity** of handwork that your **current** job requires (circle the number that best corresponds to your response):

        0- none
        1- very weak
        2- weak (light)
        3- moderate
        4
        5- strong (heavy)
        6
        7- very strong
        8
        9
        10- extreme

Past work practices

14. What is the nature of your **previous** work? (Select ALL that apply)	Information- Services and Data Processing
Homemaker	Legal Services
Retired	Manufacturing- computer and electronics
Student	Manufacturing- Other
Unemployed	Military
Agriculture, forestry, fishing or hunting	Mining
Arts, entertainment, or recreation	Publishing
Broadcasting	Real Estate, Rental or Leasing
Education	Religious
Construction	Retail
Finance and Insurance	Scientific or Technical Services
Government and Public Administration	Software
Health Care and Social Assistance	Telecommunications
Hotel and Food Services	Transportation and Warehousing
	Utilities
	Other:_____

15. How many years were you at your **previous** job(s)?
    1) Job: _____
    Number of years: _____
    2) Job: _____

    Number of years: _____
    3) Job: _____

    Number of years: _____
    4) Job: _____

    Number of years: _____

16. Overall, how do your **previous** job(s) compare to your **current** job, in terms of:
    a) Frequency of hand use (please circle one)
        More frequent   As frequent as current job   Less frequent

    b) Intensity of hand use (please circle one)

        More intense   As intense as current job   Less intense

Non-work related activity

17. How many hours **per week** do you engage in other **non-work-related** activities requiring your **hands** (including exercise)? _____ hours/week

18. What is the nature of your non-work-related activities, and how much time **per week** do they require/occur? (list up to 5). **Total time must equal time indicated in question 17.**
        1) Activity_____
        Amount of non-work related time:_____
        2) Activity_____
        Amount of non-work related time:_____
        3) Activity_____
        Amount of non-work related time:_____
        4) Activity_____
        Amount of non-work related time:_____
        5) Activity_____
   Amount of non-work related time:_____

19. Please indicate the **frequency** of repetitive handwork that your **non work-related activities** require (circle the number that best corresponds to your response):

        0- hands idle most of the time, no regular exertions
        1
        2- consistent slow, conspicuous pauses, or very slow motions
        3
        4- steady exertion/ motion, may have frequent pauses
        5
        6- steady exertion/motion, may have infrequent pauses
        7
        8- rapid steady exertion/motion, few, if any pauses
        9
        10- rapid steady exertion/motion, no pauses, difficulty keeping up

20. Please indicate the **intensity** of handwork that your **non-work related activities** require (circle the number that best corresponds to your response):

        0- none
        1- very weak
        2- weak (light)
        3- moderate
        4
        5- strong (heavy)
        6
        7- very strong
        8
        9
        10- extreme

Appendix F: Katz Hand Diagram and Classification from Chapter 4
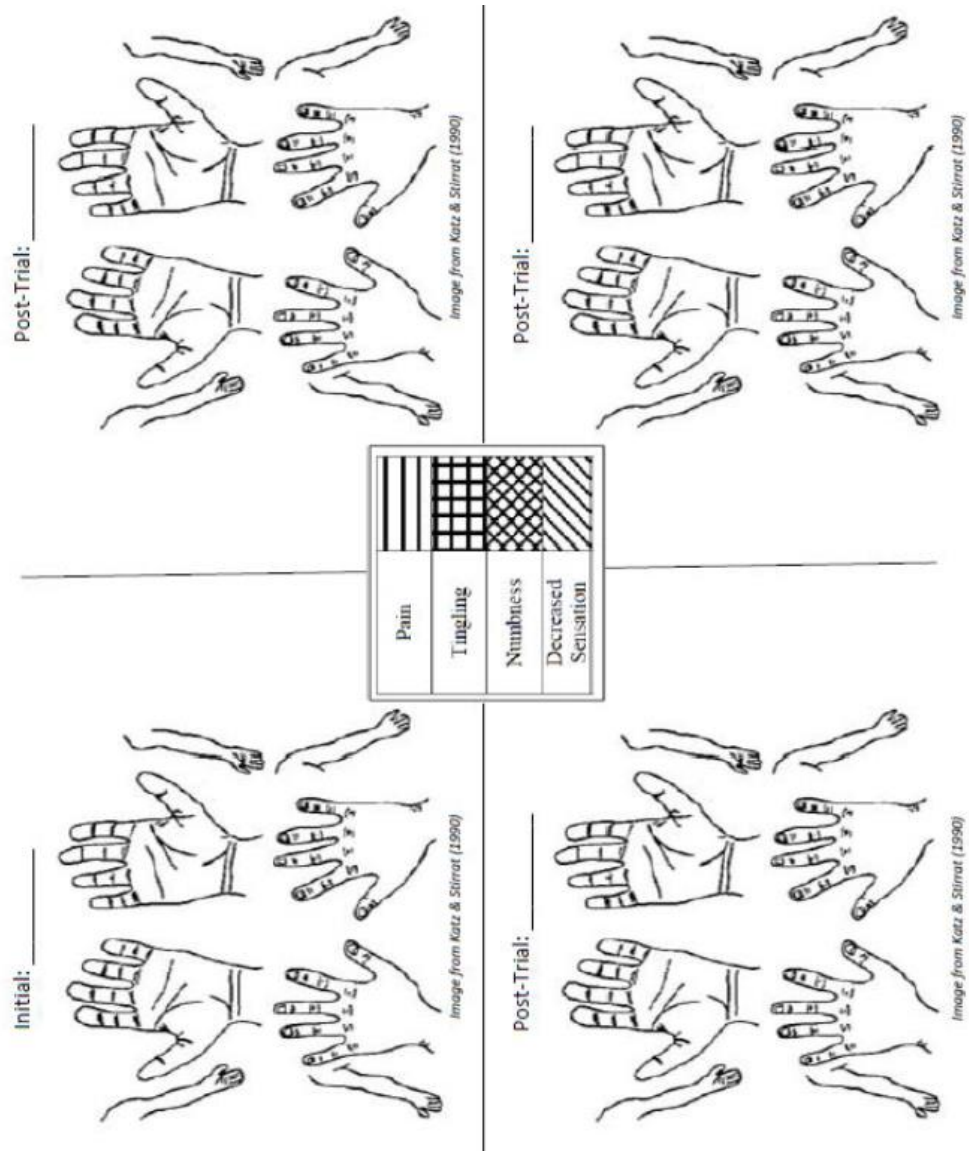
Appendix G: Levine's CTS Questionnaire from Chapter 4

CTS QUESTIONNAIRE

The following questions refer to your symptoms for a typical twenty-four hour period during the past two weeks (circle one answer to each question).

SEVERITY SCALE: 0 = None or Never; 1 = Mild; 2 = Moderate; 3 = Severe; 4 = Very severe

SYMPTOM SEVERITY SCALE

QUESTION SEVERITY SCORE 0= NONE; 4=SEVERE	0	1	2	3	4
1. How severe is the hand or wrist pain that you have at night?	0	1	2	3	4
2. How often did hand or wrist pain wake you up during a typical night in the past two weeks (times/night)?	0	1	2-3	4-5	5+
3. Do you typically have pain in your hand or wrist during the daytime?	0	1	2	3	4
4. How often do you have hand or wrist pain during the daytime (times/day)?	0	1-2	3-5	5+	constant
5. How long, on average, does an episode of pain last during the daytime (minutes)?	0	<10	10-60	>60	constant
6. Do you have numbness (loss of sensation) in your hand?	0	1	2	3	4
7. Do you have weakness in your hand or wrist?	0	1	2	3	4
8. Do you have tingling sensations in your hand?	0	1	2	3	4
9. How severe is numbness (loss of sensation) or tingling at night?	0	1	2	3	4
10. How often did hand numbness or tingling wake you up during a typical night during the past two weeks?	0	1	2-3	4-5	5+
11. Do you have difficulty with the grasping and use of small objects such as keys or pens?	0	1	2	3	4

FUNCTIONAL STATUS SCALE

QUESTION SEVERITY SCORE 0= NONE; 4=SEVERE	0	1	2	3	4
1. Writing	0	1	2	3	4
2. Buttoning of clothes	0	1	2	3	4
3. Holding a book while reading	0	1	2	3	4
4. Gripping of a telephone handle	0	1	2	3	4
5. Opening of jars	0	1	2	3	4
6. Household chores	0	1	2	3	4
7. Caring of grocery bags	0	1	2	3	4
8. Bathing and Dressing	0	1	2	3	4

COMMENTS:

_____

_____

_____

_____

ID _____

DATE _____

M /F _____   AGE_____   DOI _____

Levine DW, Simmons HP, Koris MJ, Daltroy LH, Hohl GG, Fossel AH, Katz JN. A self-Administered questionnaire for the assessment of severity of symptoms and functional status in carpal tunnel syndrome. J Bone and Joint Surgery, 1993; 75-A:1585-1592.